MODELING A FIELD APPLICATION OF *IN SITU* BIOREMEDIATION OF PERCHLORATE-CONTAMINATED GROUNDWATER USING HORIZONTAL FLOW TREATMENT WELLS (HFTWs)

Peter G. Chosa, Captain, USAF
AFIT/GEM/ENV/04M-05

DEPARTMENT OF THE AIR FORCE
AIR UNIVERSITY
AIR FORCE INSTITUTE OF TECHNOLOGY

Wright-Patterson Air Force Base, Ohio

APPROVED FOR PUBLIC RELEASE; DISTRIBUTION UNLIMITED.

The views expressed in this thesis are those of the author and do not reflect the official policy or position of the United States Air Force, Department of Defense, or the U. S. Government.

AFIT/GEM/ENV/04M-05

MODELING A FIELD APPLICATION OF *IN SITU* BIOREMEDIATION OF PERCHLORATE-CONTAMINATED GROUNDWATER USING HORIZONTAL FLOW TREATMENT WELLS (HFTWs)

THESIS

Presented to the Faculty

Department of Systems and Engineering Management

Graduate School of Engineering and Management

Air Force Institute of Technology

Air University

Air Education and Training Command

In Partial Fulfillment of the Requirements for the

Degree of Master of Science in Engineering Management

Peter G. Chosa, B.S.

Captain, USAF

March 2004

APPROVED FOR PUBLIC RELEASE; DISTRIBUTION UNLIMITED.

AFIT/GEM/ENV/04M-05

MODELING A FIELD APPLICATION OF *IN SITU* BIOREMEDIATION OF PERCHLORATE-CONTAMINATED GROUNDWATER USING HORIZONTAL FLOW TREATMENT WELLS (HFTWs)

Peter G. Chosa, B.S.
Captain, USAF

Approved:

//signed//	18 Mar 04
Dr. Mark N. Goltz Chairman, Advisory Committee	date
//signed//	18 Mar 04
Dr. Charles Bleckmann Member, Advisory Committee	date
//signed//	18 Mar 04
Dr. Junqi Huang Member, Advisory Committee	date

AFIT/GEM/ENV/04M-05

Abstract

Perchlorate contaminated groundwater is rapidly becoming a significant environmental remediation issue for the Department of Defense. In this study, an existing numerical model that simulates the operation of a Horizontal Flow Treatment Well (HFTW) system to effect the *in situ* biodegradation of perchlorate through the addition of an electron donor is modified to include a submodel that describes bioclogging. Bioclogging restricts flow out of the HFTW due to the accumulation of biomass directly adjacent to the well. The modified model is then applied to an existing perchlorate contaminated site that will be used for an evaluation of the HFTW technology. Simulations were conducted to determine the impact of altering various engineered parameters on HFTW performance. Simulation results indicate that higher time averaged electron donor concentrations and HFTW pumping rates lead to more perchlorate degradation in terms of total mass of perchlorate removed. Simulation results also indicate that varying the electron donor addition schedule has little impact on HFTW performance. The simulations conducted in this study show that, regardless of the engineered parameter values, bioclogging does not impact the ability of the HFTW technology to effect *in situ* biodegradation of perchlorate at the evaluation site.

Acknowledgements

There are several people and organizations I would like to recognize for helping me complete this thesis. First, I want to thank my wife for her love, support, encouragement, and sacrifice over the past eighteen months. I must also thank my son for not taking it personally when I had to spend long hours in front of the computer instead of playing with him. Words cannot describe how indebted I am to Dr. Goltz and Dr. Huang who both endured many hours of questions and patiently guided me through this thesis effort. Additionally, I would like to thank the Environmental Security Technology Certification Program (ESTCP) for their financial support of this work through project CU-0224. Although I never met him in person, I would be remiss if I did not thank Scott Neville, the Senior Environmental Analyst at Aerojet General Corporation, for promptly providing me with numerous site specific documents needed to finish this thesis. I would also like to thank Dr. Bleckmann for being on my advisory committee and providing invaluable classroom discussion and advice regarding microorganisms and the world they live in. I shall never look at my fingernails the same again.

Pete Chosa

Table of Contents

Page

Page

Page

List of Figures

Page

Page

Page

Page

Page

List of Tables

Page

Page

MODELING A FIELD APPLICATION OF *IN SITU* BIOREMEDIATION OF PERCHLORATE-CONTAMINATED GROUNDWATER USING HORIZONTAL FLOW TREATMENT WELLS (HFTWs)

1.0 INTRODUCTION

1.1 MOTIVATION

Perchlorate (ClO_4^-) contaminated groundwater is an emerging problem in the western United States, particularly in Utah, California, Arizona, and Nevada (Urbansky, 1998). Critical drinking water sources like Lake Mead and the Colorado River have been found to contain perchlorate (Urbansky, 1998) and it is estimated that the drinking water of more than 18 million people has tested positive for perchlorate (Strategic Environmental Research and Development Program, 2003). Recently, perchlorate at the eight parts per billion (ppb) level has been discovered in lettuce grown in areas irrigated with water from the Colorado River (Weise, 2003; Hogue, 2003). Perchlorate has also been found in milk samples taken from supermarkets in Lubbock, Texas (Kirk *et al.*, 2003).

Most perchlorate is hypothesized to have entered surface waters and groundwater aquifers primarily through the at-the-time legal dumping of perchlorate-containing wastes into the environment by the Department of Defense (DoD) and various aerospace industry companies who used perchlorate containing salts as a constituent in solid rocket boosters (Urbansky, 1998, 2002). As a major contributor to the perchlorate

contamination problem, DoD, through its Strategic Environmental Research and Development Program (SERDP) and Environmental Security Technology Certification Program (ESTCP), has taken a lead role in developing new technologies to address perchlorate-contaminated waters as well as evaluating the health risks associated with perchlorate exposure (ESTCP, 2000).

Low level doses of perchlorate ($\leq$ 1 g/day) have long been known to inhibit iodide uptake by the thyroid gland and therefore potentially disrupt normal metabolic activity within humans leading to the formation of goiters and the onset of muscle spasms (Urbansky, 1998; Wolff, 1998). Perchlorate was once clinically administered to those suffering from Grave's disease, an overactive thyroid, as well as to combat the side effects of chemotherapy (Urbansky, 1998). As a result of several cases of aplastic anemia having been discovered in patients who were administered perchlorate in the 1960's, the ion is now only used within the United States as a diagnostic tool to evaluate thyroid activity (Wolff, 1998). However, Wolff (1998) notes that low dosages of perchlorate over short times may not have any adverse health effects. Nevertheless, both Wolff (1998) and Urbansky (1998) caution that perchlorate has been shown to readily cross the placenta (of guinea pigs) and therefore the potential exists that perchlorate ingestion by pregnant women may cause reproductive problems, including congenital hypothyroidism.

As Pontius *et al*. (2000) points out, the chronic effects of low level perchlorate exposure are still being researched, so the United States Environmental Protection Agency (EPA) has yet to establish a federal drinking water standard. On January 22, 2003, the EPA

issued a memorandum updating its 1999 Interim Guidance on perchlorate. In this memorandum, the EPA suggests that states and other interested parties who are setting perchlorate cleanup criteria carefully consider setting standards at the low end of the provisional cleanup range of 4-18 part per billion (ppb) which was established by EPA in their 1999 Interim Guidance. This recommendation is based upon an analysis conducted by the EPA and the State of California that suggests a new oral health risk benchmark for perchlorate will likely lead to provisional cleanup levels slightly below the 1999 Interim Guidance range (USEPA, 2003a).

In addition to EPA efforts to establish a federal drinking water standard for perchlorate, several states have already set regulatory limits on perchlorate levels in drinking water that range from 1 ppb to 18 ppb (United States Army, 2002). Additionally, the "Preventing Perchlorate Pollution Act of 2003" was introduced into the House of Representatives on May 15, 2003 and the "Perchlorate Community Right to Know Act of 2003" was introduced into the Senate on April 8, 2003. Both of these bills are aimed at amending the Federal Water Pollution Control Act in order to establish notification guidelines in the event of a perchlorate discharge incident and to document information about perchlorate storage facilities (United States House of Representatives, 2003; United States Senate, 2003). Further, the House Bill amends the Safe Drinking Water Act, requiring EPA to establish a perchlorate maximum contaminant level (MCL) no later than July 1, 2004 (United States House of Representatives, 2003).

Remediating perchlorate-contaminated groundwater is a challenge. First, even though perchlorate reduction is thermodynamically favorable, natural reduction of perchlorate to either chlorate (ClO_3^-) or chloride (Cl^-) is extremely slow due to a large kinetic activation barrier (Urbansky, 1998). Second, the solubility of perchlorate salts is very high (Flowers and Hunt, 2000). The solubility of ammonium perchlorate is 200 g L^{-1}, and the sodium, magnesium, and calcium salts of perchlorate are even more soluble (Flowers and Hunt, 2000). Because of its high solubility, perchlorate is highly mobile. In addition, highly concentrated perchlorate brine is denser than water (Flowers and Hunt, 2000). Due to these properties, it is hypothesized that a dense perchlorate brine solution will behave like a dense non-aqueous phase liquid, DNAPL, traveling rapidly down through an aquifer, eventually pooling on top of, and diffusing into, low permeability confining layers (Flowers and Hunt, 2000). Figure 1.1 illustrates how a surface release of perchlorate may be distributed in the subsurface (Parr, 2003). Particularly note the potential for a large dissolved perchlorate plume to form as flowing groundwater passes through the source area.

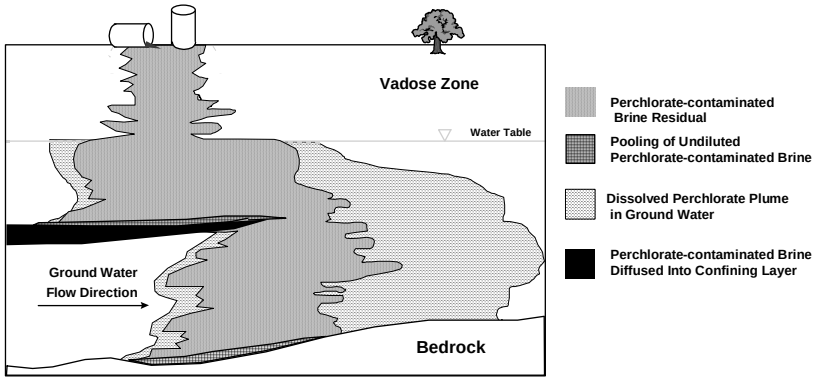

Figure 1.1 Conceptual cross-section of a perchlorate brine source area (Parr *et al.*, 2003)

There are several physicochemical treatment technologies that have been applied *ex situ* to treat perchlorate-contaminated groundwater that has been extracted from the subsurface by pumping wells as part of a "pump-and-treat" remediation strategy. Ion exchange resins have been developed that selectively remove perchlorate from contaminated water. However, waste products (brine or resins) containing concentrated perchlorate must still be treated or disposed of properly (Damien and Pontius, 1999). The same problem of dealing with perchlorate-contaminated residuals also plagues reverse osmosis, another technology that may be applied *ex situ* to treat perchlorate-contaminated water (Giblin *et al.*, 2002). Chemical reduction of the perchlorate ion has been demonstrated by exposing aqueous perchlorate simultaneously to ultraviolet light and metallic iron as well as by exposing perchlorate to metallic iron or iron oxide in the presence of phosphoric acid (Cao *et al.*, 2003; Gurol and Kim, 2000). The cost of pumping groundwater to the surface, along with the risk posed by bringing contaminants to the surface for treatment, are limitations of pump-and-treat technologies. Furthermore, the inability of chemical methods to degrade low-level concentrations of perchlorate (Gurol and Kim, 2000) as well as the nonselective removal of all ions from the water by reverse osmosis (Urbansky and Shock, 1999) may also reduce the usefulness of these technologies.

Bioremediation, using microorganisms to degrade the contaminant, appears to be the most economically feasible, efficient, and safe method of addressing perchlorate-contaminated waters at all concentration levels (Urbansky, 1998). Two strategies for implementing bioremediation are commonly used: *ex situ* bioremediation, which is an

aboveground technology applied as part of a pump-and-treat scheme; and *in situ* bioremediation, where conditions in the subsurface are established so that the contaminant is biodegraded without the need to extract water to the surface for treatment. Several *ex situ* bioremediation technologies have been successfully implemented. A biological fluidized bed reactor has been successfully installed at the Longhorn Army Ammunition Plant in Texas (Polk *et al*., 2002). A packed bed biological reactor has also been shown to degrade perchlorate (Losi *et al*., 2002). However, these *ex situ* systems, as with all pump-and-treat systems, such as those discussed earlier, are limited by high operation and maintenance costs, as well as the risks associated with pumping contaminant to the surface (Cox *et al*., 2000). *In situ* bioremediation, that is, remediation without having to extract contaminated groundwater from the subsurface, is widely believed to be the most promising of the many different treatment technologies currently available (Dupin *et al.*, 2001b).

Most commonly, *in situ* bioremediation involves biostimulation of indigenous microorganisms capable of degrading the contaminant of interest when another compound (either an electron donor or acceptor) is injected into the subsurface and made available to the organisms. *In situ* biodegradation of perchlorate is affected by bacteria that grow and gain energy through reduction of perchlorate, using an injected substrate as a source of electrons and carbon (Cox *et al*., 2000). Through this biochemical reaction, perchlorate is reduced to nontoxic oxygen and chloride (Cox *et al*., 2000). The pathway for the reduction of perchlorate as proposed by Kengen *et al*. (1999) is perchlorate (ClO_4^-) to chlorate (ClO_3^-) to chlorite (ClO_2^-) to chloride (Cl^-) and oxygen (O_2). The first two of

these reductive steps requires the presence of an electron donor, such as acetate, lactate, ethanol, methanol, or some sugar mixture such as molasses (Cox *et al*., 2000). The final step, the dismutation of chlorite to chloride and oxygen, requires an enzyme, chlorite dismutase, and will be discussed in detail in chapter two.

Fortunately, indigenous bacteria capable of reducing perchlorate in the presence of a suitable electron donor appear to be ubiquitous. Current research has identified more than thirty unique strains of naturally occurring bacteria capable of reducing perchlorate to chloride and oxygen in a variety of subsurface environments (Coates *et al*., 1999; SERDP, 2003). As Coates *et al*. (1999) point out, this discovery is quite remarkable given the fact that chlorine oxyanions such as perchlorate are not commonly found in the natural environment and have only been introduced into the ecosystem in the past 100 years through human activities.

An innovative system for *in situ* mixing of substrate into contaminated water and delivery of the mixture to indigenous microorganisms without the need to extract water from the subsurface has been demonstrated by McCarty *et al*. (1998). This system, known as a horizontal flow treatment well (HFTW) system, consists of two dual-screened treatment wells, one pumping water in an upflow direction, the other in a downflow direction (Figure 1.2). As shown in the figure, the two wells work in tandem to mix chemicals into the groundwater flowing through the wells in order to stimulate biodegradation of the contaminant in bioactive zones that form outside the injection screens of the wells. In addition, the wells establish a zone of recirculating groundwater. The groundwater flow

field that results from operation of an HFTW system is shown in Figure 1.3. As seen in the figure, which depicts the flow field induced in the lower part of the aquifer, where the upflow well is an extraction well and the downflow well is an injection well, groundwater recirculates between the downflow and upflow wells. Note that the flow lines shown in Figure 1.3 would be mirrored in the upper part of the aquifer where the downflow well would function as the capture well and the upflow well would act as the injection well. Due to this recirculation, contaminated groundwater passes through the bioactive zones several times. Multiple passes through the bioactive zones increase overall treatment efficiency and is a key advantage of an HFTW system. We see from Figure 1.3 that the HFTW system is meant to serve as a barrier to plume migration. Contaminated water flowing from upgradient is captured by the HFTW system, while water that has been biologically treated in the system moves downgradient. Note that contaminated water is never brought to the surface, as treatment is *in situ*.

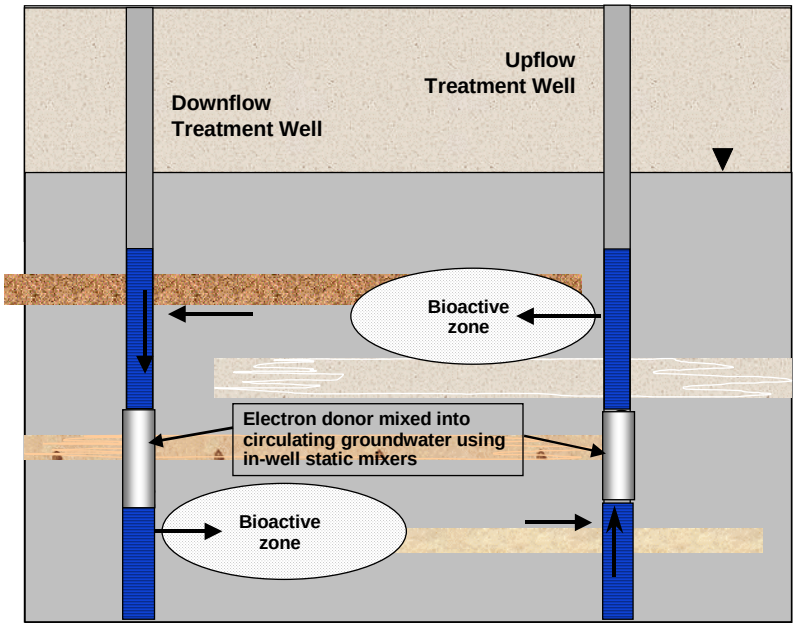

Figure 1.2 HFTW operating concept (Parr *et al.*, 2003)

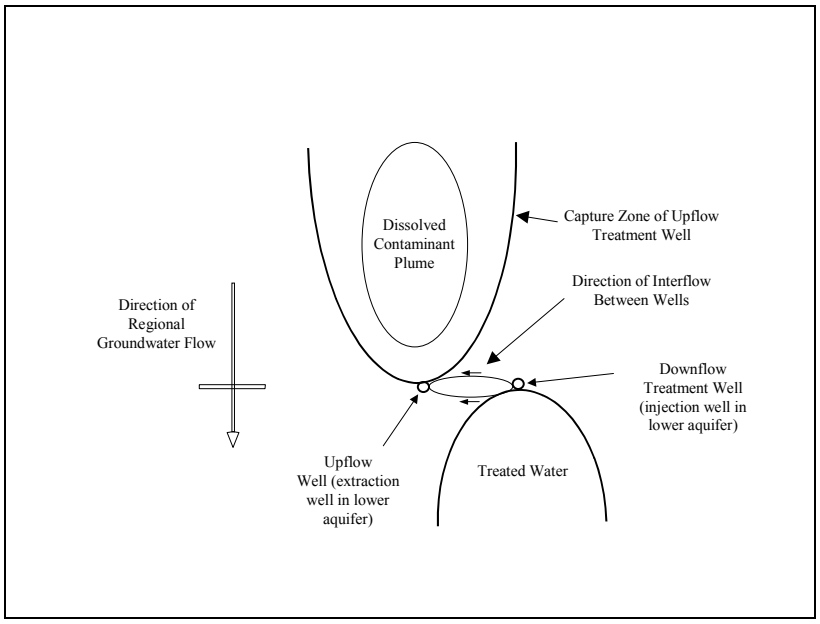

Figure 1.3 Plan view of HFTW treatment area in lower part of aquifer (Parr *et al.*, 2003)

A technology that uses HFTWs to affect *in situ* bioremediation of a subsurface perchlorate plume has been proposed for application at the Aerojet facility near Sacramento CA (Hatzinger, 2001). The technology that is being proposed for application at the Aerojet site has been modeled by Parr *et al.* (2003) who combined a three dimensional subsurface fate and transport model with a model that describes biological degradation of perchlorate. The technology model simulated performance of an HFTW system being used to remediate perchlorate-contaminated groundwater.

The HFTW system provides a practical way of delivering the required electron donor to the subsurface environment in order to stimulate the growth of the indigenous bacteria capable of degrading perchlorate. However, McCarty *et al.* (1998) and Hatzinger (2001) both point out that a major drawback (and area requiring further study) of *in situ* bioremediation technologies is the potential for bioclogging to occur near the injection

screens of the treatment wells. Kildsgaard and Engesgaard (2001) define bioclogging as the increase in biomass to the point where porosity and thus hydraulic conductivity of the medium is affected. The accumulation of biomass decreases the hydraulic conductivity of the soil by clogging pore spaces (Seki and Miyazaki, 2001). When the conductivity of the medium is reduced, it may be difficult to transport the mixture of contaminant and injected substrate to the indigenous microorganisms (Oya and Valocchi, 1998) and treatment efficiency may decrease. *In situ* remediation technologies such as the HFTW system discussed above are particularly subject to this phenomenon since the success of the technology rests upon the stimulation of growth in the bioactive zones near the well injection screens of the very organisms that tend to cause bioclogging. Previous HFTW technology models have not addressed bioclogging (Gandhi *et al.,* 2002b; Parr *et al*., 2003). Because of the importance of bioclogging to the success of *in situ* bioremediation technologies, the University of New Mexico is currently conducting laboratory studies to investigate ways to manage bioclogging. This work is being accomplished as part of the same project that is demonstrating use of the HFTW system to effect bioremediation (Hatzinger 2001).

1.2 RESEARCH OBJECTIVE

The objective of this thesis research is to better understand the potential impact of bioclogging on the ability of the HFTW system to biodegrade perchlorate *in situ*. The following research questions will be answered to achieve this goal.

(1) What biological, chemical, and physical processes affect biomass accumulation in porous media and subsequent bioclogging?

(2) What subsurface conditions influence bioclogging?

(3) How can the relevant physical, chemical, and biological bioclogging processes be modeled?

(4) How does bioclogging impact performance of an HFTW system being used to effect *in situ* perchlorate biodegradation?

1.3 RESEARCH APPROACH

(1) Conduct a literature review to determine the processes that cause bioclogging, the subsurface conditions that promote bioclogging, methods to prevent bioclogging, and techniques to model bioclogging. In order to motivate the research, the literature review will also address health risks posed by perchlorate exposure, environmental effects of perchlorate-contaminated groundwater, updated state and federal regulatory issues pertaining to perchlorate remediation, and current applications of HFTW systems for remediation of other contaminants.

(2) Based on the results of the literature review and the experimental data from the University of New Mexico laboratory studies, develop a submodel that couples microbial growth with hydraulic conductivity reduction, and incorporate this submodel into the technology model developed by Parr *et al*. (2003).

(3) Obtain site characteristics from the Aerojet site and using the modified technology model, predict system performance over a range of operating conditions. Also, propose a system design to be implemented.

1.4 SCOPE AND LIMITATIONS OF RESEARCH

(1) It is assumed that the technology model developed by Parr *et al.* (2003) is a valid representation of the important processes affecting perchlorate and electron donor transport and biodegradation during operation of an HFTW system.

(2) The bioclogging submodel will be developed based upon a review of the literature and experimental data made available from the University of New Mexico studies. No independent laboratory studies will be conducted as part of this research**.**

(3) Validation of the technology model, with the bioclogging submodel incorporated, may not be possible since the results from the Aerojet project will not be available to compare/contrast the field data to the model predictions.

(4) Efforts to optimize the technology model will not be undertaken as part of this study.

2.0 LITERATURE REVIEW

2.1 INTRODUCTION

This chapter briefly reviews the sources and extent of perchlorate-contaminated groundwater, the health and ecological effects associated with perchlorate in groundwater, and the regulatory issues surrounding perchlorate-contaminated groundwater. Following the regulatory issues section, subsequent sections explain the behavior and degradation of perchlorate in the subsurface environment, describe techniques that have been used to engineer *in situ* and *ex situ* perchlorate bioremediation, and outline the concept of operations of a horizontal flow treatment well system to effect *in situ* perchlorate bioremediation.

The final section of this chapter describes in some detail the phenomenon of bioclogging as it relates to the *in situ* biodegradation of perchlorate. After defining bioclogging, the mechanisms by which biological mass grows and accumulates in a porous media are investigated; the conditions which influence bioclogging are reviewed; and several models that have been used to predict the effects of bioclogging on groundwater flow and contaminant transport are examined in detail. Finally, this section concludes with a discussion on ways to prevent bioclogging.

2.2 SOURCES AND EXTENT OF PERCHLORATE CONTAMINTATION

As discussed in the previous chapter, perchlorate contamination of subsurface aquifers is generally attributed to the Department of Defense (DoD) and its contractors, who used perchlorate as a constituent of solid rocket fuel (Urbansky, 1999, 2002). Damien and Pontius (1999) point out that nearly 90% of all perchlorate salts manufactured, primarily in the form of ammonium perchlorate (NH_4ClO_4), are used as oxidizers in propellants for solid rocket motors. To a lesser extent, perchlorate salts are also used in nuclear reactors, electronic tubes, finishing of leather products, explosives, fireworks, and matches (USEPA, 1999a; Hatzinger *et al.*, 2002; Damien and Pontius, 1999). Chilean caliche, a nitrate salt found in Chile, is the only confirmed natural source of perchlorate (Bohlke *et al*., 1997; USEPA, 2001; Urbansky, 2002). The principal pathway by which perchlorate is introduced to the environment is through the process of washing out the residual solid propellant from rocket motors (Damien and Pontius, 1999). This process produces a perchlorate containing waste effluent that in the past was legally disposed of by pouring onto the ground (Damien and Pontius, 1999; Hatzinger *et al*., 2002; Urbansky, 1998).

The extent of perchlorate contamination is still being fully appreciated. An ion chromatographic method capable of detecting perchlorate in water at the 4 μg/L (4 parts per billion) level has been available only since April 1997 (USEPA, 1999a; Damien and Pontius, 1999; Jackson *et al*., 2000, Jackson and Chassaniol, 2002). More recently, Magnuson *et al.* (2000) have developed a mass spectrometry technique, called flow injection electrospray mass spectrometry, with a method detection limit for perchlorate of 100 ng/L (100 parts per trillion).

As a result of these advances in analytical chemistry, perchlorate has recently been detected in the surface and ground water of a number of states: Arizona, Arkansas, California, Iowa, Kansas, Maryland, Nevada, New Mexico, New York, Pennsylvania, Texas, Utah, and West Virginia (USEPA, 1999a; Damien and Pontius, 1999). The shaded states on the following map have confirmed perchlorate releases as of April 2003. The dots on the map represent the locations of the perchlorate releases within each state.

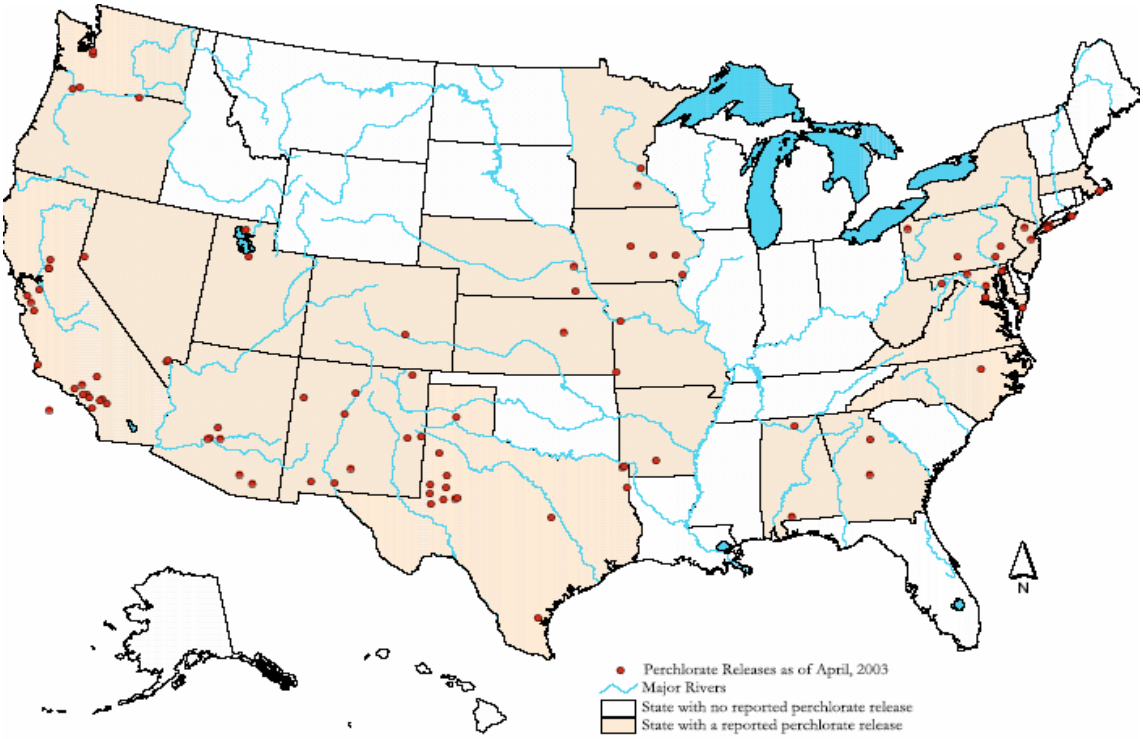

Figure 2.1 Map of U.S. perchlorate releases (USEPA, 2003b)

The perchlorate contamination problem is most pronounced in the western United States where the estimated number of people exposed to perchlorate-contaminated water range from 15 to 18 million in Arizona, California, and Nevada alone (USEPA, 1999a; Strategic Environmental Research and Development Program, 2003).

2.3 HEALTH AND ECOLOGICAL EFECTS

2.3.1 HUMAN HEALTH EFFECTS

Perchlorate has long been known to competitively inhibit iodide uptake by the thyroid gland (Clark, 2000; Wolff, 1998). In fact, because of this effect, the anion was used as a pharmacological treatment for people suffering from hyperactive thyroids, also known as Grave's Disease (Urbansky, 1998; Wolff, 1998). Wolff (1998) points out that the inhibition of thyroid activity is fully reversible; that is, once exposure to the anion ceases, the thyroid resumes normal activity. At first glance, perchlorate does not appear to pose a serious health threat since its effects on the thyroid are reversible. However, several cases of aplastic anemia, suspected to be the result of prescribed perchlorate dosages, eliminated the pharmacological use of the perchlorate anion and demonstrated that adverse health effects of perchlorate could be significant (Wolff, 1998).

Much of the concern regarding perchlorate-contaminated drinking water comes from the potential vulnerability of young children and pregnant women to perchlorate (Pontius *et al.*, 2000; Texas Department of Health, 2002). Pregnant women with critically low levels of iodide, as a result of the competitive inhibition of iodide uptake by perchlorate in their drinking water may miscarry, or the fetus may develop incorrectly due to congenital hypothyroidism (Texas Department of Health, 2002; Urbansky, 1998). This effect is most pronounced during the first two trimesters of pregnancy (Texas Department of Health, 2002). Wolff (1998) points out that perchlorate anions readily cross the

placenta of guinea pigs; he cautions that women exposed to perchlorate in their drinking water may experience reproductive problems. The results of a study conducted on newborns in Arizona by Brechner *et al.* (2000) suggest that an infant's brain function, fine motor skills, speech, vision, and hearing may be negatively impacted by perchlorate contamination, even at low levels (< 10 µg/L).

Several other recently completed studies do not support the hypothesis that subpopulations such as young children and pregnant women are particularly sensitive to perchlorate contamination. The results of studies which used data obtained from the state health departments in California and Nevada do not support the theory that exposure to the perchlorate anion increases the incidence of congenital hypothyroidism (Lamm and Doemland, 1999; Li *et al.*, 2000). Results from a study conducted by Crump *et al.* (2000), which investigated the effects of perchlorate in drinking water on thyroid function in newborns and school-age children in three cities in northern Chile, found no evidence supporting the hypothesis that perchlorate in drinking water at concentrations as high as 120 μg/l (ppb) had an adverse health effect.

2.3.2 ECOLOGICAL EFFECTS

Aside from the potential effects on human health, perchlorate appears to have an effect on the environment. Studies conducted at Texas A&M and Texas Tech (Thuett *et al.*, 2002; Goleman *et al.*, 2002) demonstrate that the perchlorate anion affected the thyroid activity of developing deer mice and South African tree frogs, leading to the hypothesis that perchlorate may pose a threat to the natural growth and development of these and

other species. Perchlorate has also been shown to bioaccumulate within trees such as salt cedar (Urbansky *et al.*, 2000), plankton (Hines *et al.,* 2002), and within the tissue of fish (Hines *et al.*, 2002).

2.4 REGULATORY ISSUES

Regulations pertaining to perchlorate-contaminated groundwater reflect the uncertainty surrounding the human health effects of the perchlorate anion. Currently there is no enforceable National Primary Drinking Water Regulation (NPDWR) for perchlorate under the Safe Drinking Water Act, although the contaminant is included on the EPA's Drinking Water Contaminant Candidate List (CCL) in the section reserved for chemicals needing additional research (Pontius *et al.*, 2000).

The EPA issued interim guidance for perchlorate in 1999 which suggests a provisional clean-up or action level between 4-18 ppb (USEPA, 1999b). The EPA placed emphasis on the lower end of this range in January 2003 (USEPA, 2003a). This range is likely to change upon the finalization of the EPA document, "Perchlorate Environmental Contamination: Toxicological Review and Risk Characterization" (the 2002 Draft Assessment) which is due to be complete sometime in 2003 (USEPA, 2003a).
Legislation has been recently introduced which pertains to the perchlorate contamination problem. On April 8, 2003 the "Perchlorate Community Right-to-Know Act of 2003" was introduced into the United States Senate. According to the legislative search engine, www.thomas.loc.gov, as of March 11, 2004, this bill is being reviewed by the Senate

Committee on Environment and Public Works. This act seeks to amend the Federal Water Pollution Control Act by:

(1) Requiring the EPA to annually publish a list of perchlorate storage facilities beginning on or before June 1, 2005 (United States Senate, 2003).

(2) Establishing notification guidelines in the event of a perchlorate discharge incident (United States Senate, 2003).

(3) Establishing a state loan program through the collection of fines and penalties for the clean-up of perchlorate contaminated water (United States Senate, 2003).

The "Preventing Perchlorate Pollution Act of 2003" was introduced into the United States House of Representatives on May 15, 2003. If passed into law, this bill will amend the Safe Drinking Water Act in order to establish a maximum contaminant level for perchlorate no later than July 1, 2004 (United States House of Representatives, 2003). The "Preventing Perchlorate Pollution Act of 2003" will also amend the Federal Water Pollution Control Act in a manner similar to the Senate Bill.

According to www.thomas.loc.gov, the "Preventing Perchlorate Pollution Act of 2003" has been referred to two committees: the Transportation and Infrastructure Committee and the Energy and Commerce Committee. On May 20, 2003, the bill was referred to the Subcommittee on Water Resources and Environment and the Subcommittee on the Environment and Hazardous Materials, both of these organizations are subcommittees of the Transportation and Infrastructure Committee and the Energy and Commerce

Committee respectively, as of March 11, 2004 there has been no other action taken regarding this legislation.

In addition to actions taken on the federal level, several states have begun to regulate perchlorate. The following table summarizes state perchlorate regulations:

Table 2.1 State perchlorate regulations/guidance (United States Army, 2002; California Department of Health, 2003)

State	Regulation/Guidance Type	Perchlorate Level
California	Action Level	4 ppb
	Draft Public Health Goal	2-6 ppb
Texas	Drinking Water Action Level	4 ppb
	Residential groundwater Cleanup Level	4 ppb
	Industrial/Commercial Groundwater Cleanup Level	7-10 ppb
Arizona	Health Based Guidance Level	14 ppb
New York	Drinking Water Planning Level	5 ppb
	Public Notification Level	18 ppb
New Mexico	Interim Groundwater Screening Level	1 ppb
Nevada	Public Notice Standard	18 ppb

The wide range of state standards and federal "recommendations" pertaining to safe perchlorate exposure levels reflects the current uncertainty regarding the health effects of the perchlorate anion. While the health and ecological effects of perchlorate may still be covered in a veil of uncertainty, the behavior of perchlorate in the subsurface is relatively well understood. A review of this behavior is included in the next section.

2.5 BEHAVIOR IN THE SUBSURFACE ENVIRONMENT

2.5.1 PHYSICAL BEHAVIOR

In chapter one, the analogy was made between a perchlorate source area and a DNAPL source area. The reader is referred to Figure 1.1 for a graphical illustration of how a surface release of perchlorate may be distributed through the subsurface. Perchlorate may be emplaced in low conductivity layers and diffuse into the passing groundwater (Flowers and Hunt, 2000). The mass transfer limitations of diffusive transport into the flowing groundwater indicate that these source areas have the potential to contaminate resident groundwater for approximately a century (Flowers and Hunt, 2000). While the need to locate source areas is obvious, doing so can be difficult due to geological heterogeneities and inaccurate perchlorate disposal records maintained by industry. The inherent difficulty associated with locating and remediating source areas of perchlorate contamination points to the need to develop a cost effective, efficient, and safe method of controlling the perchlorate containing groundwater plume that emanates from the source area.

Perchlorate contamination in the subsurface environment poses many remediation challenges because of the anion's behavior. Experiments have shown that perchlorate does not adsorb well to soil particles (Tipton *et al*., 2003). Additionally, the salts of perchlorate are very soluble as Table 2.2 suggests, resulting in high perchlorate anion mobility in the subsurface environment.

Table 2.2 Solubility of perchlorate containing compounds (@25°C)

Compound	Solubility (g/L)	Reference
Lithium Perchlorate $LiClO_4$	474.15	Linke (1965)
Sodium Perchlorate $NaClO_4$	1,141.41	Linke (1965)
Potassium Perchlorate $KClO_4$	20.49	Linke (1965)
Rubidium Perchlorate $RbClO_4$	13.28	Linke (1965)
Beryllium Perchlorate $Be(ClO_4)_2$	595.00	Linke (1958)
Magnesium Perchlorate $Mg(ClO_4)_2$	1,000.00	Linke (1965)
Calcium Perchlorate $Ca(ClO_4)_2$	653.5	Linke (1958)

The high solubility of perchlorate salts is a result of the anion's structure. The perchlorate anion has a tetrahydral shape with a large volume and a highly delocalized charge (Urbansky, 1998; 2002). In the case of an anion, this indicates that no area of the molecule preferentially attracts the negatively charged electron. Urbansky (1998) indicates that the reduced charge density of the perchlorate anion results in a reduced affinity for positively charged cations; this reduced affinity is responsible for the high solubility of the various perchlorate salts in aqueous and non-aqueous liquids.

2.5.2 CHEMICAL BEHAVIOR

The reduction of perchlorate to less toxic substances such as chloride and molecular oxygen is thermodynamically favorable, as the positive values of the reduction potentials for the following equations indicate (Emsley, 1989):

$$ClO_4^- + 8\,H^+ + 8\,e^- \Leftrightarrow Cl^- + 4\,H_2O \quad E^o = 1.287\ V \qquad (2.1)$$

$$ClO_4^- + 2\,H^+ + 2\,e^- \Leftrightarrow ClO_3^- + H_2O \quad E^o = 1.201\ V \qquad (2.2)$$

Given these thermodynamics and the solubility of perchlorate salts, one would expect perchlorate to rapidly be reduced in the natural environment. However, although thermodynamics define the realm of possible reaction, kinetics define what actually happens. In the case of perchlorate reduction, a large kinetic barrier exists that prevents the energetically favorable reduction of perchlorate (Urbansky, 1998).

Urbansky and Schock (1999) attribute this kinetic barrier to the fact that the initial step in the reduction of perchlorate must occur via oxygen atom abstraction rather than direct involvement of the central chlorine atom. The strength of the chlorine-oxygen bond is reflected in the height of E_a, the activation energy that is required for the reduction of ClO_4^- to ClO_3^- in Figure 2.2. In this figure, ΔE is the change in energy states between the reactants and the products, "R" represents a reducing agent or electron donor, and "RO" is the reducing agent with the attached oxygen atom from the perchlorate anion (Urbansky and Schock, 1999).

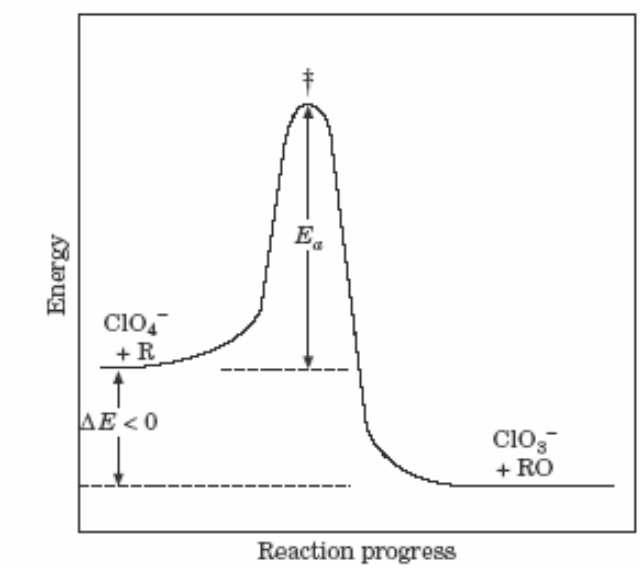

Figure 2.2 Kinetic barrier to perchlorate reduction (Urbansky and Shock, 1999)

As Urbansky (1998) points out, it is fortunate that perchlorate is stable in the subsurface environment due to kinetics rather than thermodynamics, as a kinetic barrier can always be overcome; the challenge is to find a method that will allow the reaction to proceed through the barrier (Urbansky, 1998). Kinetic barriers are often overcome by the addition of energy to the system in the form of heat or light (Gurol and Kim, 2000). The presence of a chemical catalyst can also serve to reduce the activation barrier and increase the reaction rate (Urbansky, 1998; Gurol and Kim, 2000; Moore *et al*., 2003). While research into the chemical catalysis of perchlorate reduction is ongoing, recent findings have shown that the reaction rate is too slow under environmental conditions, or the associated cost of implementing the technology at the field scale may be prohibitively expensive (Urbansky, 1998; Gurol and Kim, 2000; Parr, 2002; Moore *et al*., 2003; Cao *et al.*, 2003). Additionally, some chemical methods are unable to reduce low-level perchlorate concentrations (<200 ppb) (Gurol and Kim, 2000). Another possible way to overcome the kinetic activation energy barrier, the degradation of perchlorate via the metabolic activities of microorganisms, will be discussed next.

2.5.3 BIODEGRADATION OF PERCHLORATE

The pathway for the biologically mediated reduction of perchlorate as proposed by Rikken *et al*. (1996) and reported by Kengen *et al*. (1999) and Cox *et al*. (2000) is as follows:

$$(ClO_4^-) \Rightarrow (ClO_3^-) \Rightarrow (ClO_2^-) \Rightarrow (Cl^-) \text{ and } (O_2) \qquad (2.3)$$

The first and second steps in this pathway, the reduction of perchlorate to chlorate and chlorate to chlorite, require the presence of an electron donor, such as acetate, lactate,

ethanol, methanol, or some sugar mixture such as molasses (Cox *et al*., 2000) along with the enzyme, (per)chlorate reductase, to catalyze the reactions (Kengen, *et al*., 1999). The reduction of perchlorate to chlorite via chlorate produces water, carbon dioxide, and energy used by the organism for growth and cellular maintenance (Rikken *et al*., 1996). The final step in the pathway, the dismutation, or breaking apart, of the chlorite ion to molecular oxygen and chloride is accomplished through catalysis by the chlorite dismutase enzyme (Kengen *et al*., 1999; Cox *et al*., 2000). This reaction does not yield a substantial amount of energy and is postulated to occur as a mechanism to degrade chlorite, which is toxic to most perchlorate-degrading bacteria (Rikken *et al*., 1996; Kengen *et al*., 1999; Logan, 2001a).

The following table presents four microbially mediated redox reactions and the associated Gibbs free energy change where an electron donor (also referred to as the reductant or reducing agent), in this case ethanol, reduces oxygen, nitrate, or perchlorate which act as electron acceptors (also known as the oxidant or oxidizing agent).

Table 2.3 Gibbs free energy changes for ethanol oxidation using oxygen, nitrate and perchlorate as electron acceptors

Stoichiometric Reaction	ΔG^o (kJ/mol ethanol)
$C_2H_6O + 3O_2 \Rightarrow 2CO_2 + 3H_2O$	-1333
$5C_2H_6O + 12\ NO_3^- + 12H^+ \Rightarrow 10CO_2 + 21H_2O + 6N_2$	-6752
$2C_2H_6O + 3ClO_4^- \Rightarrow 4CO_2 + 3Cl^- + 6H_2O$	-3034
$C_2H_6O + 3ClO_4^- \Rightarrow 2CO_2 + 3ClO_2^- + 3H_2O$	-1256
$ClO_2^- \Rightarrow Cl^- + O_2$	-148.2

The Gibb's free energy of formation values used to calculate the above ΔG^o values were obtained from the 84th Edition of the CRC Handbook of Chemistry and Physics (CRC,

2003). Table 2.3 is relevant to the present work as it shows that the complete reduction of perchlorate (ClO_4^-) to chloride (Cl^-) is thermodynamically more favorable than the aerobic oxidation of ethanol. It would appear then, that the degradation of perchlorate should naturally occur in the subsurface environment assuming that there is an abundance of ethanol present.

However, other investigations into the microbially mediated reduction of perchlorate indicate that oxygen is preferentially used as an electron acceptor (Parr *et al*., 2003; Chaudhuri *et al*., 2002; Tipton *et al*., 2003). The free energy values listed in Table 2.3 support this empirical evidence. The second to last stoichiometric equation in Table 2.3, which represents the proposed pathway of microbial perchlorate degradation, indicates that the incomplete reduction of perchlorate to chlorite, which is then dissmutated, is less energetically favorable than aerobic oxidation of ethanol. Therefore, bacteria will preferentially use oxygen as an electron acceptor when it is available, leaving perchlorate relatively untouched (Coates *et al*., 2000; Chaudhuri *et al*., 2002).

Experimental evidence indicates that nitrate is also preferred over perchlorate as an electron acceptor by some, though not all, perchlorate-reducing bacteria (Giblin *et al*., 2000; Chaudhuri *et al*., 2002). This observation is reflected in Table 2.3 where we see that the magnitude of the Gibbs free energy change for perchlorate reduction to chlorite or chloride is much smaller than the free energy change of nitrate reduction to molecular nitrogen, indicating that nitrogen is the preferred electron acceptor. The values shown in Table 2.3 also indicate that nitrogen is the energetically preferred electron acceptor

compared to oxygen. The studies of Chaudhuri *et al*. (2002) contradict this observation; however, acetate was used as the electron donor in this study.

The extent of natural perchlorate biodegradation depends upon site specific parameters such as the prevalent subsurface environmental conditions and the indigenous microbial population (Maier *et al*., 2000). The presence of nitrate and oxygen, which, as discussed above, compete with perchlorate for electrons, is an important factor that directly impacts whether or not perchlorate will be reduced (Coates *et al*., 2000; Chaudhuri *et al*., 2002). However, Xu *et al*. (2003) postulate that the greatest impact of the presence of oxygen and nitrate on perchlorate bioremediation may be to increase the requirement for electron donor.

To date, researchers have isolated more than thirty different strains of perchlorate reducing bacteria (O'Connor and Coates, 1999; SERDP, 2003). Parr (2002) provides an exhaustive review of bacterial strains capable of degrading perchlorate and the conditions favorable to their growth. Bacteria capable of using perchlorate in metabolic processes have been identified in environments as diverse as pristine soils, soils contaminated with hydrocarbons, aquatic sediments, farm animal waste lagoons, and paper mill waste sludge (Coates *et al*., 1999; Coates *et al*., 2000; Michaelidou *et al*., 2000). Studies have shown that environments previously contaminated with perchlorate have a higher number of perchlorate-respiring microorganisms than environments that were never exposed to the anion (Tipton *et al*., 2003; Wu *et al*., 2001). Techniques have recently been developed to determine the presence of these bacteria in the subsurface environment (O'Connor and

Coates, 2002; Bender *et al*., 2002; Xu and Logan, 2003; Coleman *et al*., 2003; Sturchio *et al*., 2003).

The elucidation of the environmental conditions which impact perchlorate reduction, uncovering the metabolic pathway for perchlorate degradation, and developing methods to determine the presence and activity of perchlorate respiring organisms have opened the door for the development of several technologies which take advantage of engineered biological technologies to remediate perchlorate-contaminated groundwater. These technologies are discussed next.

2.6 BIOREMEDIATION OF PERCHLORATE

The use of bacteria capable of producing enzymes which lower the kinetic barrier to perchlorate reduction is thought to be the most practical way of addressing the perchlorate contamination problem (Urbansky, 1998). The bioremediation of perchlorate can be separated into two broad categories of treatment, *ex situ* and *in situ*. As was stated earlier, *ex situ* treatment takes place above ground while *in situ* treatment occurs in the subsurface environment. This section will provide a review of the *ex situ* and *in situ* biological treatment options currently available and their applications to date at different perchlorate-contaminated sites.

2.6.1 *EX SITU* BIOREMEDIATION TREATMENT TECHNIQUES

Ex situ biological treatment technologies generally require that perchlorate-contaminated groundwater be pumped into an above bioreactor that contains a consortium of

perchlorate-reducing bacteria (AFCEE, 2002a). Bioreactors are distinguished by how the perchlorate-degrading bacteria grow within the reactor vessel (Logan, 2000). Suspended cell reactors maintain the bacterial population in the water, while fixed film reactors provide the bacteria with a surface upon which they can attach themselves and grow (Logan, 2000). The following table summarizes the different categories of bioreactors.

Table 2.4 Common bioreactor designs (Logan, 2000)

Suspended Cell Reactors	Fixed Film Reactors
Completely mixed reactor: Continuously Stirred Tank Reactor (CSTR)	Packed bed-saturated flow: Trickling Filter
Activated Sludge: Either CSTR or Plug Flow Reactor (PFR)	Packed bed-unsaturated flow: PFR
Up-flow anaerobic sludge blanket: PFR	Fluidized bed: CSTR

According to calculations carried out by Logan (2000), suspended cell bioreactors may not be adequate for groundwater remediation purposes because the detention times required to degrade influent water with low-level perchlorate concentrations would be too long. Losi *et al*. (2002) concurred with this assessment in a subsequent study. Therefore, only fixed film bioreactors will be discussed here.

Packed bed bioreactors, also referred to as fixed bed bioreactors, provide the microorganisms with an immobile growth platform, typically sand, plastic media, granular activated carbon (GAC), or some other solid which provides a large surface area

(Logan, 2001b). Packed bed bioreactors are operated in both saturated and unsaturated flow configurations.

2.6.1.1 SATURATED FLOW PACKED BED REACTORS

Saturated flow packed bed bioreactors have been widely studied. Figure 2.3 illustrates the saturated flow packed bed bioreactor concept. Acetate, perchlorate and a phosphate buffer were combined in the mixer and pumped upwards through the granular activated carbon (GAC) bed (Kim and Logan, 2000). The vertical numbers represent sampling ports used to monitor the concentration of perchlorate, chlorate, chloride and acetate (Kim and Logan, 2000). In their study, Kim and Logan (2000) demonstrated that GAC, or any other perchlorate absorbing material, should not be used as a support medium in packed bed bioreactors because desorbing perchlorate can increase effluent concentrations after the system is backwashed.

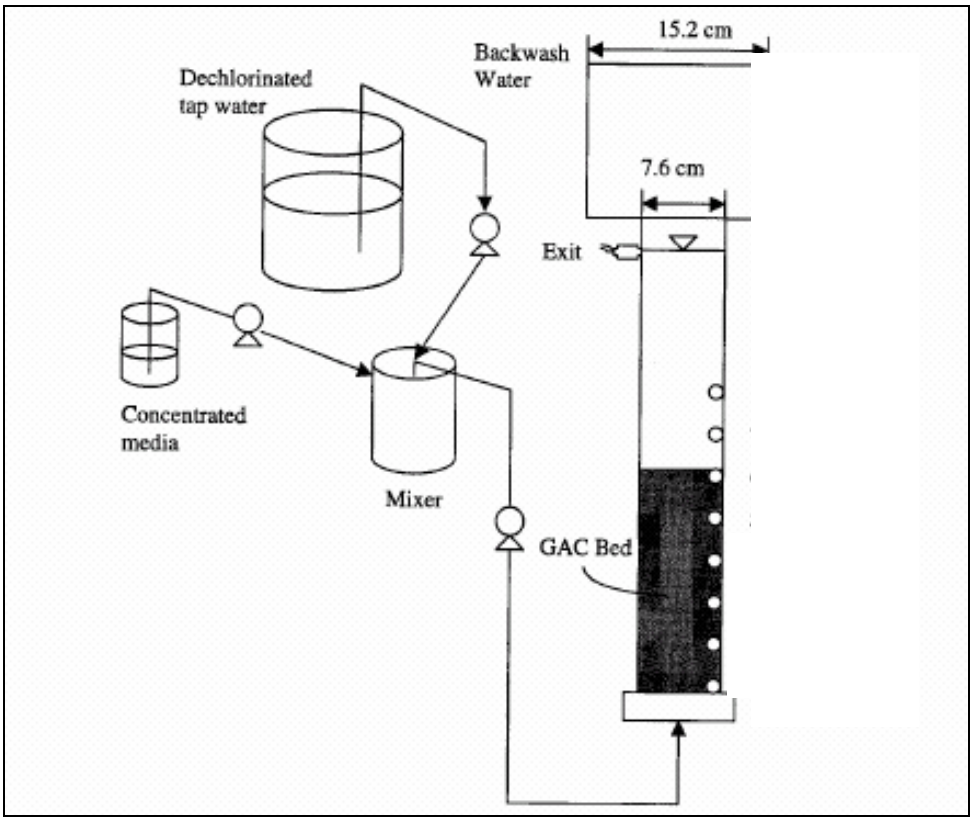

Figure 2.3 Bench scale packed bed reactor schematic (Kim and Logan, 2000).

A bench scale packed bed bioreactor that used Celite (R-635) as a growth platform and acetate as the electron donor was shown to be capable of degrading influent perchlorate concentrations of 800 ppb to less than 4 ppb (Losi *et al*., 2002). In a similar study, Giblin *et al*. (2002) demonstrated that the same packed bed bioreactor setup was capable of reducing perchlorate concentrations in secondary reverse osmosis rejectate from 5 ppm to less than 4ppb. Similar experiments conducted by Logan *et al*. (2001) using a pure culture and a mixed consortium of perchlorate-reducing bacteria suggest that perchlorate degradation rates in packed bed biological reactors are highly correlated with the log-mean perchlorate concentration within the reactor. Giblin *et al*. (2000) used a bench-scale, saturated flow, packed bed bioreactor to demonstrate for the first time that an

autotrophic, that is, hydrogen oxidizing, consortium of bacteria was capable of perchlorate reduction.

2.6.1.2 UNSATURATED FLOW PACKED BED REACTORS

Unsaturated flow packed bed bioreactors are also being tested. These studies focus on the use of gas-phase hydrogen as an electron donor (Miller and Logan, 2000; Logan and LaPoint, 2002). Figure 2.4 depicts the apparatus used by Logan and LaPoint (2002) to investigate the potential of using gas phase hydrogen as a reductant.

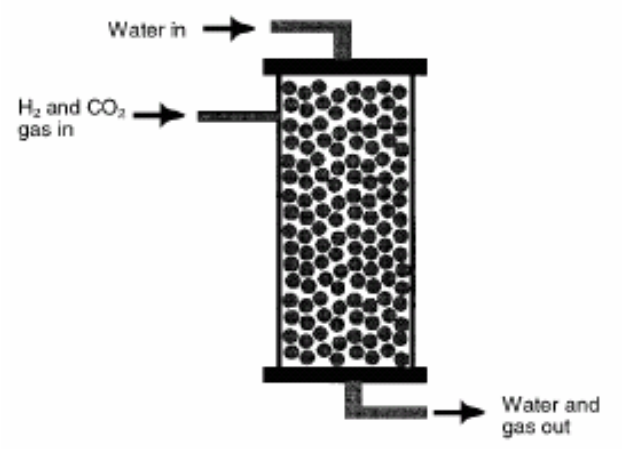

Figure 2.4 Unsaturated, packed bed bioreactor (Miller and Logan, 2000).

Unlike saturated packed bed bioreactors where the groundwater is pumped up through the column, unsaturated flow packed bed bioreactors introduce the influent at the top of the column. The groundwater is then exposed to gas phase hydrogen just prior to entering the packed bed. Finally, the treated groundwater exits the system through the bottom of the column.

Using hydrogen in lieu of other electron donors such as acetate or ethanol has several advantages. First, in drinking water applications, organic electron donors that are added in lieu of hydrogen may remain in the effluent, thereby allowing biological growth in downstream distribution systems (Miller and Logan, 2000; Logan 2001a). Second, chlorinated aliphatic pollutants such as PCE, can be reductively dehalogenated by microorganisms in the presence of aqueous phase hydrogen (Miller and Logan, 2000). Finally, perchlorate degradation by hydrogen oxidizing bacteria has been shown to be uninhibited by the presence of dissolved nitrate in some studies, an observation first reported by Giblin *et al*. (2000) and confirmed by Logan and LaPoint (2002). Research involving packed bed, unsaturated flow bioreactors has shown that the rate of perchlorate degradation is similar to the rates obtained from other bioreactor configurations (Logan and LaPoint, 2002).

Packed bed bioreactors, in both saturated and unsaturated configurations, have primarily been developed at the bench scale for use in laboratory studies (Hatzinger *et al*., 2002). However, a pilot scale packed bed saturated flow reactor has been constructed in Redlands, California (Evans *et al*., 2002). This bioreactor is seven feet tall, has a two square foot cross sectional area, and was shown capable of reducing perchlorate levels from 75 ppb influent to under 4 ppb at a rate of 1 gallon per minute (Evans *et al*., 2002). Typically, though, fluidized bed bioreactors, rather than packed beds, have been implemented at field scale. The primary drawback of packed bed bioreactors is the potential of clogging and channeling to occur, especially near the inlet of the vessel, due to the growth and accumulation of biomass, commonly referred to as bioclogging

(Hatzinger *et al*., 2002; Logan, 2000; Logan, 2001a). Several studies describe the need to periodically backwash the packed column with either water or air in order to remove accumulated biomass and restore the original hydraulic characteristics of the column (Kim and Logan, 2000; Miller and Logan, 2000; Evans *et al*., 2002). On the other hand, Hatzinger *et al*. (2002) contend that the growth media within the bioreactor must be completely replaced if clogging occurs because backwashing techniques are inefficient. The cost of developing an efficient mechanism for dealing with clogging in packed bed bioreactors is probably the primary reason that so few field scale evaluations of the technology have occurred to date. More information regarding the phenomenon of bioclogging is provided in the last section of this chapter. The next subsection discusses several fluidized bed field-scale applications, along with a description of the how fluidized bed bioreactors work.

2.6.1.3 FLUIDIZED BED REACTORS

Fluidized bed biological reactors are reactors that rely on microorganisms grown on a hydraulically fluidized bed of particles to degrade the target compound (Togna *et al*., 2001; Polk *et al*., 2002; Hatzinger *et al*., 2002). Fluidization is maintained through injection of influent water into the bottom of the reactor vessel at high velocity, resulting in a well mixed system (Urbansky and Schock, 1999; Togna *et al*., 2001; Logan, 2000). As the influent moves upwards in the reactor, velocity slows due to the increasing cross-sectional area (see Figure 2.5). This velocity reduction allows the growth media and microorganisms to settle out before the effluent leaves the system (Urbansky and Schock, 1999).

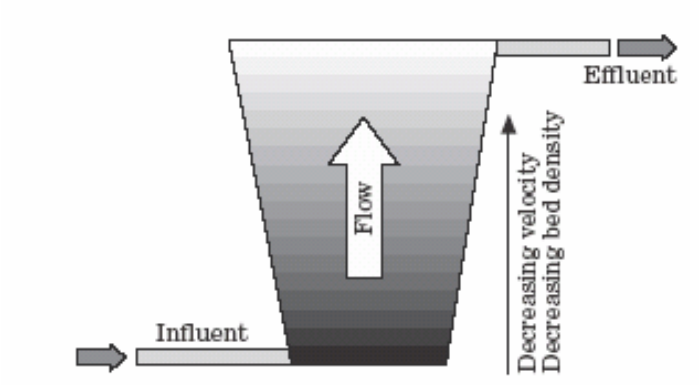

Figure 2.5 Fluidized bed bioreactor schematic (Urbansky and Schock, 1999)

Fluidized bed bioreactors have been in operation at the field scale for several years. In 1998, engineers from Envirogen and USFilter Envirex Products installed four, 4.27 m diameter fluidized bed reactors at the Aerojet Superfund Site in Rancho Cordova, California (Greene and Pitre, 2000; AFCEE, 2002a; Hatzinger *et al*., 2002). Working in unison, these bioreactors are capable of degrading groundwater with a perchlorate concentration of approximately 3,500 ppb to below the detection limit of 4 ppb at a rate above 3,000 gallons-per-minute (gpm) (Hatzinger *et al*., 2002; Greene and Pitre, 2000).

The first DoD installation to utilize a fluidized bed bioreactor to remediate perchlorate was the Longhorn Army Ammunition Plant (LHAAP) in Karnack, Texas (AFCEE, 2002a; Hatzinger *et al*., 2002; Polk *et al*., 2002; Togna *et al*., 2001). This system has the capacity to treat 50 gpm of groundwater to below the 4 ppb analytical detection limit (AFCEE, 2002a; Hatzinger *et al*., 2002; Polk *et al*., 2002; Togna *et al*., 2001).

The promising results from the field scale demonstrations discussed above have led environmental regulators to accept fluidized bed bioreactors as a perchlorate remediation option. In fact, the California Department of Health Services has recently granted approval for the use of fluidized bed technology to treat perchlorate-contaminated water for drinking water use (CDHS, 2002). Nevertheless, fluidized bed bioreactors have limits and drawbacks. First, fluidized bed biological reactors suffer from the high cost of pumping groundwater at accelerated flow rates in order to maintain fluidization of the media (Logan, 2001b). Fluidized bed bioreactors designed to degrade perchlorate contaminated groundwater also have low cellular growth and reaction rates because the bulk perchlorate concentration within the reactor must be as low as or lower than the desired effluent perchlorate concentration (4-18 ppb) (Logan, 2000).

These drawbacks are in addition to the general limitations of all *ex situ* treatment options. That is, *ex situ* treatment technologies are hampered by high costs as well as the health and safety risks associated with pumping contaminated groundwater to the surface (Cox, *et al*., 2000). *In situ* or "in-place" technologies reduce these costs and risks by eliminating the requirement for aboveground treatment. Several *in situ* remediation techniques which exploit biological metabolic pathways to degrade perchlorate will be discussed in the next section.

2.6.2 *IN SITU* BIOREMEDIATION TREATMENT OPTIONS

In situ biotreatment technologies can be broadly categorized as either bioaugmentation or biostimulation strategies. *In situ* bioaugmentation involves the addition of non-native

microorganisms to the subsurface in order to enhance the biodegradation of the target contaminant. Bioaugmentation is a difficult strategy to implement, as non-native microorganisms are often unable to establish a niche in the contaminated environment and do not survive long after introduction (Maier *et al*., 2000) even though bioaugmentation techniques have been successfully used for chlorinated aliphatic compounds such as trichloroethelyne (TCE) (Ellis *et al*., 2000). Fortunately, as stated earlier in this chapter, perchlorate-respiring bacteria have been found in a variety of subsurface environments. Since perchlorate-reducing bacteria are typically present in the subsurface, bioaugmentation strategies are probably not required, and therefore, for the purposes of this study, we will focus on *in situ* biostimulation.

In situ biostimulation strategies require the addition of either an electron donor, electron acceptor, and or other nutrients to the subsurface to promote the growth of indigenous bacterial populations. We will now review three methods of effecting *in situ* biodegradation via biostimulation: permeable reactive biobarriers (PRB), groundwater extraction-injection systems, and horizontal flow treatment wells (HFTWs).

2.6.2.1 PERMEABLE REACTIVE BARRIERS (PRB)

Permeable reactive barriers are engineered regions within the subsurface that contain a reactive material to chemically or biologically degrade a target contaminant (AFCEE, 2002b). Permeable reactive barriers consist of trenches which are dug perpendicular to the direction of groundwater flow and backfilled with reactive material (AFCEE, 2002b). To effect perchlorate biological reduction, permeable reactive barriers consist of gravel

and sources of electron donor, typically organic material such as compost (Perlmutter *et al*., 2000; AFCEE, 2002b). Figure 2.5 shows a conceptual installation of a permeable reactive barrier.

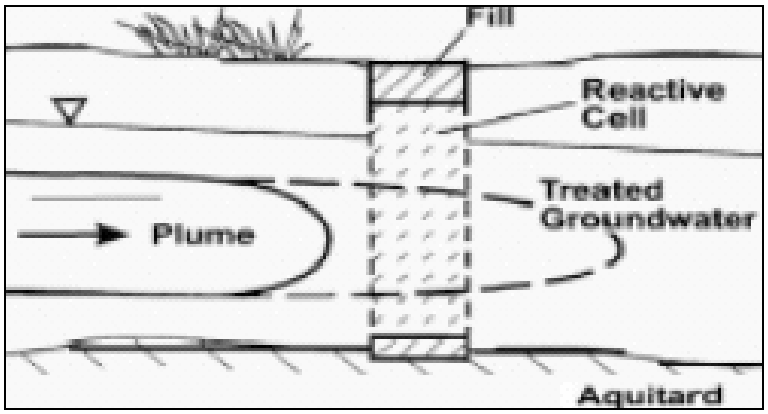

Figure 2.6 Permeable reactive barrier concept (AFCEE, 2002b)

The DoD has effectively used PRB technology to degrade perchlorate contaminated groundwater at the inactive Naval Weapons Industrial Reserve Plant McGregor near Waco, Texas (AFCEE, 2002b; Perlmutter *et al*., 2000; Logan, 2001). In this full-scale field demonstration, approximately a mile of 25 foot deep trench was dug perpendicular to the regional groundwater flow (AFCEE, 2002b). The trench, which was backfilled with gravel and organic amendments, successfully reduced perchlorate concentrations 90% from 27,000 ppb. In addition, TCE and nitrate, which were also present, were co-reduced to below detection limits (AFCEE, 2002b; Perlmutter *et al*., 2000; Logan, 2001). Another example of PRB application for perchlorate remediation is the multi-layer permeable reactive barrier being developed for the remediation of a shallow groundwater aquifer contaminated with radionuclides, metals, nitrate, and perchlorate at the Los Alamos National Laboratory (Taylor *et al*., 2002). Perchlorate reduction is accomplished

in this layered system by providing an Apatite II layer to act as an electron donor followed by a layer of pecan shells which serve as a growth surface for perchlorate reducing bacteria (Taylor *et al*., 2002).

While particularly appealing for shallow aquifer remediation, PRB technology is not generally applicable or cost effective for deep aquifer remediation (Hatzinger *et al*., 2002). Additionally, as a passive remediation technology, permeable reactive barriers are susceptible to being bypassed by contaminants when environmental conditions, such as groundwater flow rate or flow direction, change. Fortunately, other *in situ* technologies may be appropriate for promoting biodegradation of perchlorate in deep aquifers; these technologies will be discussed next.

2.6.2.2 EXTRACTION-INJECTION SYSTEMS

The extraction-injection method of *in situ* bioremediation involves pumping the perchlorate-contaminated groundwater to the surface, mixing in an electron donor, and then re-injecting the mixture back into the aquifer (McMaster, *et al*., 2001; Hatzinger *et al*., 2002). In May 2000, the first phase of a pilot scale demonstration of this technology was performed at the Aerojet site (Area 20) in Rancho Cordova, California (McMaster, *et al*., 2001; Hatzinger *et al*., 2002). In this study, perchlorate concentrations declined from 12,000 ppb to less than 4 ppb within fifteen feet of the injection well when acetate or lactate was used as the electron donor (McMaster, *et al*., 2001; Hatzinger *et al*., 2002; GeoSyntec Consultants, 2002a; 2002b). Additionally, nitrate was reduced within the pilot test area, while sulfate reduction did not occur (McMaster *et al*., 2001). The

following figure shows the rapid reduction of perchlorate at two monitoring wells located 15 feet and 35 feet away from the electron donor injection well (GeoSyntec Consultants, 2002a).

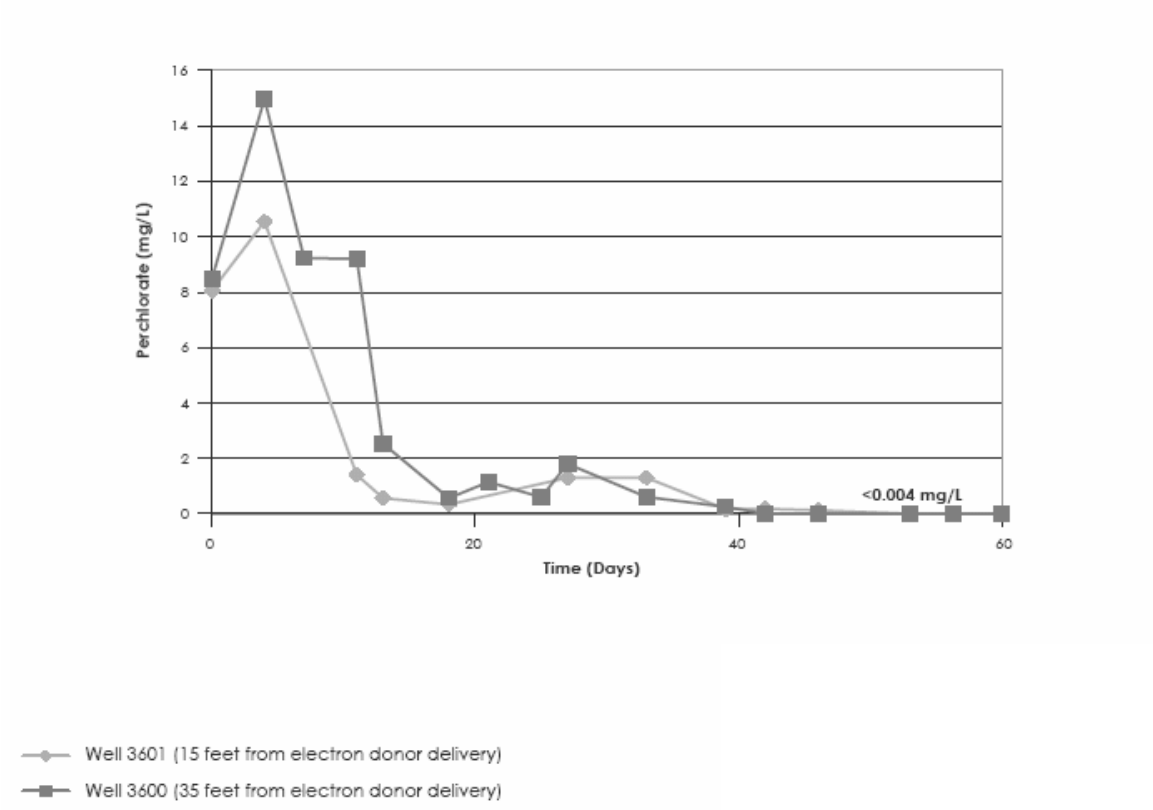

Figure 2.7 Phase 1 perchlorate reduction at Aerojet Area 20 site (GeoSyntec Consultants, 2002a)

As a second phase to the Aerojet Area 20 pilot scale field demonstration, groundwater from two extraction wells was mixed with ethanol and injected back into the aquifer through a single recharge well. The following schematic provides a plan view of the second phase of the pilot study.

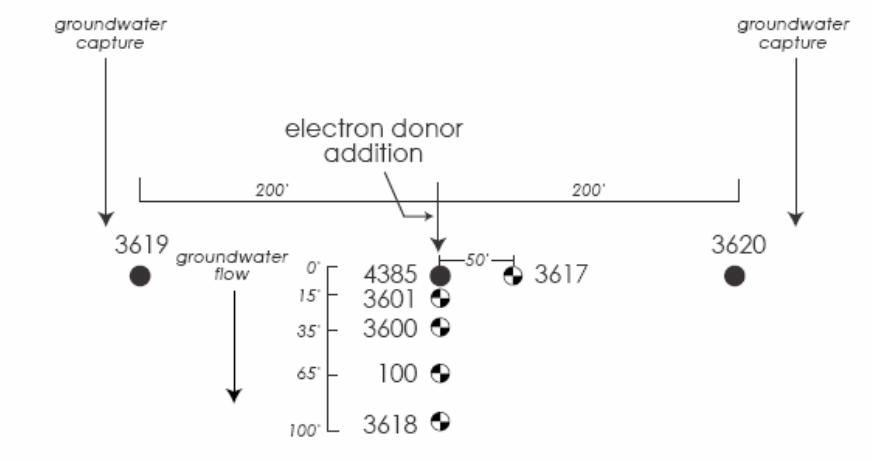

Figure 2.8 Plan view of phase 2 of Aerojet Area 20 pilot study (GeoSyntec Consultants, 2002a, 2002b)

Groundwater is pumped from well 3619 and 3620, amended with ethanol and reinjected into the aquifer via recharge well 4385. Initial data from this study indicate that perchlorate concentrations are reduced from 8,000 ppb to 4 ppb within thirty-five feet of the recharge well (Hatzinger *et al*., 2002; GeoSyntec Consultants, 2002a, 2002b). The following figure illustrates the decrease in perchlorate concentration observed at the various downstream monitoring wells.

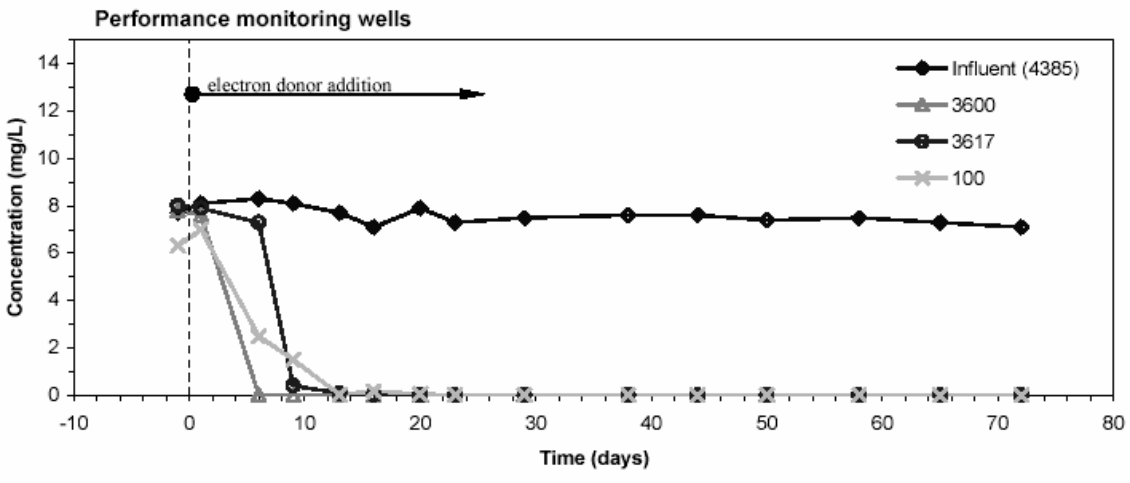

Figure 2.9 Phase 2 perchlorate reduction at Aerojet Area 20 site (GeoSyntec Consultants, 2002b)

GeoSyntec Consultants also conducted pilot extraction-injection *in situ* bioremediation studies at the Groundwater Extraction and Treatment Facility D (GET D) at the Aerojet facility in Rancho Cordova, California (GeoSyntec Consultants, 2002a). The location of GET D study and the Area 20 projects in relation to the HFTW demonstration site is shown in Figure 3.1. The GET D studies were similar to those conducted in the phase one testing at the Aerojet Area 20 site. The GET D facility is comprised of 25 extraction wells and 6 recharge wells; the facility is designed to remove volatile organic carbon compounds such as TCE via air stripping (GeoSyntec Consultants, 2002a). This pilot study consisted of adding an electron donor delivery system at various recharge wells in order to effect *in situ* perchlorate biodegradation. In addition to the donor delivery system, monitoring wells were installed downstream of the recharge wells as part of the study. Key results of this pilot study include: (1) addition of electron donor by low concentration, long duration pulses can limit the amount of manganese and iron that is reduced and consequently mobilized, (2) ethanol and citric acid appear to be more cost effective electron donors, and (3) biofouling of recharge wells is a significant challenge that must be overcome in order for *in situ* bioremediation of perchlorate to be successful. A more detailed discussion of biofouling, also known as bioclogging, is contained in latter portions of this work.

While the results of extraction-injection systems used for *in situ* perchlorate biodegradation have been favorable, the technology suffers from many of the same drawbacks as *ex situ* treatment technologies. While extraction-injection systems avoid the costs associated with the construction of an aboveground treatment system,

groundwater must still be pumped to the surface and injected back into the aquifer. The costs associated with extracting and injecting groundwater from deep aquifers (>100 ft) can be a significant portion of the remediation project budget (Hatzinger *et al*., 2002). Given that many of the perchlorate contaminated aquifers in the western United States are anywhere from 100 to 700 feet below ground, any technology that relies upon pumping contaminated water to the surface may be prohibitively expensive (Hatzinger *et al*., 2002). The next *in situ* bioremediation technology to be discussed, horizontal flow treatment wells, eliminates the need to bring groundwater to the surface in order to promote perchlorate biodegradation through the addition of an electron donor.

2.6.2.3 HORIZONTAL FLOW TREATMENT WELLS (HFTWs)

An HFTW system consists of a pair of dual screened treatment wells pumping in opposite directions in order to create a zone of recirculating groundwater (McCarty *et al*., 1998; Gandhi *et al*., 2002a; Gandhi *et al*., 2002b; Parr *et al*., 2003; Munakata *et al*., 2002). The reader is referred to Figure 1.2 and Figure 1.3 of Chapter 1 for a schematic of the HFTW concept. HFTW systems allow electron donor and other nutrients to be added within the treatment wells without the need to bring contaminated groundwater to the surface, a feature especially suited for the treatment of perchlorate and other contaminants in deep aquifers (Hatzinger et al., 2002; McCarty *et al*., 1998; Gandhi *et al*., 2002a; b; Parr *et al*., 2003; Munakata *et al*., 2002). HFTW systems act like a deep aquifer version of the permeable reactive barrier technology discussed earlier (Munakata *et al*., 2002); modeling studies have shown that an HFTW system is capable of capturing a portion of the contaminant plume several times larger than the space between the wells (Gandhi *et*

al., 2002a; b). Additionally, a substantial fraction of the contaminated water that passes through a bioactive treatment zone for perchlorate reduction recycles through the treatment zones several times, thereby increasing the overall degradation efficiency of the system, where overall degradation efficiency is defined in terms of perchlorate concentrations upgradient and downgradient of the HFTW system (McCarty *et al*., 1998; Parr *et al*., 2003; Gandhi *et al*., 2002a; Munakata *et al.*, 2002). The ability to change pumping rates and nutrient concentrations in response to changing environmental conditions is also an advantage of an HFTW remediation system.

Horizontal flow treatment wells have been used primarily to treat other contaminants, particularly halogenated solvents such as TCE. The seminal work in the field of HFTW applications was done by McCarty *et al*. (1998). This study used HFTW technology to introduce toluene, oxygen, and hydrogen peroxide to a TCE-contaminated aquifer at Edwards Air Force Base, California in order to stimulate the *in situ* cometabolic biodegradation of TCE. Over the course of the 410-day study, reductions in TCE concentration of 97% - 98% were observed. HFTW systems are also being implemented at the field scale for the palladium catalyzed *in situ* degradation of TCE at the same site in California (Stoppel and Goltz, 2003; Munakata *et al*., 2002).

HFTW technology, like any engineered system, is not without its drawbacks. When an HFTW system is used to stimulate the growth of subsurface microorganisms through the addition of nutrients, the microorganisms are going to grow faster near the injection well screens where the nutrient concentration is the highest. As the microorganisms grow,

they reduce the porosity of the soil matrix, thereby reducing the hydraulic conductivity of the porous media, ultimately resulting in reduced water flow and inefficient mixing of contaminant, nutrients, and microorganisms. The loss of hydraulic conductivity due to microbial growth is often referred to as bioclogging in the literature and was a concern during the McCarty *et al*. (1998) study. Several strategies were used by McCarty *et al.* (1998) to avoid the effects of bioclogging. The treatment wells were routinely shut down for redevelopment. Toluene, the electron donor and carbon source, was delivered in pulses in order to stimulate bacterial growth away from the well screens. This strategy was supported by model simulations presented by Goltz *et al*. (2001). Another approach used by McCarty *et al*. (1998) to eliminate bioclogging was to add hydrogen peroxide to inhibit bacterial growth near the well screens.

In a model of TCE degradation using an HFTW system (Gandhi *et al*., 2002b), the inhibitory effects of hydrogen peroxide on the resident microbial population were simulated; however, the effects of biological growth, that is to say biomass, on hydraulic conductivity were not. The effects of biogrowth on conductivity were also not included in a model of HFTW-induced perchlorate biodegradation developed by Parr *et al*. (2003). While Gandhi *et al*. (2002b) indicate that their simulations were able to closely fit observed data without having to model bioclogging; the need to accurately simulate the impact of biological growth on groundwater flow is highlighted as an area where further research is required. In order to extend existing mathematical models of HFTW bioremediation performance to include the effects of bioclogging, an understanding of the phenomenon is required. The next section provides an in-depth review of bioclogging to

include: how bacteria grow in the subsurface environment, what factors influence their growth, the mechanisms by which bacteria reduce the hydraulic conductivity of a porous media, and current models that have been developed to simulate bioclogging.

2.7 BIOCLOGGING

2.7.1 DEFINITION

Kildsgaard and Engesgaard (2001) define bioclogging as the increase in biomass to the point where porosity and thus hydraulic conductivity, K_s, of a porous medium is reduced. The accumulation of biomass decreases the hydraulic conductivity of the soil by clogging pore spaces (Seki and Miyazaki, 2001).

The fundamental law describing groundwater flow in a porous medium, Darcy's law, provides the starting point for mathematically modeling bioclogging. In one spatial dimension (x), Darcy's Law is:

$$Q/A = -K_s(dh/dx) \qquad (2.4)$$

where

A is the cross sectional area (L^2) through which groundwater flowing at rate Q (L^3/T) passes

K_s = *hydraulic conductivity (L/T)*

h = piezometric head (L)

Piezometric head is a measure of the potential energy (elevation plus pressure) of the fluid (Bear, 1972). The negative sign in equation 2.4 indicates that groundwater flow is

from regions of high piezometric head to regions of low piezometric head. Note that the term Q/A is commonly referred to as the Darcy velocity, q.

Bear and Verruijt (1987) define hydraulic conductivity, K_s, as the ease with which a fluid is able to travel through a porous media. Consequently, hydraulic conductivity depends upon both the porous media properties and the properties of the fluid (Bear and Verruijt, 1987). Important fluid properties include density and viscosity; relevant porous media properties include the grain size distribution, grain shape, tortuosity, specific surface area, and porosity (Bear, 1972). Hydraulic conductivity is often expressed as

$$K_s = (k*\rho*g)/\mu \qquad (2.5)$$

where

$$k = \text{permeability } (L^2)$$

$$\rho = \text{fluid density } (M/L^3)$$

$$g = \text{acceleration due to gravity } (L/T^2)$$

$$\mu = \text{fluid dynamic viscosity } (M*L^{-1}*T^{-1})$$

Permeability, k, depends only on the properties of the porous media (Bear, 1972). Numerous formulas have been formulated which relate permeability to the various properties of the porous media; some of these relationships are purely empirical, others are purely theoretical, and a third class of formula which defines permeability in terms of the properties of the porous media are considered semi-empirical (Bear, 1972). According to Bear (1972), semi-empirical formulas are theoretically derived from conceptual models of a porous media, but the coefficients involved in the theoretical formula must be experimentally determined for each porous media type. The following

general equation is an example of a semi-empirical formula relating permeability to the properties intrinsic to the porous media (Bear, 1972).

$$k = f_1(s)*f_2(n)*d^2 \qquad (2.6)$$

where

$f_1(s)$ = *dimensionless grain shape factor*

$f_2(n)$ = *dimensionless porosity factor*

d = *mean grain diameter (L)*

Bear (1972) indicates that the porosity factor is often evaluated using the following equation:

$$f_2(n) = n^3/(1-n)^2 \qquad (2.7)$$

where

n = *measured porosity of porous media (pore volume/total volume)*

Equations 2.6 and 2.7 are important to the current topic of bioclogging because they establish that permeability is directly related to the porosity of the porous media. If the accumulation of biomass reduces the porosity of a porous media, Equations 2.5 through 2.7 clearly show that the hydraulic conductivity, and ultimately the flow rate of the fluid through the porous media will be reduced as well. In the following sections we will describe what is currently understood about bioclogging, in order that we may, in the final section of the chapter, examine bioclogging models that relate microbial growth and porosity reduction to hydraulic conductivity reduction.

2.7.2 BIOCLOGGING MECHANISMS

Intuitively, we recognize that if biological cells accumulate and physically block the pore spaces of a medium, the hydraulic conductivity of the medium will be reduced. Studies conducted by Vandervivere and Baveye (1992b, 1992c) show that biomass can occupy upwards of 8.5% of the pore volume of a porous media. On the other hand, Vandevivere *et al.* (1995) note that net biomass accumulation is not the only biological process responsible for reducing hydraulic conductivity within the biologically active zones of an aquifer.

Vandevivere *et al.* (1995) and Baveye (1998) review an extensive body of work that indicates the production of extra cellular polymers and gas bubbles also result in bioclogging. Vandevivere and Baveye (1992a) investigated the clogging effects of four different bacteria; their results indicate that all four strains produced nearly the same bacterial mass but the strain which produced extra cellular polymers resulted in a greater loss of hydraulic conductivity. Observations made by Thullner *et al*. (2002) in a two-dimensional flow cell also attribute the cause of bioclogging to the bacterial production of extra cellular polymers. Cunningham *et al.* (1991) and Rittman (1993) identified an increase in the friction factor of the soil due to the absorbed bacteria as a cause of hydraulic conductivity reduction. In the next section, we review the various ways biomass has been observed to accumulate within a porous media.

2.7.3 BIOMASS MORPHOLOGY

A considerable source of debate within the literature has centered on how bacteria grow in a porous media. Several authors (Cunningham *et al.*, 1991; Dupin and McCarty, 2000; Suchomel *et al.*, 1998; Taylor and Jaffé, 1990a, 1990b, 1990c; Taylor *et al.*, 1990) have put forth evidence that biomass accumulates in a continuous layer, known as biofilms, that grow on the outer surface of the porous medium grains. Others (Molz *et al.*, 1986; Widdowson, 1991) suggest that incomplete biofilms, or microcolonies, develop on the grain surface. Vandervivere and Baveye (1992a, 1992b, 1992c), Baveye *et al.* (1989), Dupin and McCarty (2000), and Dupin *et al.* (2001a, 2001b) postulate that the formation of biomass aggregates within the pore throats between particles is the primary way biomass accumulates. Two other biomass morphologies have also been explored: Dupin and McCarty (1999, 2000) and Seki *et al*. (2002) identified the growth of fungi in the form of filaments that spanned several pores and Paulson *et al.* (1997) along with Dupin and McCarty (2000) identified the formation of biowebs, thin strips of biomass that stretch between the pore walls. The following is a listing of the most prevalent biomass morphologies described in the literature:

(1) Biofilms

(2) Microcolonies

(3) Aggregates

(4) Fungi filaments

(5) Biowebs

The accumulation of biomass is not a uniform process. The morphology of the biomass may change with time; Paulsen *et al.* (1997) described the temporal shift of the biomass

morphology from biofilms to biowebs. Also, Dupin and McCarty (2000) point out that the presence of one biomass morphology does not exclude the growth of other types of biomass.

Several authors (Dupin and McCarty, 2000; Paulsen *et al.*, 1997; Rittman, 1993) suggest that the conditions within the porous media have a dramatic effect on the manner which biomass accumulates and thereby affects bioclogging. The next section reviews some of the conditions within a porous media and their influence on bioclogging.

2.7.4 CONDITIONS WHICH INFLUENCE BIOCLOGGING

Bioclogging has been found to occur in a wide variety of soil types and conditions. Cunningham *et al.* (1991), Cunningham and Wanner (1995), Thullner *et al.* (2002), and Seki *et al*. (2002) investigated biomass accumulation on uniform glass beads. Vandevivere and Baveye (1992a, 1992b, 1992c) explored bioclogging in sand. Other researchers (Rice, 1974; Chang *et al*., 1974; Davis *et al*., 1973; Ragusa *et al*., 1994) have observed bioclogging in porous media as diverse as: loamy sand, sandy soil, loamy soil, silty clay, dairy waste pond soil, and irrigation channel soil.

2.7.4.1 CHEMICAL CONDITIONS WHICH INFLUENCE BIOCLOGGING

The predominant opinion within the literature for many years has been that anaerobic conditions are necessary to observe large reductions in the hydraulic conductivity of a porous media due to biological growth (Vandevivere and Baveye, 1992c; Baveye *et al*., 1998). However, Baveye *et al*. (1998) provides an extensive review of research which

suggests that aerobic conditions as well as anaerobic conditions within a porous media can promote bioclogging. Additional evidence of bioclogging under aerobic conditions has been presented by Vandevivere and Baveye (1992c) who demonstrated that a strictly aerobic strain of bacteria was capable of reducing the hydraulic conductivity of a sand column by three to four orders of magnitude.

Aerobic conditions within the subsurface lead to bioclogging via several mechanisms. Vandevivere and Baveye (1992c) demonstrate via scanning electron microscopy that the aerobic bacteria, *Arthrobacter* AK19, form aggregates within the pore space of the soil matrix and did not produce extra cellular polymers. Cunningham *et al*. (1991) were able to grow the bacteria, *Pseudomonas aeruginosa,* as a biofilm under aerobic conditions. Taylor and Jaffé (1990a) also observed the development of a biofilm under aerobic conditions by using a consortium of bacteria derived from primary sewage and activated sludge. Dupin and McCarty (1999, 2000) identified the growth of fungal filaments within an aerobic environment. Finally, a small body of literature is presented by Baveye *et al*. (1998) which points towards the production of gaseous nitrogen by bacteria under aerobic conditions as a cause of hydraulic conductivity reduction.

Anaerobic conditions are often times prevalent in subsurface aquifers. Paulsen *et al*. (1997) determined that bacteria indigenous to seawater which were grown under anaerobic conditions formed biowebs. Thullner *et al*. (2002) demonstrated that in the absence of oxygen, a nitrate reducing bacteria, *Pseudomonas* strain PS^{+}, produced significant clogging effects by producing extra cellular polymers. During the same study,

bacterial cells were found to occupy only 0.01% of the pore space (Thullner *et al*., 2002). By using PCE as an electron acceptor and lactate as an electron donor, Nambi *et al.* (2003) were able to demonstrate that the anaerobic halorespiring microorganism, *Sulfurospirillum multivorans,* was capable of altering the flow path and creating higher pore water velocities. Additionally, Nambi *et al.* (2003) indicated that biomass initially grew in the form of aggregates with diameters smaller than the pore diameter and later developed into finger like structures similar to biowebs. Results of this study also indicated that biomass did not accumulate in the pore throats as the authors expected (Nambi *et al.*, 2003). Methane gas production by anaerobic bacteria can also result in hydraulic conductivity reductions within a porous media (Baveye *et al*., 1998). Anaerobic iron reducing bacteria tend to produce exopolymers which can clog or plug the pore space inside a porous media (Baveye *et al*., 1998).

Acidic conditions within the subsurface can also promote hydraulic conductivity reductions due to bioclogging. Dupin and McCarty (1999, 2000) observed the growth of biomass, in the form of fungal filaments, in laboratory conditions with a pH as low as 3. In their experiments, Dupin and McCarty (2000) also indicate that biofilms and aggregates were the prevalent morphology at neutral pH.

Another chemical condition which can significantly impact the extent of bioclogging that can occur in a porous medium is the amount of substrate available for utilization by bacteria and other microorganisms. Rittman (1993) presents a concept known as normalized loading to help define how substrate concentration can impact biomass

morphology. Rittman (1993) describes the concept of normalized loading graphically. The following figure taken from Rittman (1993) is a typical normalized loading curve. While not specifically for perchlorate reducing bacteria, this curve is valid for nearly all bacteria found in the subsurface (Rittman, 1993).

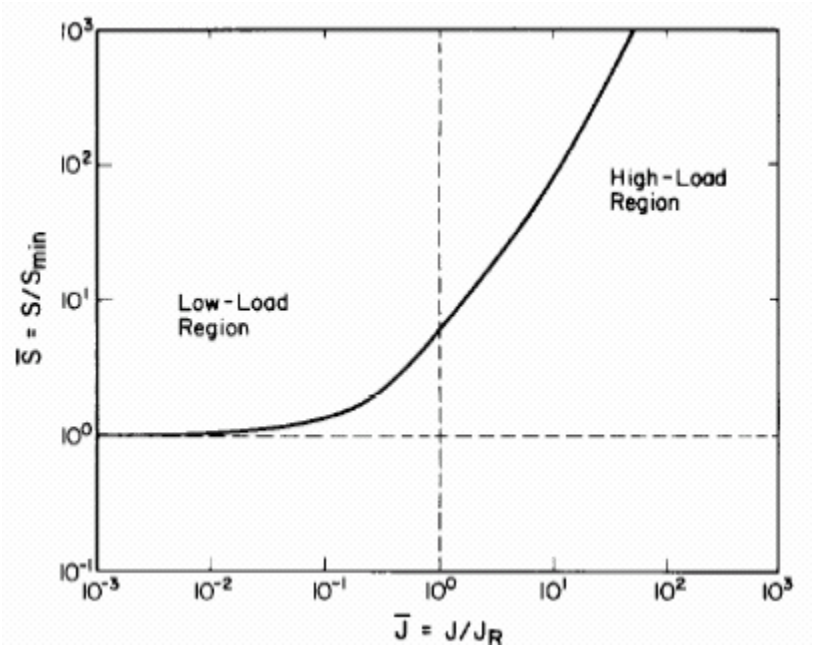

Figure 2.10 Substrate normalized loading curve (Rittman, 1993)

$\bar{S}$ is defined as the normalized substrate concentration where

S = substrate concentration in the effluent of control volume (M/L^3)

S_{min} = minimum substrate concentration to maintain a steady state biofilm (M/L^3)

$\bar{J}$ is defined as the normalized substrate loading where

J = actual substrate flux into biofilm (M/L^2T)

J_r = minimum substrate flux giving a steady state biofilm that is deep (M/L^2T)

Rittman (1993) defines a deep biofilm as one in which the thickness of the biofilm and consequently, the diffusional resistance of the biofilm is large enough that the substrate concentration within the biofilm approaches zero at some point.

The key point presented in Figure 2.10 is that as the normalized substrate concentration increases, the normalized substrate flux into the biofilm increases exponentially. Rittman (1993) points out that in the high load region, the biomass will accumulate within the porous medium as a complete biofilm, while in the low loading region the concept of biological microcolonies may be more appropriate.

Baveye *et al.* (1998) criticize the normalized substrate loading concept. Rittman (1993) mathematical defined *J* as:

$$J = \frac{Q(S^o - S)}{aV} \qquad (2.8)$$

where

Q = *flow rate into the system* (L^3/T)

So = *substrate concentration into the system* (M/L^3)

S = *substrate concentration in system effluent* (M/L^3)

a = *specific surface area of the biofilm* ($1/L$)

V = *system volume* (L^3)

Baveye *et al.* (1998) point out the fact that the value of *J* can be manipulated by altering the system volume. Therefore, if the system volume is small, the resulting value of *J* will

be large. The arbitrariness of the volume variable limits the use of the normalized loading concept in porous media where samples can be taken at a variety of scales (Baveye *et al., 1998).*

It must also be noted that conditions within an aquifer are not always uniform. In fact, chemical conditions can vary within a few millimeters; aerobic and anaerobic environments can exist next to each other (Maier *et al.*, 2000). Furthermore, the physical properties of a porous medium interact with the chemistry to influence the nature and severity of bioclogging (Baveye *et al*., 1998). The next section describes how the physical properties of the subsurface environment, particularly the grain size distribution, affect bioclogging.

2.7.4.2 PHYSICAL CONDITIONS WHICH INFLUENCE BIOCLOGGING

The presence of fine particles in porous media has been shown to magnify the effect of bioclogging. Baveye *et al*. (1998) reviews literature that indicates that small soil particles subject to advective transport are particularly susceptible to being trapped by extra cellular polymers produced by subsurface bacteria. As more and more of these particles are collected over time, the hydraulic conductivity is reduced.

The rate of groundwater flow is another physical property of the subsurface environment that has been shown to affect bioclogging. Taylor and Jaffé (1990a) attributed the reduction of hydraulic conductivity in regions that did not have the proper nutrients to promote biological growth to the migration of detached bacteria from regions upstream.

The detachment of bacteria has been suggested to increase as the pore water velocity increases due to the thickening biofilm reducing the cross-sectional area of the pore space and thereby increasing pore velocity (Taylor and Jaffé, 1990a).

Paulsen *et al*. (1997) also demonstrated that the morphology of the growing bacteria can be influenced by the groundwater flow rate. In their research, Paulsen *et al*. (1997) demonstrated that bacterial cells developed thicker biowebs sooner under increased flow conditions than under low flow conditions. Paulsen *et al*. (1997) does not present a hypothesis explaining this difference, however it seems plausible that the high flow rate delivered nutrients at a rate fast enough to stimulate the observed accelerated growth.

The size of the particles which compose the porous media matrix is also an important condition which influences how and where biomass accumulates. Work originally reported by Cunningham *et al*. (1991) and reviewed by Vandevivere *et al.* (1995) and Baveye *et al.* (1998) indicates that the reduction of hydraulic conductivity is more severe in fine grained soils than in coarse grained soils. The following figure which includes data from Cunningham *et al*. (1991) and Vandevivere and Baveye (1992b) illustrates this trend.

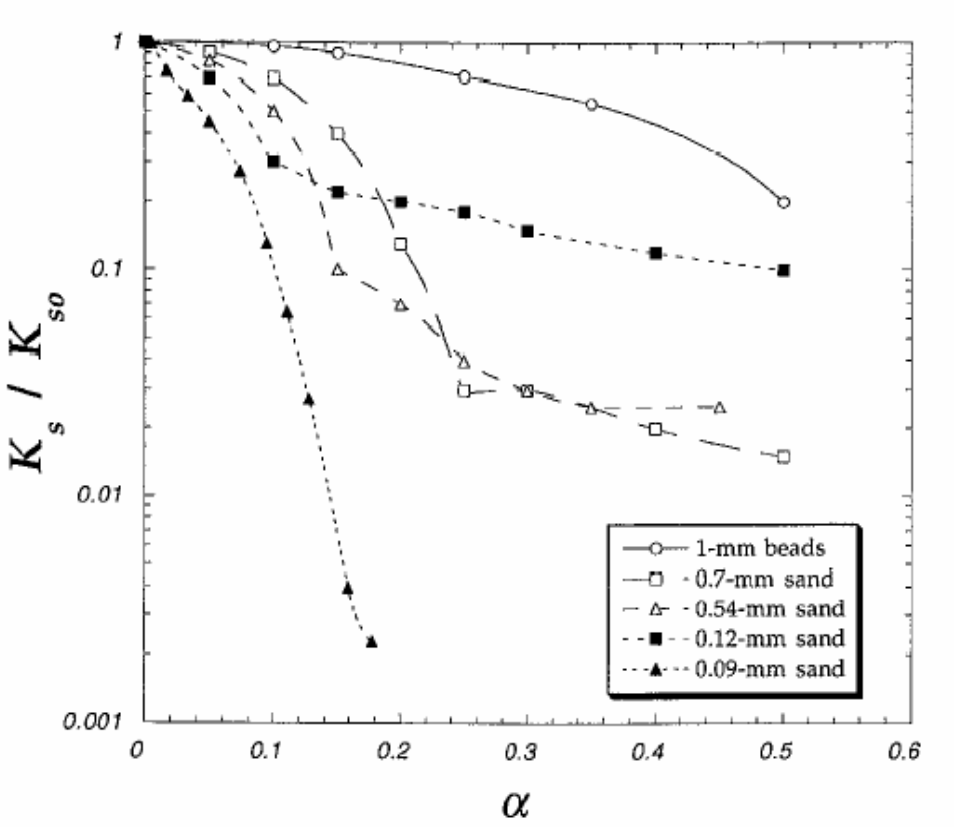

Figure 2.11 Hydraulic conductivity reduction observed in uniform porous media of different grain size (Vandevivere *et al.*, (1995)

In Figure 2.11, the x-axis, α, is referred to as the biovolume ratio which is defined as the bulk volume of biomass per unit pore volume of the unclogged porous media (Vandevivere *et al*., 1995). Mathematically, the biovolume ratio is defined as:

$$\alpha = (n - n_c)/n \ (L^3/L^3) \qquad (2.9)$$

where

n_c = *clogged porosity* (L^3/L^3)

n = *initial porosity* (L^3/L^3)

Fine grained soils tend to have a higher porosity than coarse grained sands; consequently, a given amount of biomass should have a lesser effect on hydraulic conductivity reduction in a fine grained soil compared to a coarse grained soil (Baveye *et al*., 1998). This does not explain the difference in the rate and extent at which hydraulic conductivity is reduced by biogrowth (Baveye *et al.*, 1998). Instead, the specific surface area, which is the ratio of particle surface area to particle volume, is believed to be a determining factor for the extent of hydraulic conductivity decrease due to biomass accumulation (Vandervivere *et al.*, 1995). Coarse-grained soils have a significantly smaller specific surface area than fine-grained soils (Baveye *et al.,* 1998). Therefore, bacteria and other microorganisms have less area to colonize in coarse-grained environments (Baveye, *et al*., 1998) which leads to a smaller reduction in hydraulic conductivity. The next section reviews methods used in the laboratory and in field applications to reduce the effects of bioclogging on porous media.

2.7.5 TECHNIQUES TO PREVENT BIOCLOGGING

An area that needs further study is the prevention or control of bioclogging. The techniques implemented by McCarty *et al*. (1998) to control bioclogging included well redevelopment, H_2O_2 addition, and substrate pulsing. These techniques were previously discussed in section 2.6.2.4. Researchers at the University of New Mexico are currently conducting column experiments in order to determine the effect different electron donors have on bioclogging (Nuttall, unpublished data). Different techniques to control bioclogging are also under investigation; some of the techniques receiving attention include electrostatic dispersion, addition of enzymes, and the use of different biocides

such as chlorine, chloroamines, chlorine dioxide, hydrogen peroxide, peracetic acid, ozone, and ultraviolet light (Nuttall, unpublished data).

An intriguing technique to reduce the effects of bioclogging involves the use of protozoans to reduce the amount of bacterial biomass in a porous media via grazing. Mattison *et al*. (2002) reported that the bacterivorous soil flagellate, *Heteromita globosa,* was capable of minimizing the loss of hydraulic conductivity due to bioclogging when introduced before the bacteria can establish themselves in porous media though it was not capable of restoring hydraulic conductivity when added to a porous medium that had already been colonized by bacterial biomass.

GeoSyntec Consultants (2002a) has conducted extensive field evaluations of several ways to limit the effects of bioclogging. In one of the trials during the GET D pilot study, citric acid was mixed with ethanol in order to provide a carbon source for perchlorate respiring bacteria while lowering the pH in the area of the recharge wells (GeoSyntec Consultants, 2002a). A lower pH environment should, in theory, limit the growth of perchlorate respiring bacteria. However, the amount of bioclogging, as measured by the water level in the recharge wells, is seen to initially drop, and then steadily increase despite the addition of the citric acid/ethanol blend. In fact, shock citric acid loading at the end of the trial appears to have had very limited effect on the water level of the recharge well.

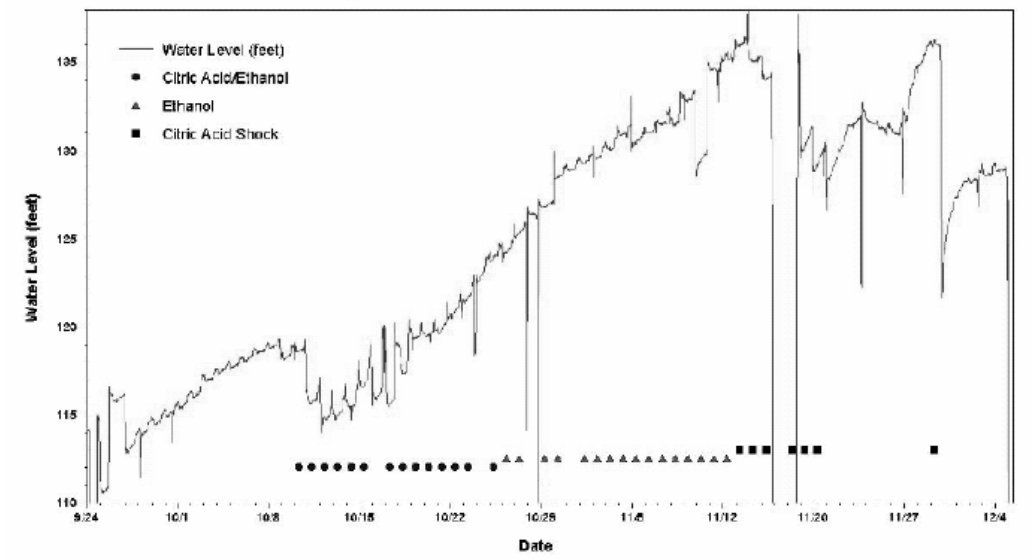

Figure 2.12 Effect of citric acid on bioclogging of recharge well as measured by the water level in well (GeoSyntec Consultants, 2002a)

In yet another trial during the GET D pilot study, another method of controlling bioclogging was explored. Instead of citric acid to control the pH near the recharge wells, chlorine dioxide (ClO_2) was periodically added to the injection water in order to kill the perchlorate respiring bacteria growing near the well screens. The following figure shows the impact of ClO_2 on the water level in one of the recharge wells of the GET D study.

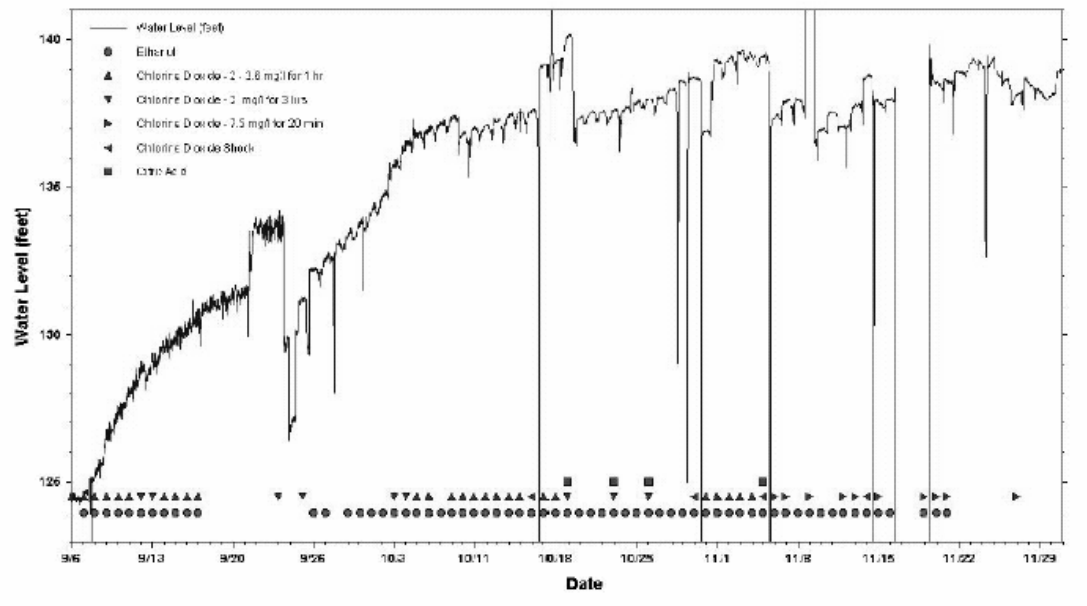

Figure 2.13 Effect of chlorine dioxide on bioclogging of recharge well as measured by the water level in well (GeoSyntec Consultants, 2002a)

While it is not initially obvious that chlorine dioxide controlled bioclogging better than citric acid, the following figure which compares the changes in well water level for the two methods clearly shows that ClO_2 outperformed citric acid.

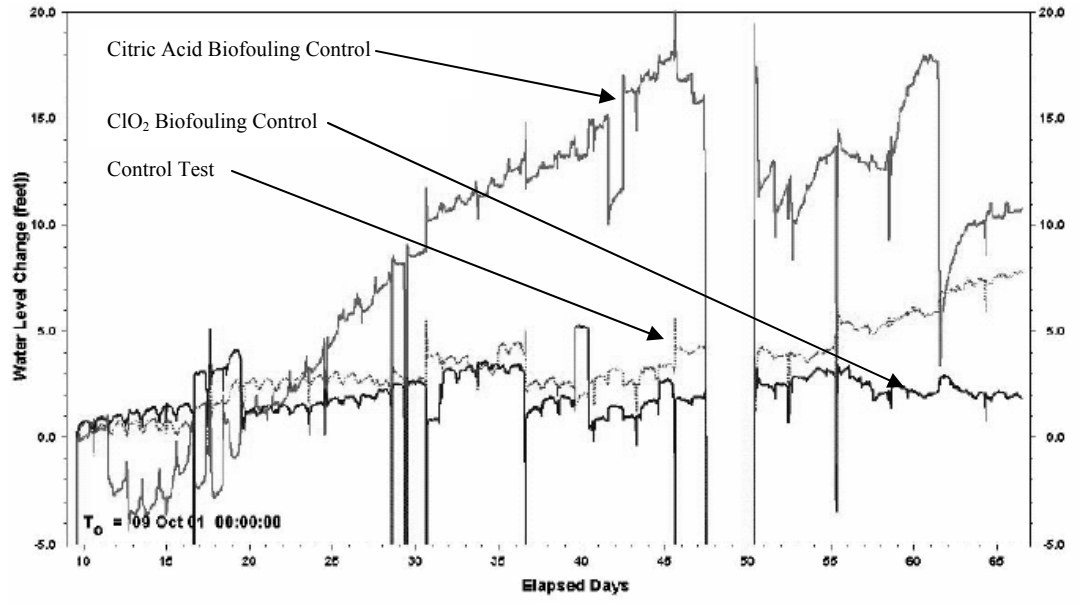

Figure 2.14 Water level trend comparison for GET D pilot study (GeoSyntec Consultants, 2002a)

In the final section of this chapter, we review the mathematical models that have been developed to describe bioclogging.

2.7.6 BIOCLOGGING MODELS

A mathematical model of bioclogging should be able to predict the spatial and temporal variation of the saturated hydraulic conductivity (K_s) of a porous medium based on the characteristics of the system: physical and chemical properties of the soil and water, flow characteristics, and features of the indigenous microbial community (Baveye *et al.* 1998). As Baveye *et al.* (1998) point out; such a model can be theoretically separated into two elements. The first element would be a collection of equations describing the accumulation of biomass and associated by-products (Baveye *et al.* 1998). The second component would estimate the reduction of K_s as a function of the accumulation of biomass and associated by-products (Baveye *et al.* 1998).

Equations describing the accumulation of biomass have been extensively reviewed by several authors (Parr, 2002; Logan, 2000; Logan, 2001b; Logan *et al*., 2001; Cox *et al*., 2000). These models of biological growth can be categorized as first order, Monod, dual Monod, and multi electron acceptor dual Monod models (Parr, 2002). The current work does not present these models. Instead, we focus on the reduction of the hydraulic conductivity of a porous medium due to the accumulation of biomass. The assumptions made regarding the morphology of the biological mass in the porous media are critical to developing a model which realistically represents bioclogging. Thus, this section will present a review of bioclogging models based upon their morphology assumptions.

2.7.6.1 MODELS WITH NO MORPHOLOGY ASSUMPTION

Using the Kozeny-Carmen equation as presented by Bear (1972), Vandevire *et al*. (1995) show that in a porous media that becomes clogged, the hydraulic conductivity ratio is given below.

$$\frac{K_s}{K_{so}} = \frac{n_c^3}{n^3} * \frac{S^2}{S_c^2} \qquad (2.10)$$

where

K_s = *clogged hydraulic conductivity (L/T)*

K_{so} = *initial hydraulic conductivity (L/T)*

n_c = *clogged porosity* (L^3/L^3)

n = *initial porosity* (L^3/L^3)

S = *initial internal surface area of porous media per unit volume* (L^2/L^3)

S_c = *clogged internal surface area of porous media per unit volume* (L^2/L^3)

Kildsgaard and Engesgaard (2002) developed a model of saturated hydraulic conductivity reduction that takes a macroscopic approach to the distribution of biomass within the porous media; consequently the biomass may accumulate in any of the previously discussed morphologies. Kildsgaard and Engesgaard (2002) begin the development of their model by defining the fraction of the total volume of a porous media occupied by biomass as:

$$n_b = \frac{X_s \rho_{bulk}}{\rho_b} \qquad (2.11)$$

where

X_s = *solid biomass concentration* (M_{bio}/M_{solid})

ρ_{bulk} = *bulk density of porous media* (M_{solid}/L^3)

ρ_b = *density of solid biomass* (M_{bio}/L^3)

Kildsgaard and Engesgaard (2002) then used this definition in the hydraulic conductivity ratio first developed by Clement *et al.* (1996).

$$\frac{K_s}{K_{so}} = (1 - \frac{n_b}{n})^{19/6} \qquad (2.12)$$

The basis for Equation 2.12 is the "cut and random rejoin model" used by Taylor *et al*. (1990). This model assumes that a porous medium contains random pores of varying width distributed within the medium and that the hydraulic conductivity across any two adjacent planes is dependent upon the number of interconnected pores. It is assumed that the hydraulic conductivity of each connected pore pair is controlled by the smaller pore (Taylor *et al.,* 1990). Interestingly, identical values for variables required by the "cut and random rejoin model" can be derived by using either the van Genuchten or the Brooks-Corey empirical equations relating relative water saturation and pressure head (Clement *et al.*, 1996). The next subsection reviews bioclogging models which assume that the biological growth takes the form of a biofilm coating the soil particles which make up the porous media.

2.7.6.2 MODELS ASSUMING BIOFILMS

Ives and Pienvichitr (1965) developed a model to predict the reduction in hydraulic conductivity based on Equation 2.10. Within this model, it is assumed that the porous media can be modeled as a bundle of tortuous capillary tubes of varying radii (Vandevivere *et al*., 1995). Suspended biological colloids are then deposited on the walls of the capillaries in a uniform thickness and reduce the radius of the capillary tubes (Vandevivere *et al*., 1995). Based on these assumptions, Equation 2.13 was developed:

$$\frac{K_s}{K_{so}} = (1-\alpha)^{3-2p} \qquad (2.13)$$

where

p = dimensionless parameter dependent on tortuosity and pore diameter variations

Chu *et al.* (2003) built a model describing the hydraulic conductivity reduction associated with the onset of biological growth in the form of a biofilm based on the Ives and Pienvichitr (1965) model with the shape parameter, *p*, set equal to 0.5. This model assumes that the porous media can be thought of as a bundle of straight capillary tubes of the same radius; as the biofilm develops it uniformly reduces the radii of the capillary tubes. Chu *et al.* (2003) also assume that the minimum hydraulic conductivity of a porous media is 2000th of the initial hydraulic conductivity in accordance with the findings of Taylor and Jaffé (1990a). The equations presented by Chu *et al.* (2003) are as follows.

$$\frac{K_s}{K_{so}} = (1-\alpha)^2 \quad if \quad \alpha \le 1 - \sqrt{\frac{K_{\min}}{K_{so}}} \qquad (2.14)$$

$$\frac{K_s}{K_{so}} = \frac{K_{\min}}{K_{so}} \quad if \quad \alpha > 1 - \sqrt{\frac{K_{\min}}{K_{so}}} \qquad (2.15)$$

where

$$K_{min} = 5x10^{-4}(K_{so})$$

Taylor *et al*. (1990) also developed an equation to represent the loss of hydraulic conductivity within a porous media due to biological growth based on Equation 2.10. Taylor *et al*. (1990) assumed that biological growth occurred in a porous media in the form of an impermeable biofilm of constant thickness. It is further assumed by Taylor *et al*. (1990) that the porous media grains can be represented as uniforms spheres packed together in one of four geometric arrangements: cubic, orthorhombic, tetragonal-spheroidal, and rhombohedral. The following equations are used by Taylor *et al.* (1990) to define the values of the variables in Equation 2.10.

$$n = 1 - (\frac{\pi}{6\alpha_m}) \qquad (2.16)$$

$$S = \frac{\pi}{2\alpha_m r} \qquad (2.17)$$

$$n_c = 1 - \frac{\pi}{\alpha_m}\left[\left[\frac{(2-m)}{12}\right]\left(\frac{L_f}{r}\right)^3 + \frac{(4-m)}{8}\left(\frac{L_f}{r}\right)^2 + \frac{1}{2}\left(\frac{L_f}{r}\right) + \frac{1}{6}\right] \qquad (2.18)$$

$$S_c = \frac{\pi}{2\alpha_m r}\left[\frac{(2-m)}{2}\left(\frac{L_f}{r}\right)^2 + \frac{(4-m)}{2}\left(\frac{L_f}{r}\right) + 1\right] \qquad (2.19)$$

where

m = number of contact points with neighboring spheres

α_m = *packing arrangement factor*

r = radius of sphere (L)

L_f = *biofilm thickness (L)*

Another model developed by Taylor *et al.* (1990) uses the "cut and random rejoin" model to represent the porous medium. As stated previously, the "cut and random rejoin" model assumes that a porous medium contains random pores of varying width distributed within the medium and that the hydraulic conductivity across any two adjacent planes is dependent upon the number of interconnected pores. It is assumed that the hydraulic conductivity of each connected pore pair is controlled by the smaller pore (Taylor *et al.,* 1990). . In the Taylor *et al.* (1990) model, as with the previous model, biofilms of uniform thickness are assumed to grow on the inside surface of the pores (Taylor *et al.*, 1990). The following equations describe the hydraulic conductivity ratio reported by Taylor *et al.* (1990).

$$\frac{K_s}{K_{so}} = \left(\frac{L_f}{R}\right)^{2+2\lambda}\left[\frac{\left(I_3\left(\frac{R}{L_f}-1,\lambda\right) - I_3\left(\frac{r_{ob}}{L_f},\lambda\right)\right)^2}{\left[\frac{1}{1+\lambda}\left[1-\left(\frac{r_o}{R}\right)^{1+\lambda}\right]\right]^2}\right](1-\alpha)^{\frac{1}{2}} \qquad (2.20)$$

$$I_n(\mu,\lambda) = \int_0^{\mu} \frac{x^n}{(1+x)^{3-\lambda}} dx \qquad (2.21)$$

where

R = *maximum pore radius (L)*

r_o = *minimum pore radius (L)*

$r_{ob} = max(r_o - L_f, 0)$

λ = *pore size distribution index*

Biofilm models of porous media clogging have been the most common presented in the literature. Nevertheless, several models which assume alternative biomass morphologies have also been developed. These models will be discussed in the next subsection.

2.7.6.3 MODELS ASSUMING A MORPHOLOGY OTHER THAN A BIOFILM

Vandevivere *et al.* (1995) developed a model which viewed a porous media as a group of parallel, cylindrical capillaries of constant radius. These capillaries become clogged by dense plugs of biological mass (Vandevivere *et al.*, 1995). It is further assumed that the head loss occurring in the unplugged portions of each capillary is insignificant because the hydraulic conductivity of the biological plug is extremely low compared to the initial hydraulic conductivity of the porous media (Vandevivere *et al.*, 1995). Finally, if Darcy's law is assumed to apply to flow through the plugs, the following equation describes the hydraulic conductivity of the plugged porous media.

$$K_s = \frac{nK_p}{n_b} \qquad (2.22)$$

where

K_p = *hydraulic conductivity of biological plug (L/T)*

Chu *et al.* (2003) recast the Vandevivere *et al.* (1995) plug model by assuming that flow occurs unimpeded until the amount of biomass in the pore volume, α, reaches a certain limit. The following equations represent this model.

$$\frac{K_s}{K_{so}} = 1 \ if \ \alpha \le \frac{K_p}{K_{so}} \qquad (2.23)$$

$$\frac{K_s}{K_{so}} = \frac{n}{n_b}\frac{K_p}{K_{so}} \ if \ \alpha > \frac{K_p}{K_{so}} \qquad (2.24)$$

Seki and Miyazaki (2001) developed a theoretical concept which they refer to as the "colony enveloping space" in order to quantify the morphology of the growing biomass in a porous media. The colony enveloping space is the hypothetical space over which a film of uniform thickness would cover a particle of the porous media. While this model can be applied to biofilm models if the coverage of the soil particles is assumed to be complete; the model is flexible enough to evaluate the loss of hydraulic conductivity due to the onset of a patchy biofilm or microcolony. Seki and Miyazaki (2001) developed their model based on the assumption that the porous media is made up of particles of uniform size. The Seki and Miyazaki (2001) model is represented in the following equation.

$$\frac{K_s}{K_{so}} = [1 - [(\frac{\alpha n}{\beta - \beta n} + 1)^{\frac{1}{3}} - 1][(\frac{\tau}{1-n})^{\frac{1}{3}} - 1]^{-1}]^3 \qquad (2.25)$$

where

α = *biovolume ratio*

β = *enveloping factor*

τ = *shape factor*

Seki and Miyazaki (2001) define the biovolume ratio in accordance with Vandevivere *et al*. (1995), as the bulk volume of biomass per unit pore volume of unclogged porous media. The enveloping factor is defined as the bulk volume of biomass per unit volume of colony enveloping space (Seki and Miyazaki, 2001). The shape factor is defined as the ratio of the volume of the solid phase of the porous media to S^3, where S is defined as the characteristic length of the solid phase particles (Seki and Miyazaki, 2001).

Other bioclogging models do not explicitly define a K_s/K_{so} ratio. Dupin *et al*. (2001a, 2001b) developed a network model which assumes that biological material forms aggregates within the pore throat. The effect of these aggregates on groundwater flow through the pores is modeled by artificially increasing the water viscosity within the biological mass (Dupin *et al*., 2001a, 2001b). Suchomel *et al.* (1998) also developed a network model which simulates flow, transport, and biological growth in a porous medium. This model assumes that clogging occurs due to biological cells adsorbing to the pore walls to form biofilms and that the radii of tubes, which represent the pores of the medium, are randomly selected based upon a normal probability distribution

(Suchomel *et al.*, 1998). The effect of the biofilm is incorporated into the network model through a reduction in the pore radius given by the following equation.

$$a_t = a_o \sqrt{1 - \frac{c_b(t)}{\rho_{film}(t)}} \qquad (2.26)$$

where

a_t = *pore radius at time, t (L)*

a_o = *initial pore radius (L)*

$c_b(t)$ = *adsorbed concentration of biomass in discretized network cell at time, t* (M_{bio}/L^3)

$\rho_{film}(t)$ = *biofilm density at time, t* (M_{bio}/L^3)

Suchomel *et al.* (1998) use the Hagen-Poiseulle equation to describe the fluid flow through the network model. This relationship is defined in the following equations.

$$q = k^*(h_i - h_j) \qquad (2.27)$$

$$k^* = \frac{\rho g \pi a^4}{8 \mu L} \qquad (2.28)$$

where

h_i = *piezometric head at network junction, i (L)*

h_j = *piezometric head at network junction, j (L)*

ρ = *fluid density* (M/L^3)

g = *acceleration due to gravity* (L/T^2)

a = *cross sectional area of pore* (L^2)

μ = *fluid dynamic viscosity* ($M*L^{-1}*T^{-1}$)

L = *length of pore (L)*

From Equations 2.27 and 2.28 it is clear that when the cross sectional area of the pore, a, is reduced, k^* and q, the fluid flow rate through the pore are both reduced. By incorporating the new biofilm affected pore radius and resolving the flow equation at various time steps, the effects of biological growth can be seen in the model simulation results (Suchomel *et al.*, 1998).

The two network models presented by Dupin *et al*. (2001a, 2001b) and Suchomel *et al.* (1998) will not be considered for integration into the Parr *et al.* (2003) technology model as the reduction of hydraulic conductivity due to bioclogging is not explicitly defined in either of these models. In Dupin *et al*. (2001a; 2001b) the effects of bioclogging are captured through the manipulation of water viscosity, μ, while Suchomel *et al.* (1998) manipulates pore radius, a. In the next chapter, we will describe a methodology to select a bioclogging submodel to be incorporated into the Parr *et al.* (2003) technology model.

3.0 METHODOLOGY

3.1 INTRODUCTION

In this chapter, a bioclogging submodel will be selected for incorporation into the Parr *et al*. (2003) model of perchlorate biodegradation. A protocol for verifying that the modified model is operating as expected will then be developed. Next, a plan for conducting model simulations in order to investigate how bioclogging impacts the performance of an HFTW system being used to effect *in situ* perchlorate biodegradation will be presented. The final portion of this plan involves using the modified model to predict the extent of *in situ* perchlorate biodegradation effected through field scale application of an HFTW system at a perchlorate-contaminated site. The site, which will be described in detail in the next section, is the Aerojet Site, a relatively well-characterized site near Sacramento, California.

3.2 BIOCLOGGING SUBMODEL SELECTION CRITERIA

In order to select the bioclogging submodel, the following criteria will be applied to each of the submodels discussed in Chapter 2 of this work.

(1) Applicability of the submodel to the Aerojet Site

(2) Ease of determination of submodel input parameters

(3) Prior applications/validations of submodel

The following subsections detail the criteria and how the criteria will be applied to each submodel.

3.2.1 APPLICABLITY OF SUBMODEL TO THE AEROJET SITE

3.2.1.1 HISTORY AND LAYOUT OF THE AEROJET SITE

The HFTW field demonstration site is located within Aerojet General Corporation's 34.4 km^2 Sacramento, California facility which has been used for solid and liquid rocket engine development, testing, and production since 1951 (Shaw Environmental and Infrastructure, 2003). Past disposal practices have resulted in an extensive perchlorate and TCE groundwater plume which affects several fluvial aquifer units up to 91.44 meters below ground surface (bgs) (Shaw Environmental and Infrastructure, 2003). Figure 3.1, although not to scale, provides the reader with the spatial relationship of the three Aerojet perchlorate groundwater remediation studies mentioned in Chapter 2. The distance between the HFTW demonstration site and the GET D facility is approximately 914.4 meters (Shaw Environmental and Infrastructure, 2003).

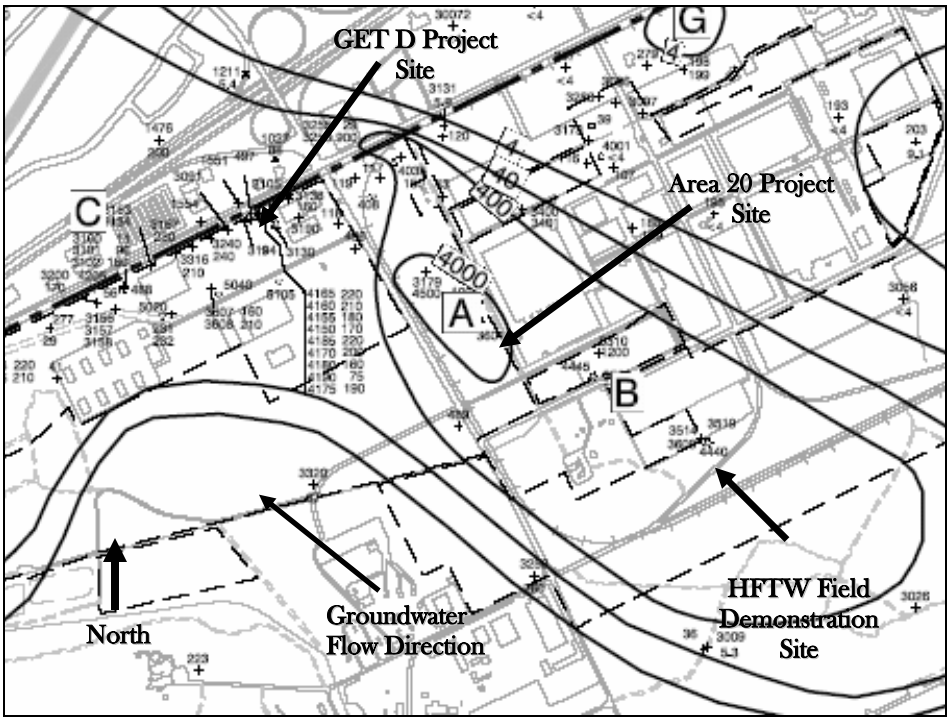

Figure 3.1 Location of perchlorate projects at Aerojet facility (after Shaw Environmental and Infrastructure, 2003)

The contours shown on Figure 3.1 are perchlorate concentrations in ppb at a depth approximately 30.48 to 60.96 meters bgs.

3.2.1.2 GEOLOGIC, HYDROGEOLOGIC, AND GEOCHEMICAL SITE CHARACTERISTICS

The soil composition of the HFTW demonstration site is mostly sand and silt with occasional interspersed gravel lenses; the average hydraulic conductivity at the Aerojet facility is approximately 21.336 m/day (Shaw Environmental and Infrastructure, 2003). Groundwater at the HFTW demonstration site flows with a gradient of approximately 0.017 m/m in a north-northwest direction; the first groundwater is encountered at a depth of 10.668 meters bgs (Shaw Environmental and Infrastructure, 2003). Six aquifer units identified as A (the shallowest) through F (the deepest) have been identified at the Aerojet site (Shaw Environmental and Infrastructure, 2003). The following table summarizes some of the key geochemical characteristics of the HFTW demonstration site. The data were obtained from four monitoring wells located at the site that are screened between 21.336 and 30.48 meters bgs (Shaw Environmental and Infrastructure, 2003).

Table 3.1 Geochemical characteristics of HFTW demonstration site

Parameter	Value
Redox	Aerobic and oxidizing
pH	6.7
Nitrate Concentration	13 mg/L
Sulfate Concentration	25 mg/L
TCE Concentration	2000 µg/L
Perchlorate Concentration	1000 µg/L
Dissolved Oxygen	2-5 mg/L

3.2.1.3 EXTENT OF PERCHLORATE CONTAMINATION

As stated earlier, the Aerojet site contains a perchlorate plume that is extensive in both the vertical and horizontal directions. The following perchlorate concentration contour maps of the shallowest aquifer units, A and B, depict the extent of perchlorate contamination near the HFTW demonstration site. Aquifer A is an unconfined aquifer which ranges in depth from 12.19 meters bgs to 30.48 meters bgs across the Aerojet facility; aquifer B ranges in depth from 18.29 meters bgs to 54.86 meters bgs (Aerojet General Corp., 2004). The units of the contour labels on Figure 3.2 and 3.3 are in ppb.

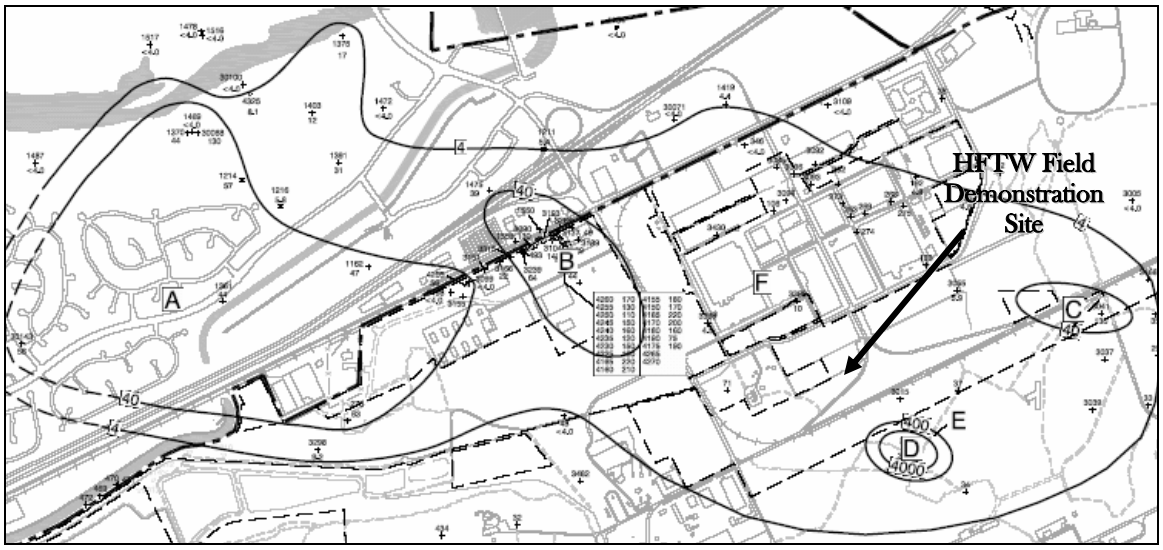

Figure 3.2 Perchlorate concentration contours in aquifer A (Shaw Environmental and Infrastructure, 2003)

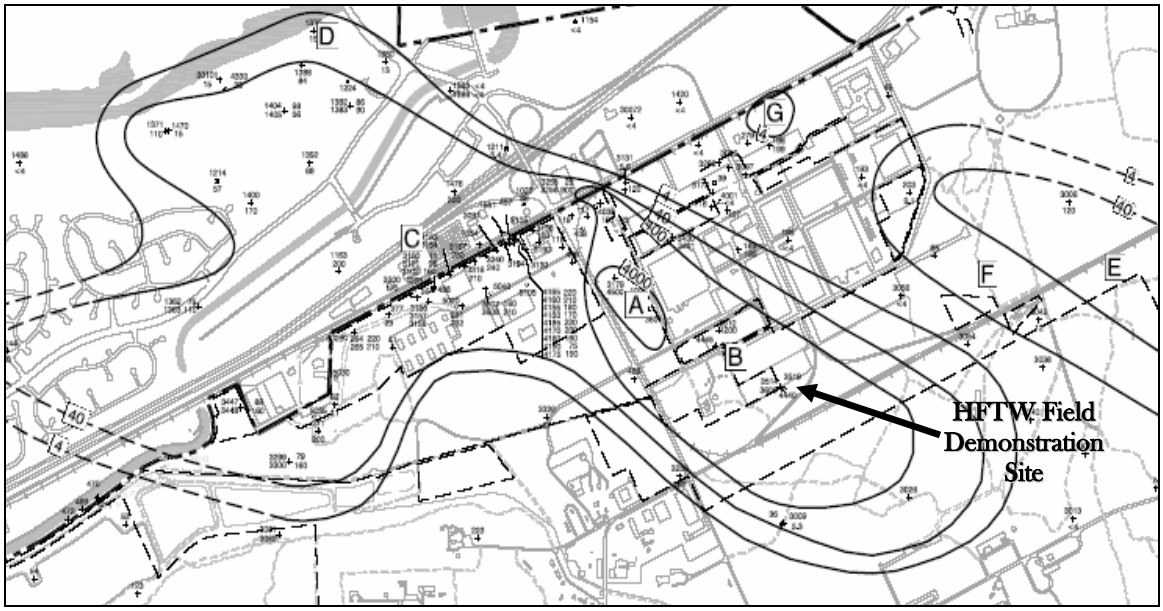

Figure 3.3 Perchlorate concentration contours in aquifer B (Shaw Environmental and Infrastructure, 2003)

Figures 3.2 and 3.3 clearly show that the majority of the perchlorate contamination beneath the Aerojet site is found in aquifer B. The HFTW demonstration site is between the 4,000 ppb and 400 ppb concentration contours of Figure 3.3. This is a much higher concentration range than is found in aquifer A, in which the HFTW demonstration site has perchlorate concentrations of 40 ppb – 400 ppb.

The vertical distribution of perchlorate at the demonstration site is further defined in the following table, which lists perchlorate concentration data obtained from various monitoring wells in the vicinity of the site (see Figure 3.4 for well locations). At the HFTW demonstration site, wells listed in Table 3.2 that penetrate to a depth of approximately 15.2 meters to 18.3 meters bgs can be considered to be in aquifer A while

wells deeper than this range can be considered to be in aquifer B (Aerojet General Corp., 2004).

Table 3.2 Vertical distribution of perchlorate near HFTW demonstration site (Shaw Environmental and Infrastructure, 2003)

Well	Perchlorate (µg/L)	Screen Interval (m bgs)
3628	330	15.85 – 17.37
3629	1,500	24.38 – 25.91
3630	3,140	29.26 – 30.79
3632	65	10.97 – 12.50
3632	155	15.85 – 17.37
3633	3,350	29.87 – 31.39
3627	970	22.86 – 28.96
3519	2,320	23.77 – 31.39
3514	3,920	23.47 – 27.43
4440	3,300	22.86 – 28.35 and 29.87 – 32.31

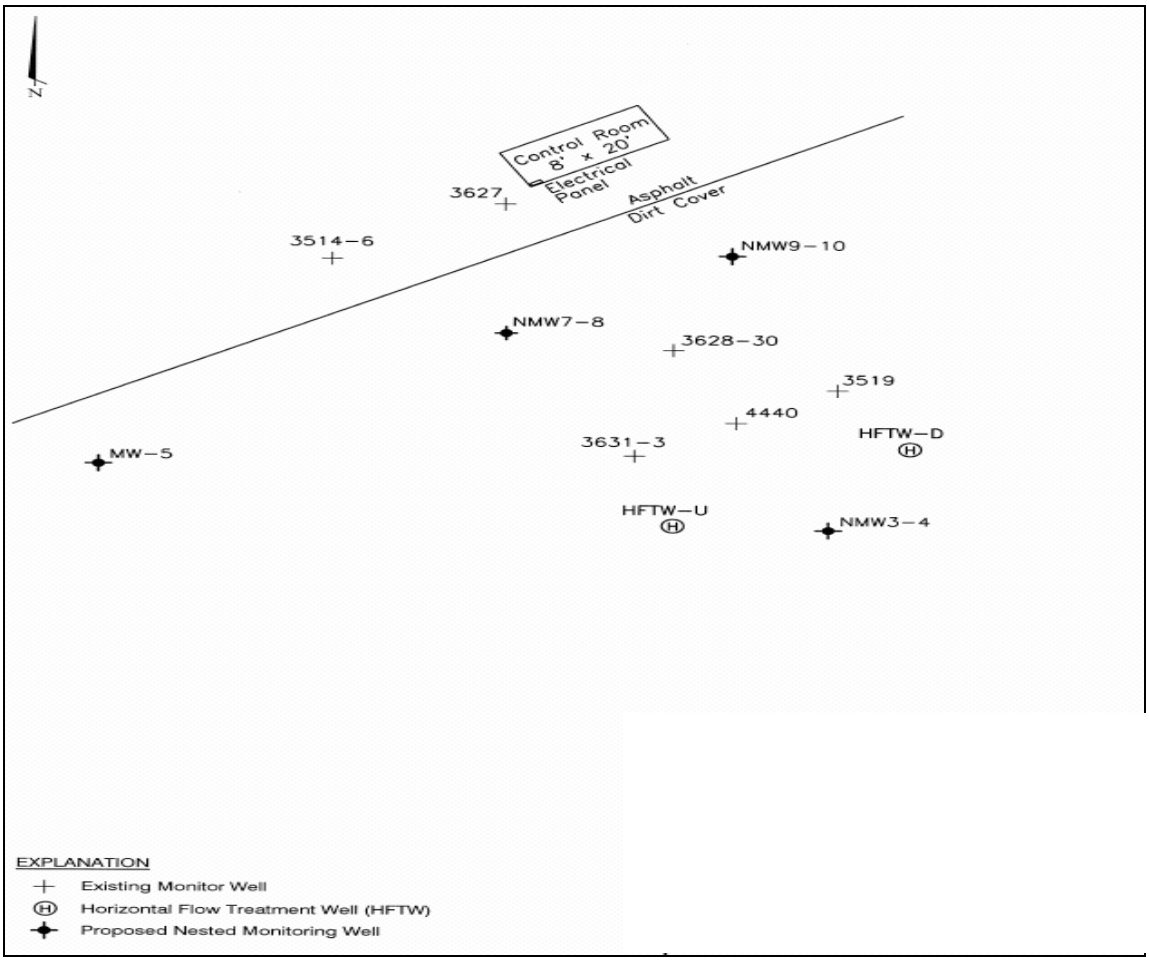

Figure 3.4 Plan view of HFTW demonstration site (Shaw Environmental and Infrastructure, 2003)

It is apparent from Table 3.2 that higher perchlorate concentrations at the HFTW demonstration site are located deeper in the aquifer. Perchlorate concentrations are particularly elevated in groundwater samples taken between 27.43 and 30.48 meters bgs**.** This observation agrees with the perchlorate contamination contours shown in Figure 3.2 and Figure 3.3 as well.

The hydrogeology, geochemistry, and perchlorate concentration at the HFTW demonstration site do not provide a basis for eliminating any of the bioclogging submodels under consideration for integration into the technology model developed by Parr *et al.* (2003). In the next section we will discuss the second selection criterion, the ease of determination of submodel input parameters.

3.2.2 EASE OF DETERMINATION OF SUBMODEL INPUT PARAMETERS

In this subsection the parameters of each bioclogging submodel will be discussed. Particular emphasis will be placed on the ease of determining submodel parameters. Those models that rely on arbitrarily determined parameters will be considered less desirable than submodels that depend upon measurable parameters. The models will be reviewed in the same order as they were presented in section 2.8.6.

The Kozeny-Carmen relationship, Equation 2.10, depends upon the specific surface area (surface area per unit porous medium volume) of the porous medium. Bear (1972) points out that no direct method of measuring the specific surface area of a porous medium exists. Only statistical and indirect methods of determining specific surface are available;

different values of the specific surface area are calculated depending upon the measurement method employed (Bear, 1972). To further complicate matters, application of the Kozeny-Carmen relationship requires knowing the specific surface area of both the clean and bioclogged medium, requiring that the area be estimated both before and after biogrowth.

The macroscopic approach to mathematically describing bioclogging put forth by Clement *et al*. (1996) and Kildsgaard and Engesgaard (2001), Equation 2.12, depends upon the ability to accurately determine the density of the solid phase biomass growing in the porous media, ρ_b, and the solid biomass concentration, X_s, in order to determine fraction of the total volume occupied by biomass, n_b, using Equation 2.11 While ρ_b and X_s may be difficult to accurately measure, n_b can be approximated by subtracting the clogged porosity from the original porosity. Bear (1972) outlines several methods by which the porosity of a porous media can be determined.

As reported in Vandevivere *et al*. (1995), the bioclogging ratio developed by Ives and Pienvichitr (1965) depends upon a parameter, α, which according to Equation 2.9 is a ratio of porosities that can be determined with relative ease. In this model, it is the dimensionless parameter, p, which depends upon the tortuosity and pore diameter variations in the porous media that is difficult to measure.

Chu *et al*. (2003) used a variation of the Ives and Pienvichitr (1965) model in which the parameter, p, is set equal to 0.5 to describe the reduction of hydraulic conductivity due to

the growth of uniform biofilm (Equations 2.14 and 2.15). While this model is less flexible than the Ives and Pienvichitr (1965) model, the resulting hydraulic conductivity ratio is based on measurable quantities, not arbitrary constants.

The model developed by Taylor *et al*. (1990a), Equations 2.16 through 2.19, is based on the assumption that a uniform biofilm of thickness, L_f, coats spherical particles of equal radius. The geometric parameters of this model, α_m and m, are set based upon the assumed packing configuration of the porous media. Accurately measuring the thickness of the biofilm, L_f, at the pore scale is difficult, but possible; destructive laboratory methods exist. Additionally, Cunningham *et al*. (1991) indicate that an estimate of biofilm thickness can be obtained using the following equation.

$$L_f = \frac{n_b * V_t}{S} \qquad (3.1)$$

where

n_b = *fraction of total volume occupied by biomass*

V_t = *total volume of sample*

S = *total surface area of the porous media sample*

Obtaining a value of S for use in Equation 3.1 is difficult, particularly for a field sample.

Several of the parameters of the second model developed by Taylor *et al*. (1990), Equations 2.20 and 2.21 are difficult to determine. First, the hydraulic conductivity ratio depends upon the maximum and minimum pore radius of the porous medium, both of which are difficult to measure. Second, according to Vandevivere *et al*. (1995) the pore

size distribution index, λ, is inversely related to the variance of the pore size distribution. Vandevivere *et al*. (1995) point out the fact that the variance of the pore sizes may not necessarily be related to any other measure of the geometry of the pore space, causing clay and sand to potentially have the same λ value. In light of the discussion in Chapter 2, the pore size geometry plays a significant role in determining the extent to which bioclogging impacts hydraulic conductivity. Therefore, the potential exists to incorrectly model the effects of bioclogging on hydraulic conductivity by using a parameter that is insensitive to the pore geometry.

The second bioclogging model proposed by Chu *et al*., (2003), Equations 2.23 and 2.24, assumes that biomass accumulates in plugs within the pore space. All of the parameters contained in these two equations are measurable. The hydraulic conductivity of the biological plug is set equal to the experimentally observed minimum hydraulic conductivity resulting from biogrowth (Taylor *et al*., 1990a).

The final model under consideration, Equation 2.25, has two parameters which are arbitrary in nature. First, the enveloping factor, β, defined as the amount of the colony enveloping space occupied by biomass, is difficult to measure. While Seki and Miyazaki (2001) used 3-dimensional scanning electron microscopy to visually estimate a value of 0.2 for β; they readily point out that one of the limitations of their bioclogging submodel is that reliable techniques to measure β for various soil types have not been developed. The shape factor, τ, which is defined as the ratio of the volume of the solid phase to S^3,, where S is the characteristic length of the solid phase, is given a value of one based on

previous work conducted by the author (Miyazaki, 1996). Lastly, *S* was defined as the mean particle diameter during the validation simulations. The authors comment that this is a valid assumption for uniform particles, but not for non-uniform natural soils. Seki and Miyazaki (2001) also point out that *S* cannot be directly measured. The next subsection evaluates the extent to which each model has been validated by comparison to experimental data and whether or not the bioclogging submodel has been used in other modeling efforts.

3.2.3 PRIOR APPLICATIONS/VALIDATIONS OF SUBMODELS

Kildsegaard and Engesgaard (2001) used the model developed by Clement *et al*. (1996) to model the effects of bioclogging induced by a nitrate reducing strain of bacteria that used acetate as an electron donor. In this experiment Brilliant Blue was used as a tracer and an image analysis technique was used to convert digital snapshots of the tracer movement into a concentration map. This map of tracer concentration showed the extent and location of biological growth and its effect on tracer movement through a two dimensional box. The model developed by Kildsegaard and Engesgaard (2001) provided fair simulations of the observed Brilliant Blue movement through the sandbox. Much of the discrepancy between the observed tracer movement and the simulations was attributed to the fact that sorption of Brilliant Blue is related to the concentration of biomass within the sandbox; and this relationship was not included in the flow-transport-reaction model.

Taylor and Jaffé (1990c) provide validation for Equations 2.20 and 2.21. However, the authors concede that directly measuring the thickness of the biofilms grown in their experiments was not possible. Therefore, Taylor and Jaffé (1990c) were not able to directly test their model against experimental data. Instead, the model was used to parameterize a one dimensional substrate transport equation which was subsequently used to fit data from the column experiments discussed in Taylor and Jaffé (1990a). This technique provided a good fit to experimental data when the specific surface area of the porous medium was determined by fitting the substrate transport model curve to previous column experiment results (Taylor and Jaffé, 1990c).

The bioclogging model of Seki and Miyazaki (2001) provides a good fit to the experimental data reported in Vandevivere *et al*. (1995). The colony enveloping space, β, and the colony thickness, L_b, were determined from the reported biovolume ratio and hydraulic conductivity ratio (Seki and Miyazaki, 2001). The results are shown in Figure 3.5.

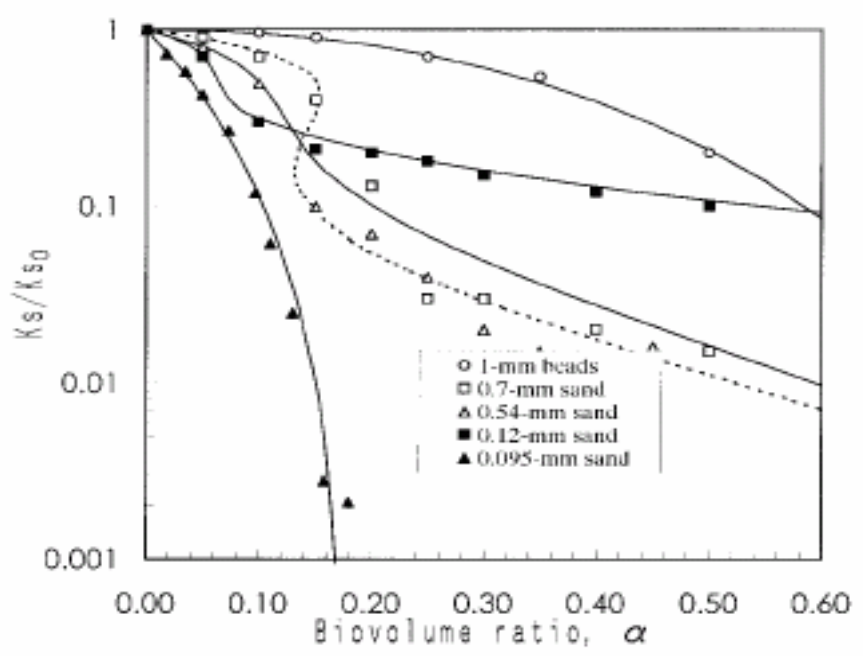

Figure 3.5 Seki and Miyazaki bioclogging model fit to experimentally determined hydraulic conductivity reduction (Seki and Miyazaki, 2001)

Figure 3.6 compares the hydraulic conductivity ratio vs. biovolume ratio predicted by four of the models under consideration: Kozeny-Carman, Ives and Pienvichitr, Taylor *et al*. model #2, and the Seki and Miyazaki model to the experimental data for 1-mm glass beads and 0.12 mm sand provided by Cunningham *et al*. (1991).

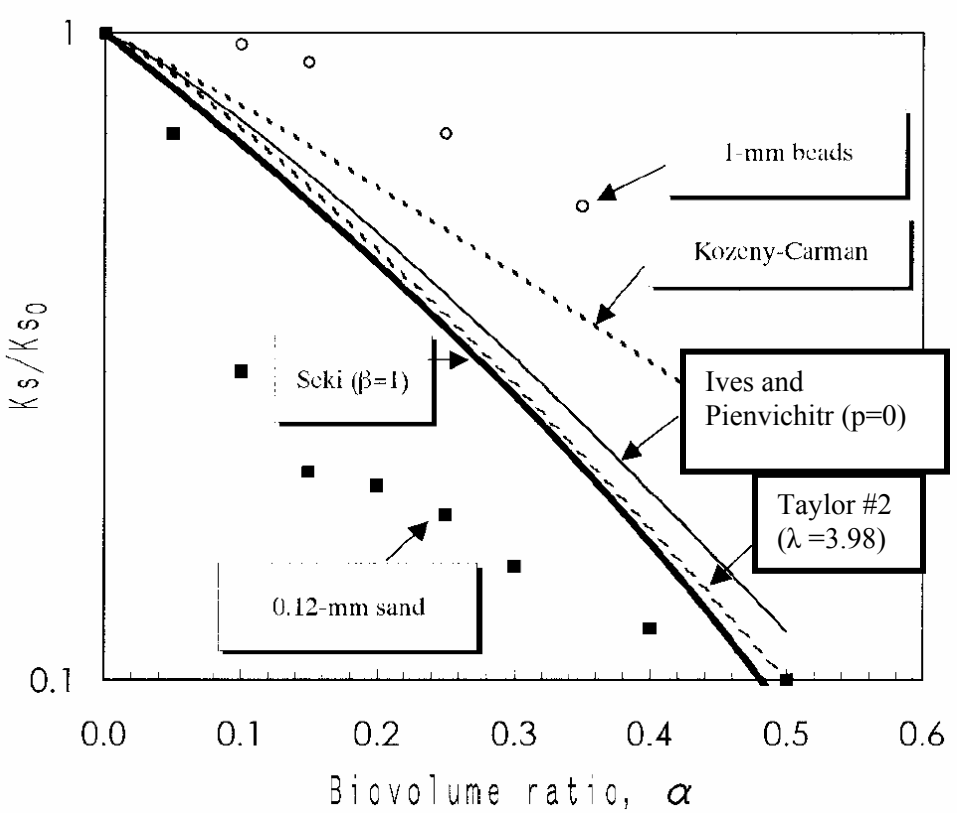

Figure 3.6 Hydraulic conductivity ratio vs. α predicted by various bioclogging submodels (Seki and Miyazaki, 2001)

It is obvious from the above figure that none of the submodels being considered very closely simulate the experimental data. It is worth noting that the Seki curve shown in Figure 3.7 was obtained with β=1, which by definition is a uniform biofilm; varying β would result in different shaped curves as can be seen in Figure 3.6 where the Seki and Miyazaki (2001) model successfully fit the experimental data. Finally, one must consider that the experimental data shown in Figure 3.6 were obtained using particles of uniform diameter. Bioclogging in natural soils made up of both coarse and fine particles may exhibit behavior more in line with submodel simulations.

3.2.4 SUBMODEL SELECTION

Table 3.3 summarizes the application of the various selection criteria discussed in the previous subsections to the eight bioclogging submodels under consideration. The placement of an "X" in the box indicates that the submodel has been determined to meet the criterion.

Table 3.3 Submodel selection criteria summary

Model	Applicability to Aerojet Site	Ease of Parameter Determination	Model Validation
Kozeny-Carman (Vandevivere *et al*., 1995) – Equation 2.10	X		X
Clement *et al*. (1996) – Equation 2.12	X	X	X
Ives and Pienvichitr (1965) – Equation 2.13	X		X
Chu Model #1 Chu *et al*. (2003) – Equation 214 and Equation 2.15	X	X	
Taylor Model #1 (Taylor *et al*., 1990a) – Equation 2.16 thru Equation 2.19	X		
Taylor Model #2(Taylor *et al*., 1990a) – Equation 2.20 and Equation 2.21	X		X
Chu Model #2 Chu *et al*. (2003) – Equation 2.23 and Equation 2.24	X	X	
Seki and Miyazaki (2001) – Equation 2.25	X		X

A review of Table 3.3 shows that the Clement *et al*. (1996) model may be the most appropriate bioclogging submodel to choose for incorporation into the perchlorate biodegradation flow-transport model. The following discussion details the thinking behind selection of the Clement *et al*.(1996) bioclogging submodel as the model that best satisfies the proposed selection criteria.

If the simplicity of the submodel is considered in terms of the number of required parameters and the amount of computational effort required, both submodels from Taylor *et al*. (1990a) along with the Seki and Miyazaki (2001) bioclogging submodel can be

eliminated from consideration. Furthermore, upon review, the models of Ives and Pienvichitr (1965), Clement *et al*., (1996), and Chu Model #1 (Chu *et al*., 2003) are essentially identical. In spite of the fact that each submodel was developed based upon different assumptions, the only difference between the three lies in the form of the exponent. Of these three submodels, Ives and Pienvichitr (1965) and Chu Model #1 (Chu *et al*., 2003) assume that biological growth in a porous media occurs as a biofilm. In the absence of experimental evidence that this assumption is valid for our system, these models are considered inferior to the Clement *et al*. (1996) bioclogging submodel which takes a macroscopic view of bioclogging and makes no assumptions regarding the morphology of the biological growth. Murray (2002) suggests that numerical models which leave out as much detail as possible provide the clearest picture of the mechanisms responsible for the experimentally observed behavior. If a model includes numerous complicated processes and interactions, insight into how the behavior of interest comes about is often lost and the model is no better at explaining the behavior than direct observations of the behavior itself (Murray, 2002).

Murray (2002) also points out that ensuring the accuracy of the details of a model simulating a small scale process thought to be responsible for a large scale phenomenon is essential to building an accurate model. Unexpected model output may result if the variables of the model cannot be accurately measured or their relationship to the behavior of interest is incorrectly modeled (Murray, 2002). This is especially true in the case of modeling bioclogging of a porous medium where pore geometry, grain size, grain type, temperature, moisture content, microorganisms present in the subsurface, metabolic

substrates used, and the biological metabolic mechanisms may all influence how, where, and to what extent biological entities are able to reduce the hydraulic conductivity of a porous medium. However, accurately measuring many of these properties is nearly impossible and the way these properties interact to affect bioclogging is poorly understood; therefore, a model which seeks to associate these properties with hydraulic conductivity reduction should be viewed with suspicion.

The use of a macroscopic bioclogging model is further justified when one considers the scales being modeled. The behavior of interest in the present work is the macro scale effects on groundwater flow and contaminant transport of a micro scale process, biological growth reducing the hydraulic conductivity of a porous media. Using pore scale assumptions such as the spatial configuration of biological mass in conjunction with flow equations, such as Darcy's law, that disregard flow in individual pores has a "conceptual disparity in problem scale" (Clement *et al*., 1996). Also, Murray (2002) states that models which simulate processes on a commensurate scale offer better explanations of how and why a behavior occurs compared to models that simulate the dynamics of the process of interest at a smaller scale.

Based on the principle that macroscopic bioclogging submodels are superior to those submodels that make assumptions regarding the morphology of the biological growth, Chu Model #2 (Chu *et al*. 2003) can be eliminated from consideration because it assumes that biomass accumulates as plugs in the interstitial space of the porous media. Finally, the Clement *et al*. (1990a) submodel is considered better than the Kozeny-Carman

(Vandevivere *et al*., 1995) bioclogging submodel because the Kozeny-Carman (Vandevivere *et al*., 1995) model depends upon the specific surface area of the porous media, which may be difficult to determine.

3.3 TECHNOLOGY MODEL DESCRIPTION

The technology model developed by Parr *et al*. (2003) to describe HFTW application to treat perchlorate-contaminated groundwater combines steady state flow, advective/dispersive transport of dissolved electron donor (ethanol), perchlorate, and competing electron acceptors, equilibrium sorption of electron donor, and biodegradation of donor and acceptors. The model further assumes that the perchlorate degrading microorganisms are immobile (Parr *et al*., 2003). The reader is referred to the Appendix for a detailed description of the model equations. In the Parr *et al*. (2003) model, MODFLOW (Waterloo Hydrogeologic Inc, 1999) is used to calculate the three-dimensional steady state flow velocities within the simulated aquifer. The steady state flow field is then used in the transport equations. Additional equations which make up the technology model include Monod equations to describe consumption of ethanol or other electron donors, consumption of perchlorate and competing electron acceptors (oxygen and nitrate) and a microbial growth/decay equation. The technology model used in this study includes all of the above elements from the Parr *et al*. (2003) model, coupled with the Clement *et al*. (1996) bioclogging model. The values of the biological parameters used in the model will be similar to those used in Parr *et al.* (2003) except where modifications are necessary to account for the use of ethanol as an electron donor.

The flow diagram in Figure 3.7 describes how the different model elements interact.

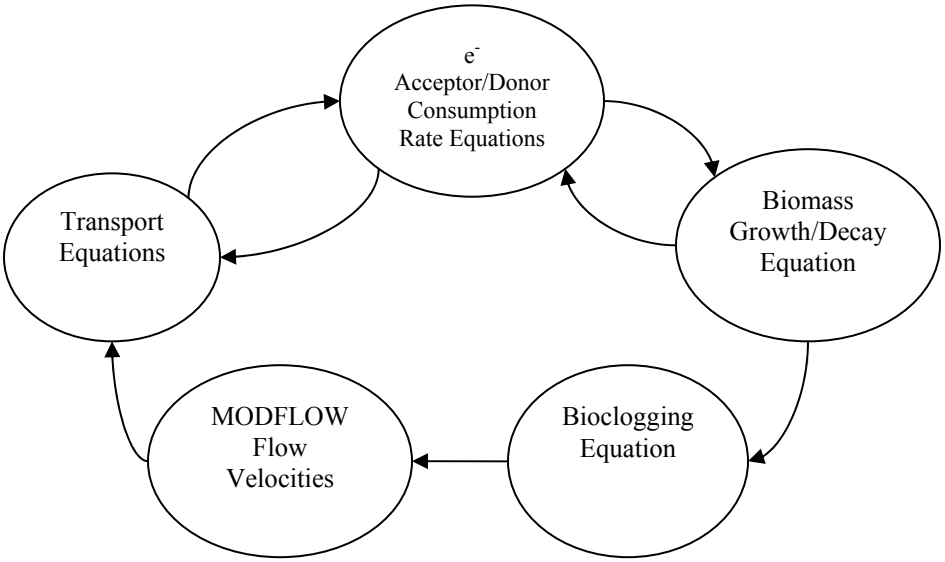

Figure 3.7 Technology model flow diagram

Each bubble in Figure 3.7 represents an equation or collection of equations describing an element of the technology model. The arrows represent how the output of one element is used as input by another element. For example, MODFLOW is used to calculate the three-dimensional steady state flow field for a set of aquifer conditions (hydraulic conductivities and hydraulic head boundary conditions). The reader is referred to the Appendix for a description of the model space used to determine the groundwater flow field in this study. The flow velocities obtained from MODFLOW are then used to determine the electron donor/acceptor advection terms in the three-dimensional advection/dispersion transport equations. These terms are then used, in conjunction with the various electron donor/acceptor consumption rate equations and biomass growth/decay equations, to determine the concentration of each electron donor/acceptor,

as well as biomass, as a function of space and time. The biomass concentration at each point in space is then used by the bioclogging equation to determine the extent of hydraulic conductivity reduction at that spatial coordinate. Finally, the resultant hydraulic conductivity is used by MODFLOW to recalculate the flow velocities within the system and the process begins again. The technology model allows the user to specify how often MODFLOW updates the flow field. Typically the flow field is updated by MODFLOW every other transport time step. This is possible because the microbial growth that affects the flow field by bioclogging is relatively slow in comparison to advection, though it is noted that reducing the number of MODFLOW simulations does not result in a significant reduction in model run time. The following mass removal tables, which show the mass of each constituent removed via biological degradation, were obtained from 360-day simulations where the flow field is updated every transport time step (Table 3.5) and every other transport time step (Table 3.4). The tables show very little difference in results when all other model parameters are held constant. The negative value in the amount of biomass removed indicates the amount of biomass grown during the simulation. The run times for both simulations approached ten hours.

Table 3.4 Mass of constituent removed, flow field updated every other time step

	Electron Donor	Oxygen	Nitrate	Perchlorate	Biomass
Mass Injected (g)	43,163,000	0	0	0	0
Mass Removed (g)	208,540	101,000	99,853	23,931	-3,008.7

Table 3.5 Mass of constituent removed, flow field updated every time step

	Electron Donor	Oxygen	Nitrate	Perchlorate	Biomass
Mass Injected (g)	43,163,000	0	0	0	0
Mass Removed (g)	208,540	101,000	99,850	23,928	-3,008.5

Table 3.4 and Table 3.5 show the amount of electron donor added during the 360-day simulations. A 60,000 g/day loading rate was used for the two injection screens of the HFTW system. Thus, the mass loaded for a 360-day simulation should be 43,200,000 grams. The model output indicates 43,163,000 grams were injected during each simulation. The difference in values may be attributed to truncation errors inherent to the finite difference solution technique employed by the technology model. The parameters for these two simulations were set to the baseline conditions as described in the Appendix. The baseline results will be discussed in more detail in Chapter 4.

3.4 SUBMODEL ANALYSIS

The basic technology model was tested by Parr (2002) and Parr *et al*. (2003). The reader is referred to these works for the details of the technology model verification process. It is assumed that the verification process carried out by Parr *et al.* (2003) is accurate and that the basic technology model is operating correctly. As such, this study will investigate the behavior of the bioclogging submodel by varying the bioclogging submodel parameters in order to determine that the submodel is operating as expected.

The first simulation to test the bioclogging submodel will examine a scenario where the biomass has accumulated to the point where flow is significantly restricted. This situation will be simulated by setting the parameter X_{as}, the maximum biomass concentration, which is used in the bioclogging relationship, to 12000 mg/L and the biomass decay rate, b, will be set to 0 day^{-1}. These adjustments will make the hydraulic conductivity reduction very sensitive to any accumulation of biomass within the porous

media. The next bioclogging submodel analysis simulation will involve a situation where the growing biomass has very little effect on the flow characteristics of the aquifer. This situation will be simulated by setting the value of p in Equation 2.12 equal to 0. Each of the bioclogging submodel test simulations will be conducted with a site model which represents the Aerojet site as described in the Appendix.

3.5 TECHNOLOGY MODEL SIMULATIONS

Once the bioclogging submodel test simulations have been run, and the technology model is deemed to be operating correctly, a series of simulations will be conducted in order to evaluate the effect that varying the dosing schedule, well flow rate, and electron donor (ethanol) concentration has on HFTW system performance, in terms of total perchlorate mass removed and the perchlorate concentration realized at down gradient monitoring wells at the Aerojet site. Simulations with a baseline dosing schedule, time-averaged electron donor concentration, and treatment well pumping rate will be run (Table 3.6) to establish how the HFTW technology performs. Next, a set of simulations will investigate the effect dosing schedule has upon HFTW system performance (Table 3.6). Additional simulations will look at how varying the electron donor concentration and treatment well pumping rate affects the performance of the HFTW technology (Table 3.6).

Table 3.6 Simulation schedule

Simulation Number	Time-Averaged Ethanol Concentration (mg/L)	Dosing Schedule (hrs on/hrs off)	Pumping Rate (m^3/day)
Baseline	600	8/0	100
1	200	8/0	100
2	400	8/0	100
3	800	8/0	100
4	1000	8/0	100
5	1200	8/0	100
6	600	7/1	100
7	600	6/2	100
8	600	5/3	100
9	600	4/4	100
10	600	3/5	100
11	600	2/6	100
12	600	8/0	75
13	600	8/0	50
14	600	8/0	25
15	600	8/0	10

Each of the above simulations will produce concentration distributions in time and space for the various electron acceptors (O_2, NO_3^-, and ClO_4^-), ethanol, and biomass. Perchlorate concentration profiles at the various observation wells will be presented for each of the simulations tabulated in Table 3.6 along with the total amount of perchlorate mass removed from the system during each simulation.

A final result of the various simulations conducted using the Aerojet site parameters will be to propose an electron time averaged concentration, an electron dosing strategy, and a treatment well pumping rate for the Aerojet site field demonstration of perchlorate

biodegradation via HFTW technology. This recommendation will be based solely on observed results of the simulations outlined above. No effort to optimize the technology model will be undertaken at this time.

4.0 RESULTS AND ANALYSIS

4.1 INTRODUCTION

In this chapter we present and discuss the results obtained by applying the integrated technology model, that is, the HFTW technology model as described by Parr *et al.* (2003) combined with a bioclogging model (as described in Chapter 3), to the perchlorate contaminated Aerojet site located in Sacramento, California. We begin the chapter by verifying that the model is operating correctly. Once the model is verified, we conduct a sensitivity analysis by varying the time averaged concentration of the electron donor, the HFTW pumping rate, and the electron donor pulsing schedule in order to determine the effect of these engineered parameters on system performance, with performance quantified in terms of perchlorate mass removed and down-gradient perchlorate concentration.

4.2 SUBMODEL ANALYSIS

As discussed in Chapter 3, the base technology model developed by Parr *et al.* (2003) was assumed to be operating correctly. In this section we investigate the behavior of the bioclogging submodel by varying the bioclogging submodel parameters. First, the parameter X_{as}, the maximum biomass concentration, which is used in the bioclogging relationship, was set to 12000 mg/L and the biomass decay rate, b, was set to 0 day^{-1}. These adjustments make the model extremely sensitive to any biomass growth.

The following figure shows the porosity of the aquifer in layer 3 after 360 days of continuous injection of donor assuming no biomass decay and a low maximum biomass concentration.

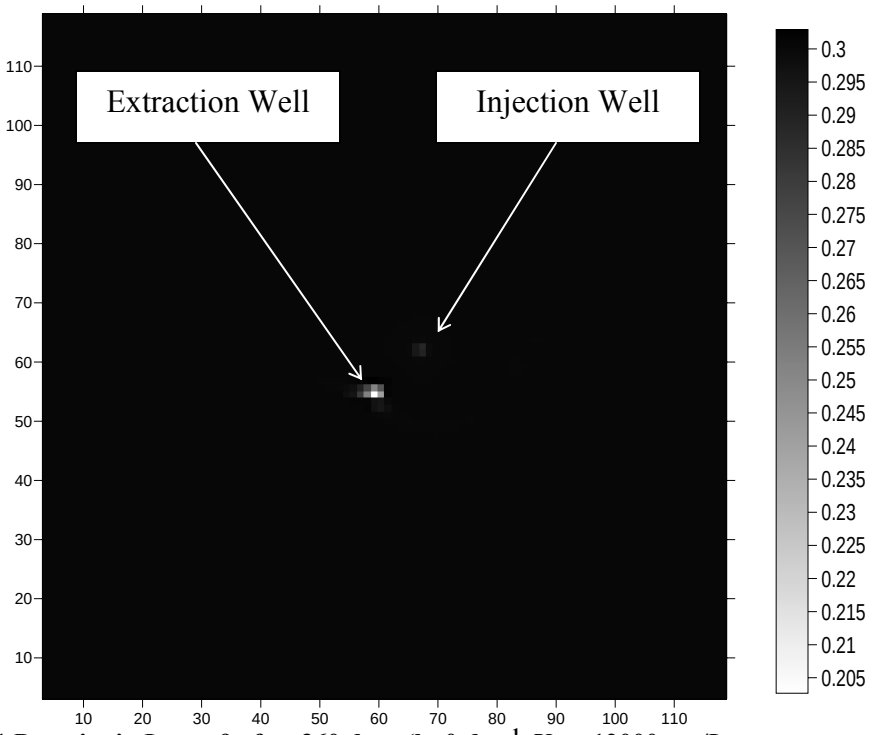

Figure 4.1 Porosity in Layer 9 after 360 days (b=0 day^{-1}, Xas=12000 mg/L, pump rate =100m^3/d, TAC=600 mg/L, continuous donor injection)

We see from Figure 4.1 that the porosity only changes in a small portion of the aquifer directly adjacent to the treatment wells located in layer nine, with a more pronounced reduction near the extraction well. Figure 4.2 shows a similar trend of increased porosity reduction near the extraction well in layer 3.

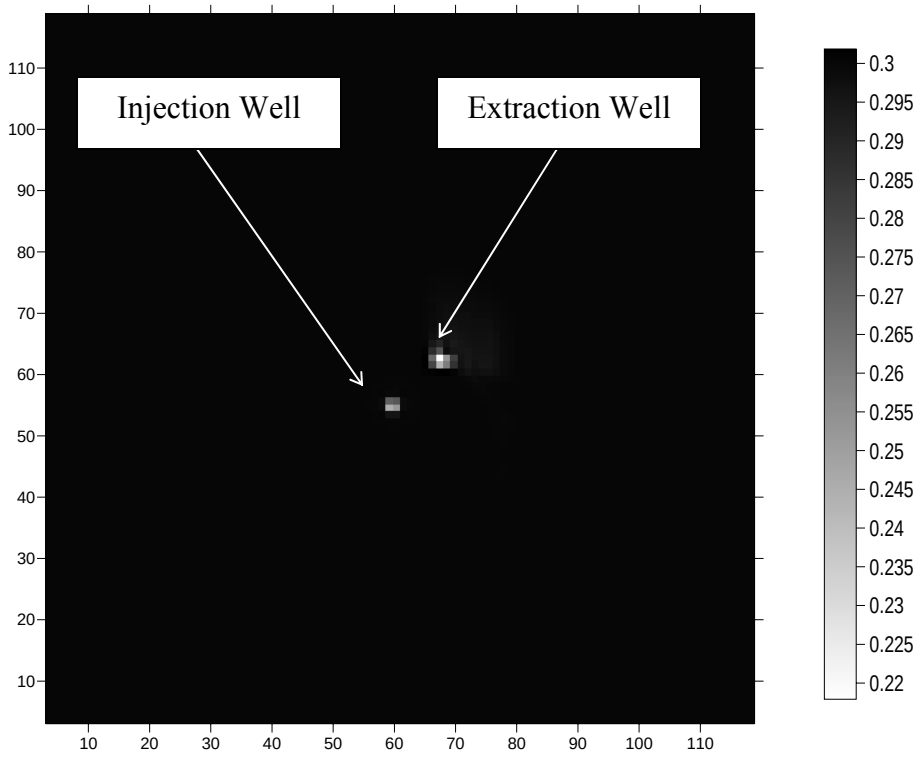

Figure 4.2 Porosity in Layer 3 after 360 days (b=0 day^{-1}, Xas=12000 mg/L, pump rate =100m^3/d, TAC=600 mg/L, continuous donor injection)

The porosity decrease is due to the accumulation of biomass that reduces the pore space available for groundwater to flow. At the electron donor injection wells, water with a high electron donor concentration is added to the aquifer. Therefore, biological growth is higher in the regions adjacent to the injection wells and the porosity decreases due to this biogrowth as evident in Figure 4.1 and Figure 4.2.

Biogrowth also occurs near the extraction well in Figure 4.1 and Figure 4.2. This occurs because near the extraction well screen electron donor-amended water that has flowed from the HFTW injection screens is mixed with water containing electron acceptors that is being captured from upgradient.

It was also noted from the figures that the porosity reduction in layer 9 was greater near the extraction well than near the injection well, while the porosity appears to be impacted to the same extent near both injection and extraction wells in layer 3. This difference may be due to the different electron acceptor concentrations in layer 9 and layer 3. While oxygen and nitrate concentrations are the same in all layers, the perchlorate concentration increases with depth; it is 2 mg/L in layer 3 and 4 mg/L in layer 9. In layer 3, water from layer 9 is mixed with electron donor and injected. This water has a higher concentration of electron donor and electron acceptor which results in a larger amount of biogrowth and porosity reduction near the injection well. Conversely, the injection well in layer 9 is injecting water from layer 3 which has a lower electron acceptor concentration and consequently, a smaller reduction in porosity is realized. Similarly, the porosity reduction at the extraction well in layer 9 is greater than the porosity reduction at the extraction well in layer 3 due to the availability of more electron acceptor in layer 9 due to higher perchlorate concentrations in that layer.

Figures 4.3 and 4.4 depict vertical cross-sections of the porosity distribution due to biological growth, as well as the resulting flow field. The location of each vertical cross section is shown in Figure 4.5.

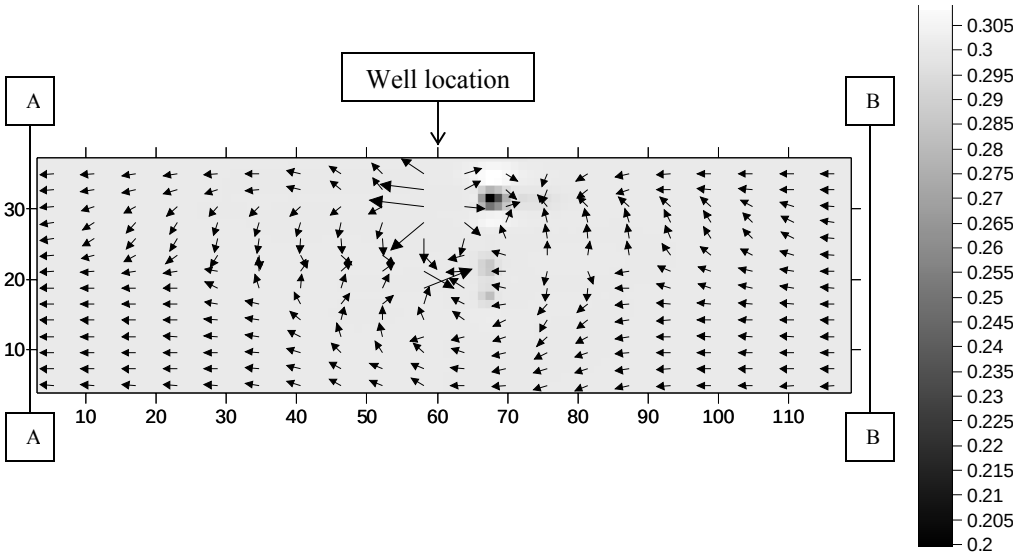

Figure 4.3 Vertical distribution of porosity and flow field along x-axis (Section A-B) after 360 days: b=0 day^{-1}, Xas=12000 mg/L, pump rate =100m^3/d, TAC=600 mg/L, continuous donor injection

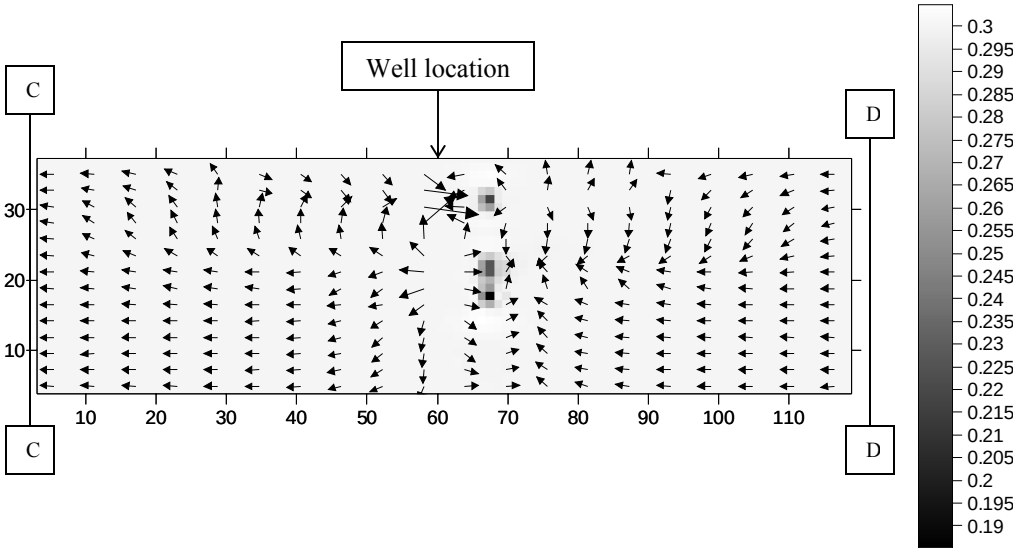

Figure 4.4 Vertical distribution of porosity and flow field along y-axis (Section C-D) after 360 days: b=0 day^{-1}, Xas=12000 mg/L, pump rate =100m^3/d, TAC=600 mg/L, continuous donor injection

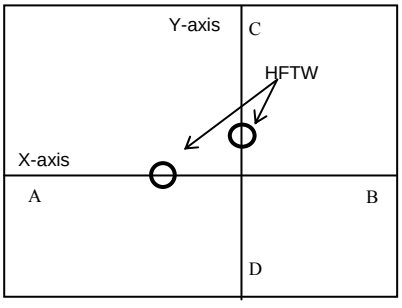

Model space schematic (NTS)

Figure 4.5 Model space schematic showing location of vertical cross sections

The porosity reductions shown in Figure 4.3 and Figure 4.4 have several effects on groundwater flow. First, the groundwater tends to flow around the regions of low porosity. This fact is evident by observing the direction of the flow vectors near the low porosity regions in Figure 4.3 and Figure 4.4. Given the fact that the porosity reduction is due to the accumulation of biological growth, it stands to reason that the treatment efficiency of the HFTW system is negatively impacted when groundwater bypasses regions of low porosity/high biomass since it is the biomass that is responsible for perchlorate degradation. It is interesting to note that the biomass does not grow directly adjacent to the well screens. Instead, the biogrowth occurs a few meters away from the well due to the slow growth kinetics of the perchlorate respiring bacteria used in this study.

Also note from Figure 4.6 that the groundwater velocity may increase due to the reduced pore area available to groundwater flow in the region of reduced porosity. Recall that the flow rate in the wells is held constant during the simulations. Since the pore volume available for flow is decreasing in the regions of biogrowth, the flow rate can only remain constant if there is an increase in groundwater velocity through these regions. From Figure 4.6 we see that the ethanol concentrations are higher farther away from the treatment wells during the simulation where the biological decay rate is reduced to zero and the maximum biomass concentration is reduced to 12000 mg/L than during the baseline simulation. The wider distribution of ethanol into the aquifer during the

simulation may be a result of higher groundwater velocities induced by the reduction of porosity near the treatment wells.

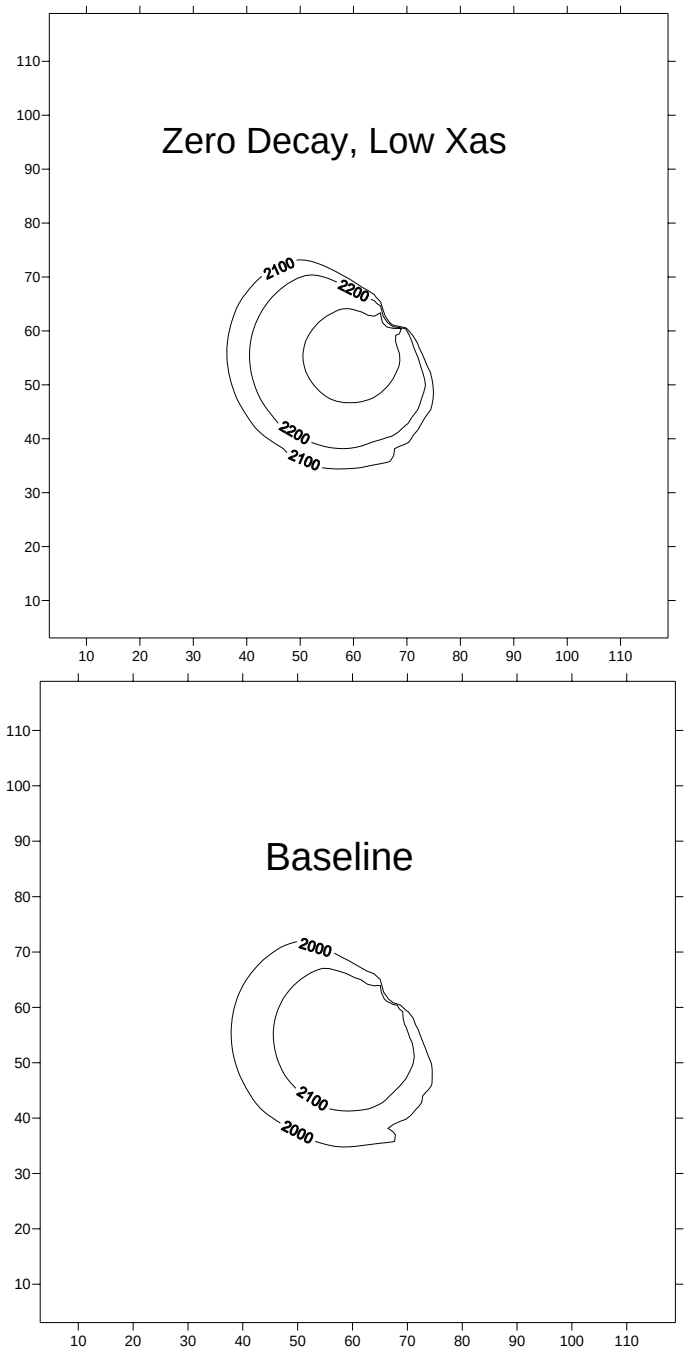

Figure 4.6 Ethanol concentration contours (mg/L) in layer 3 after 360 days (a) assuming no biomass decay and low maximum biomass concentration (b=0 day^{-1}, Xas=1200 mg/L, pump rate =100m^3/d, TAC=600 mg/L, continuous donor injection) and (b) baseline conditions

The final piece of evidence that suggests that the groundwater velocity may increase due to the biological growth that occurs near the well screens is the vertical distribution of hydraulic head within the aquifer.

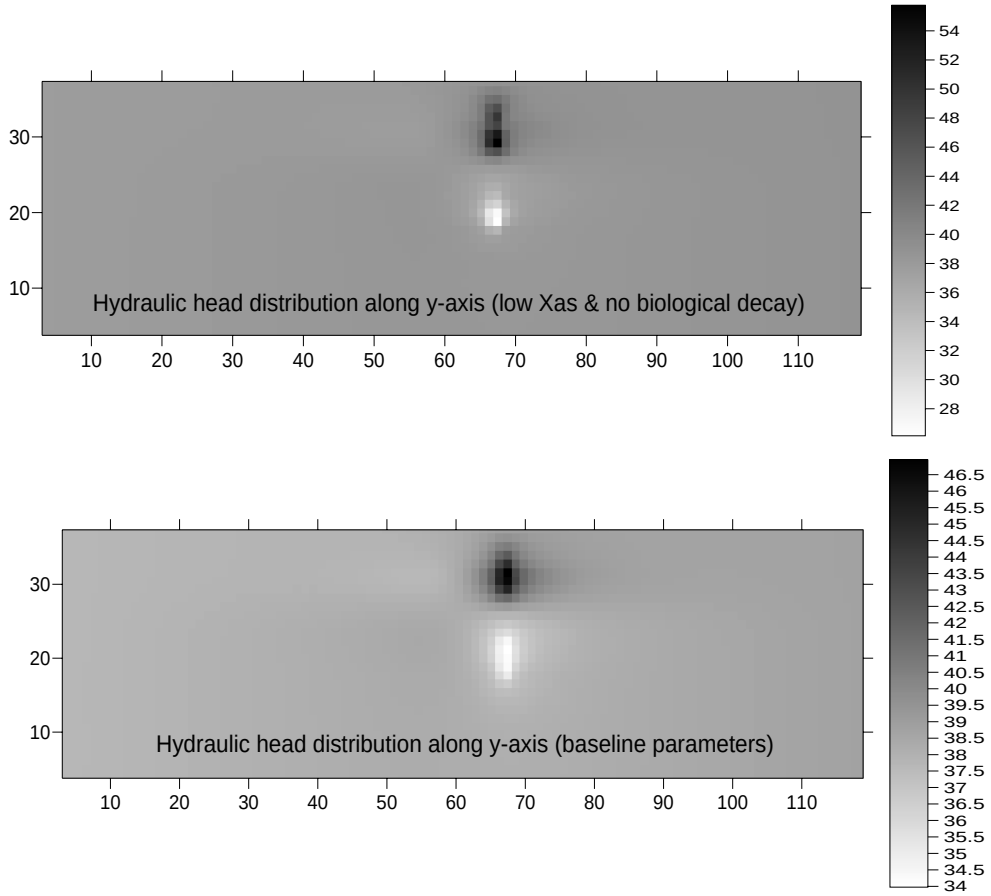

Figure 4.7 Hydraulic head (m) distribution along y-axis after 360 days (a) assuming no biomass decay and low maximum biomass concentration (b=0 day^{-1}, Xas=1200 mg/L, pump rate =100m^3/d, TAC=600 mg/L, continuous donor injection) and (b) baseline conditions

We see from Figure 4.7 that the range of hydraulic head values is greater at the end of the low X_{as}, no biological decay, simulation than during the baseline simulation. An inspection of Equation 2.4 may explain why the magnitude of the hydraulic head increases during the "clogged" simulation. Recall that the flow rate is constant throughout the simulation. In order to maintain a constant flow rate when the hydraulic

conductivity of the porous medium, K_s, is decreasing, the hydraulic gradient must increase. A similar trend was observed in the distribution of hydraulic head along the x-axis as well (data not shown).

The second test to verify that the technology model was operating correctly involved setting the parameter *p*, the exponent in the bioclogging submodel, equal to zero. This effectively "turns off" the bioclogging subroutine. The electron donor should be able to travel through the aquifer unimpeded by the growing biomass. The following figure shows the ethanol concentration distribution (mg/L) in layer 3.

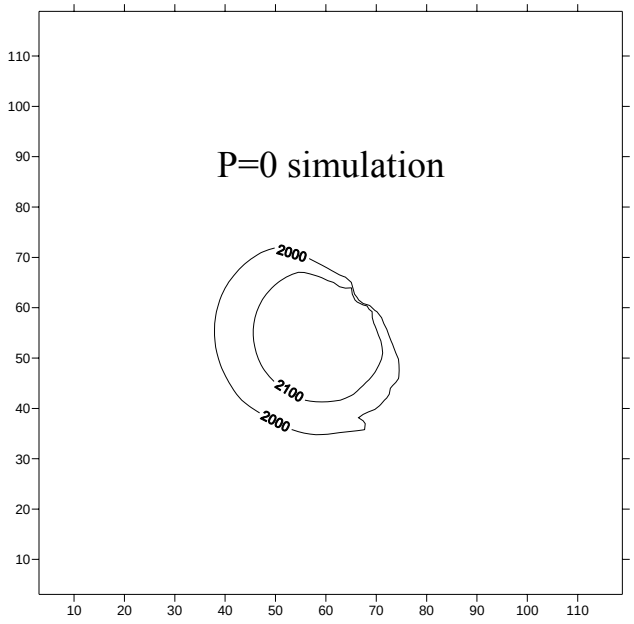

Figure 4.8 Ethanol concentration contours (mg/L) in layer 3 after 360 days (baseline parameters, p=0)

If there was a reduction in hydraulic conductivity due to bioclogging in the baseline simulation, we might expect that the ethanol concentration contours in Figure 4.8 would differ from contours obtained from the baseline simulation in Figure 4.6. However, we see that the contours of the baseline simulation shown in Figure 4.6 and the contours

obtained from the simulation where p = 0 are virtually identical. This indicates that there is little difference between simulations run with p = 0 and simulations run with p=3.16; the *p* value suggested by Clement *et al*. (1996).

Figures 4.9 and 4.10 compare the porosity change when p = 0 after 360 days with the resultant porosity when p = 3.16 after an equal amount of time.

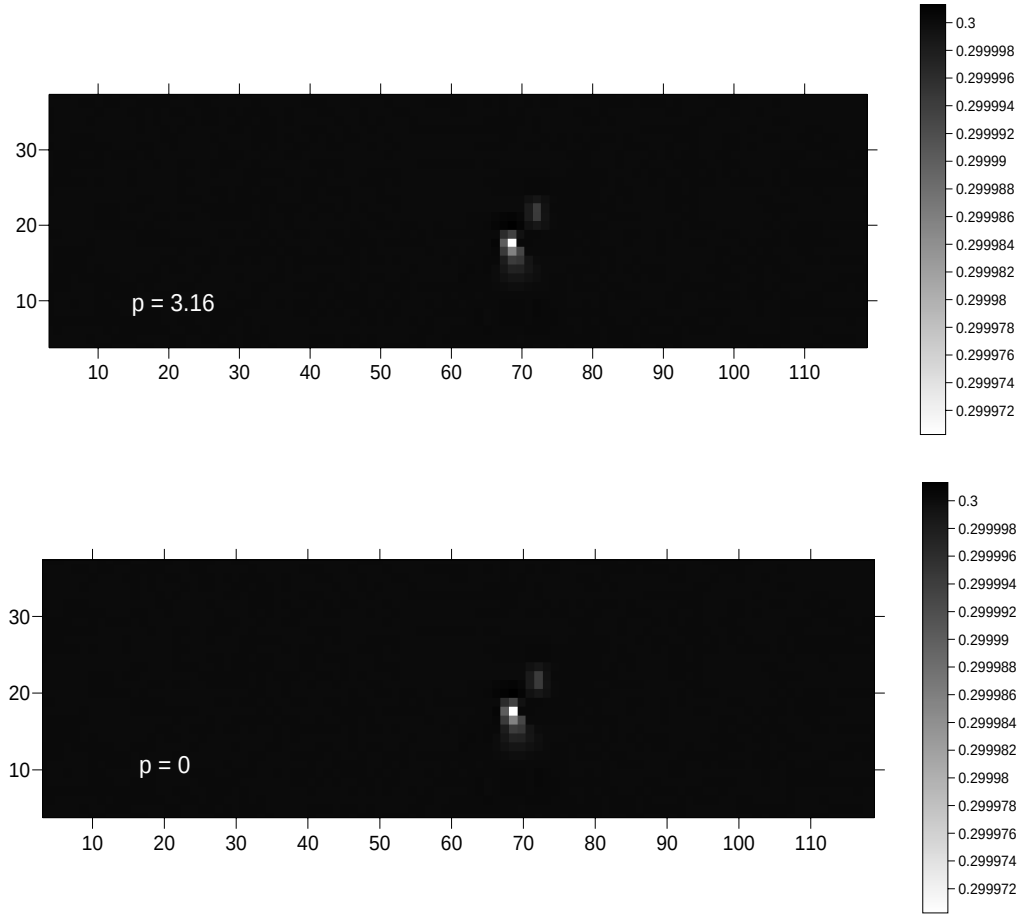

Figure 4.9 Vertical porosity distribution along the y-axis after 360 days with (a) baseline parameters and p = 3.16 and (b) baseline parameters and p = 0

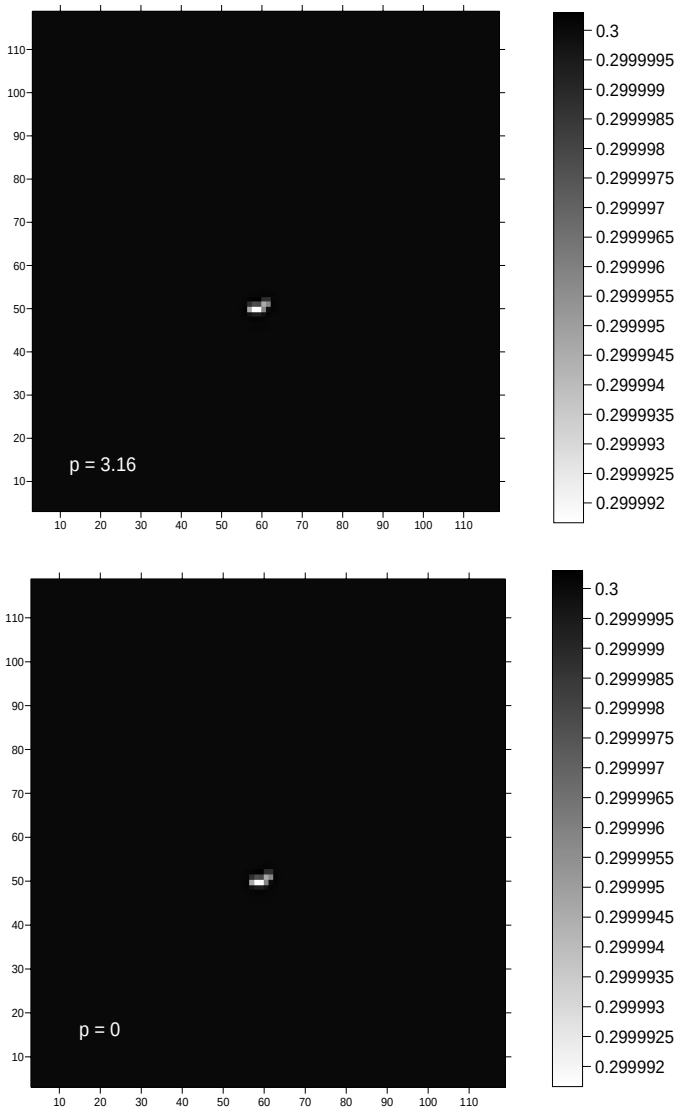

Figure 4.10 Layer seven porosity after 360 days when (a) baseline parameters and p = 3.16 and (b) baseline parameters and p = 0

Figure 4.9 and Figure 4.10 show that the porosity within the simulated aquifer does not perceptibly change when X_{as} and the biological decay factor are reset to the baseline values (see Appendix). Also, Figure 4.9 and Figure 4.10 show that there is no difference in model results when p = 0 and when p = 3.16. Table 4.1, which lists the total mass of perchlorate and other electron acceptors degraded when p=0 and when p = 3.16 confirms this observation.

Table 4.1 Comparison of constituent mass removed during technology operation over 360 days, bioclogging model exponent p=0 and p=3.16, baseline parameters

	p	Electron Donor	Oxygen	Nitrate	Perchlorate	Biomass
Mass Injected (g)	0	43,163,000	0	0	0	0
Mass Removed (g)	0	208,530	101,000	99,851	23,928	-3,008.3
Mass Injected (g)	3.16	43,163,000	0	0	0	0
Mass Removed (g)	3.16	208,540	101,000	99,853	23,931	-3,008.7

The reason the simulation results are very similar when p = 0 and when p = 3.16 appears due to the assumed value of X_{as}, the maximum biomass concentration. The assumed value for this parameter is very large (the reader is referred to the Appendix for a discussion regarding the determination of X_{as}), making the bioclogging subroutine insensitive to relatively low levels of biomass accumulation.

At this point it appears that the model is operating as expected. Porosity, and hence electron donor transport, is affected by the accumulation of biomass when the technology model is altered to simulate unrestricted biomass accumulation. The technology model simulations when bioclogging is "turned off" are similar to the model baseline simulations obtained when bioclogging is modeled with p = 3.16. However, this result is explained by the assumed value of X_{as} used in this study. More results from the baseline simulation, along with the results of varying the time averaged electron donor concentration, the donor pulsing schedule, and the HFTW pumping rate are presented in the next section.

4.3 APPLICATION OF TECHNOLOGY MODEL TO AEROJET SITE

4.3.1 BASELINE RESULTS

Once it was verified that the model was operating as expected, the first simulation was conducted using the set of engineered parameters identified in Table 3.6 as "baseline" along with the site conditions described in the Appendix in order to establish the initial performance of the HFTW system. This performance level will be used to compare to the results of subsequent simulations conducted using differing engineered parameters to determine the impact of the parameters on system performance.

The following figure shows the extent of the ethanol plume in layers 1 through 6 after operating the HFTW system for 360 days. The dark areas represent areas of higher concentration than the white areas. This convention of displaying relative concentration intensities will be used throughout this paper. The HFTW is screened over the thickness of layer 2, 3, and 4. The larger transmissivity of layer 3 is evident by the large ethanol plume observed in that layer compared to the plume in layers 2 and 4. The butterfly pattern of the ethanol plume observed in layer 5 is caused mainly by short-circuiting of the groundwater between the screens of the HFTW; not all water from the injection point flows toward the extraction well in the same layer. Some groundwater "short circuits" by flowing vertically between the injection and extraction screens of the same treatment well. This causes the ethanol plume to disperse not only horizontally, but vertically as well, especially near the treatment wells.

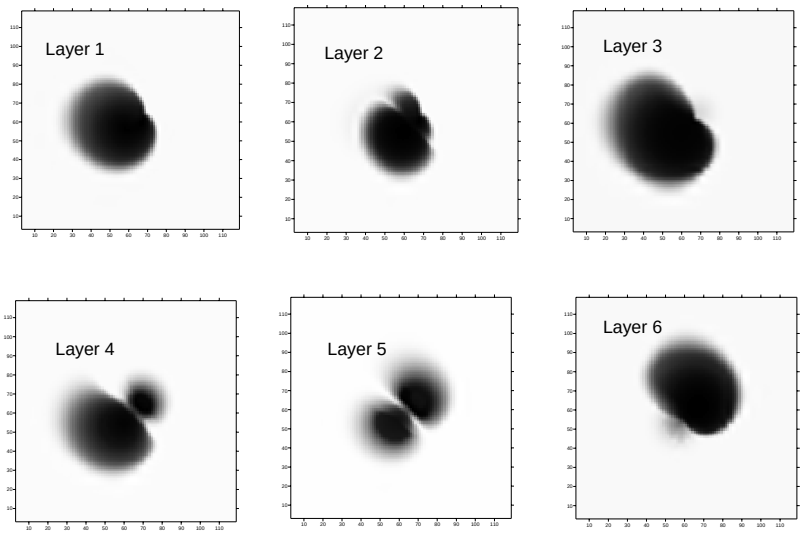

Figure 4.11 Relative ethanol concentrations in layers 1 through 6 after 360 days (baseline parameters)

The next figure displays the perchlorate concentration profile in layer 2 after 360 days of treatment.

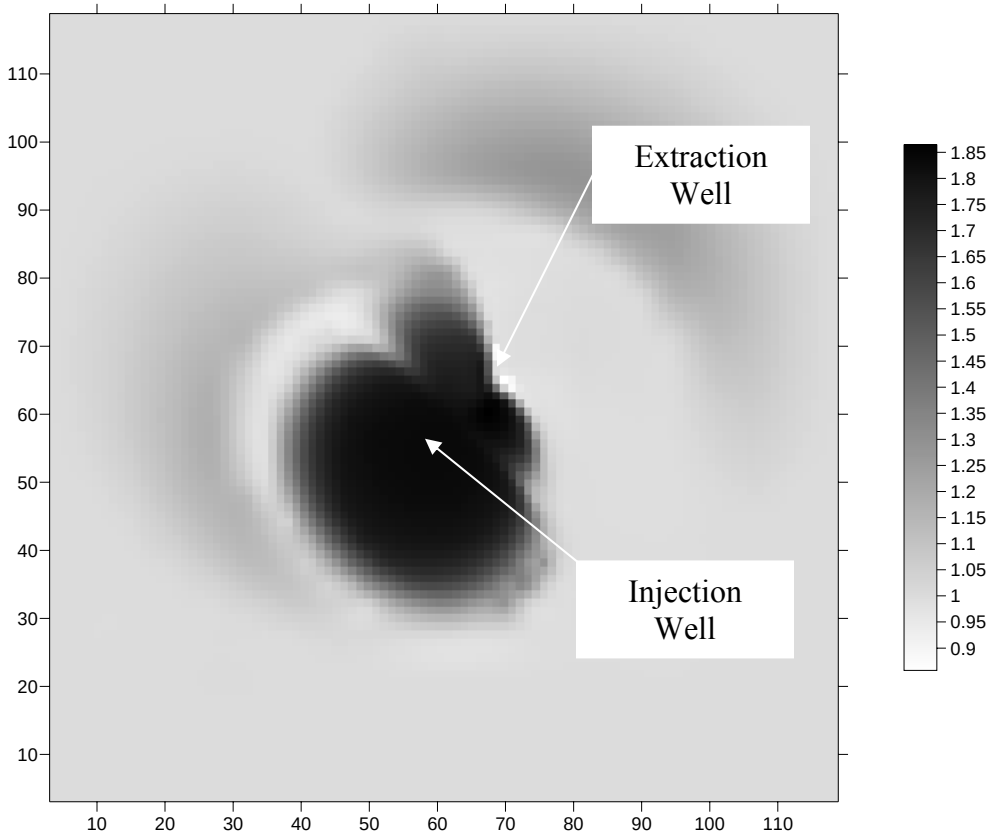

Figure 4.12 Perchlorate concentration (mg/l) in layer 2 after 360 days (baseline parameters)

Figure 4.12 indicates that the perchlorate plume in layer 2 increased in concentration after 360 days of treatment. This phenomenon occurs because perchlorate concentration increases with depth. Groundwater is recycled between the well screens of an HFTW system. Essentially, groundwater containing a higher concentration of perchlorate is brought from layers 7 through 9 (initial perchlorate concentration of 4 mg/l) and is injected into layer 2 which has a lower perchlorate concentration (initially 1 mg/l). The spreading of perchlorate to the upper aquifer is an issue of concern. The impact the different engineered parameters have on the extent of this spreading will be analyzed later in this chapter.

The next figure displays the perchlorate concentration in layer 3.

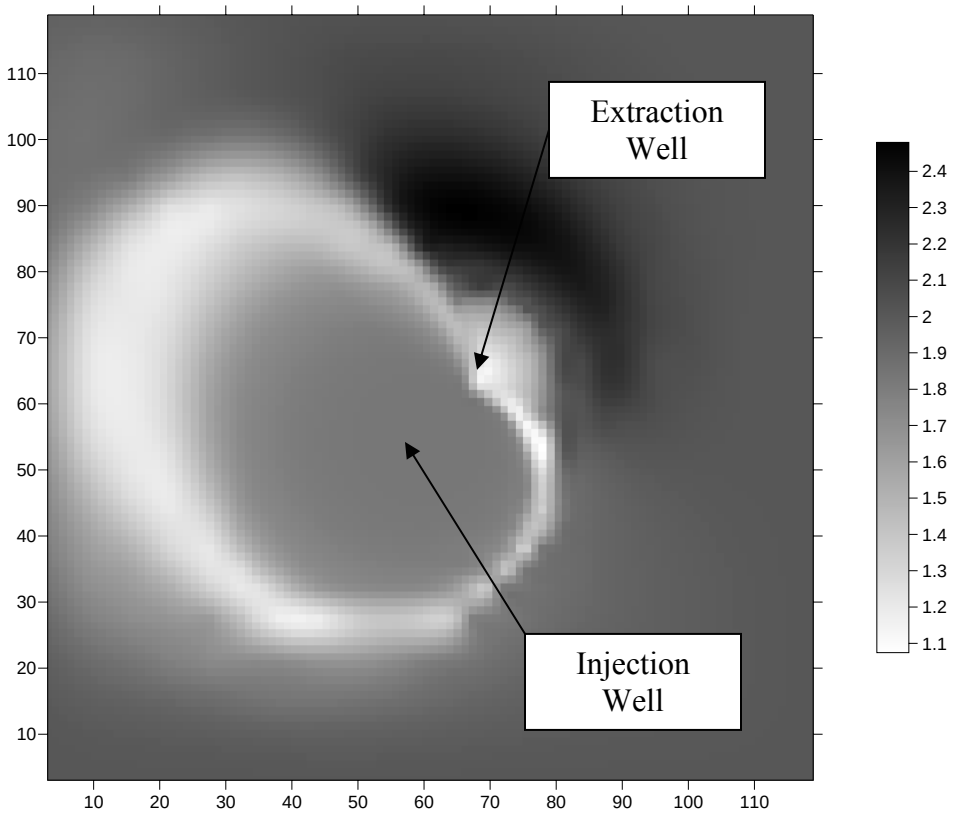

Figure 4.13 Perchlorate concentrations (mg/l) in layer 3 after 360 days (baseline parameters)

The initial perchlorate concentration in layer 3 was 2.0 mg/l. The injected groundwater had a perchlorate concentration very close to the background (initial) perchlorate concentration of layer 3. However, the white ring around the injection well indicates that perchlorate degradation is occurring away from the treatment wells. The dark band surrounding the extraction well in Figure 4.13 may be due to untreated (or less extensively treated) groundwater from the lower aquifer being captured by the extraction well located in layer 3. A similar pattern is present in layer 4 (data not shown).

Perchlorate was reduced throughout most of the lower aquifer, layer 6 through 11, from 4 mg/l to less than 2 mg/l. Very little perchlorate degradation was observed in layer 12 (data not shown). The following figure shows the extent of the perchlorate degradation in layers 7 through 9 under the baseline engineered parameters.

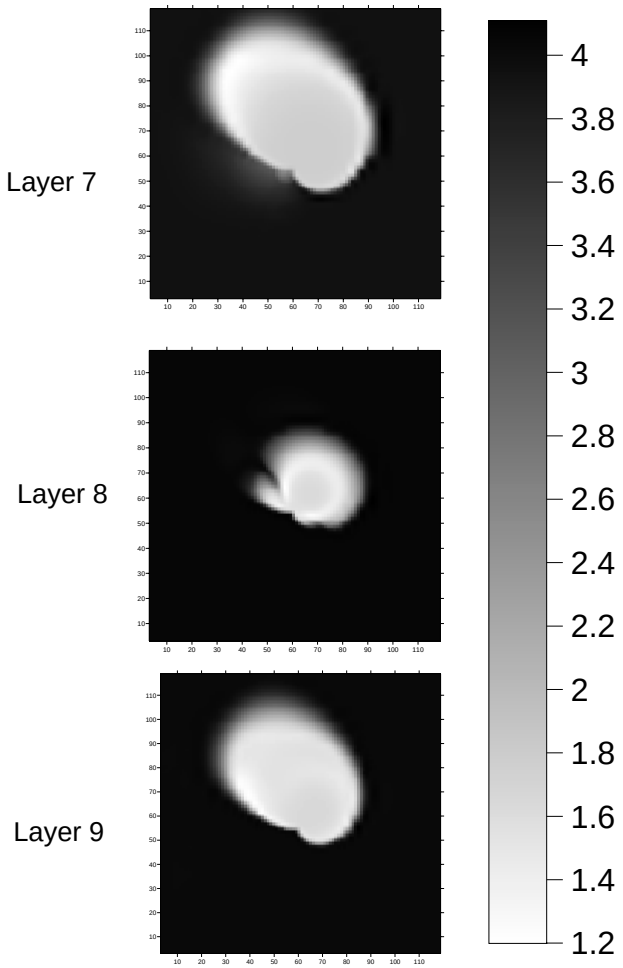

Figure 4.14 Perchlorate concentration (mg/l) in layer 7 through 9 after 360 days (baseline parameters)

The low transmissivity of layer eight is indicated by the smaller area of perchlorate degradation compared to layer 7 and layer 9.

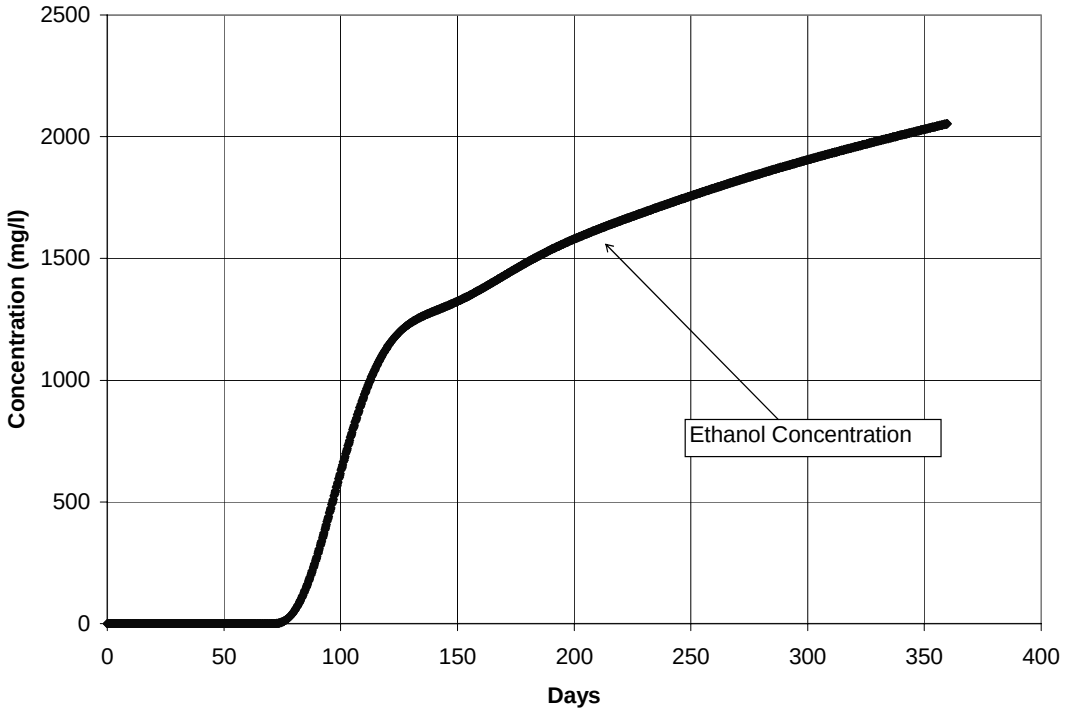

Figure 4.15 Ethanol concentration time series at well 3627 (baseline parameters)

Figure 4.15 shows time series ethanol concentration data from observation well 3627 which is located approximately 19 meters downgradient of the treatment wells (Figure A.1). We notice from Figure 4.15, that it takes the injected ethanol nearly 75 days to reach well 3627.

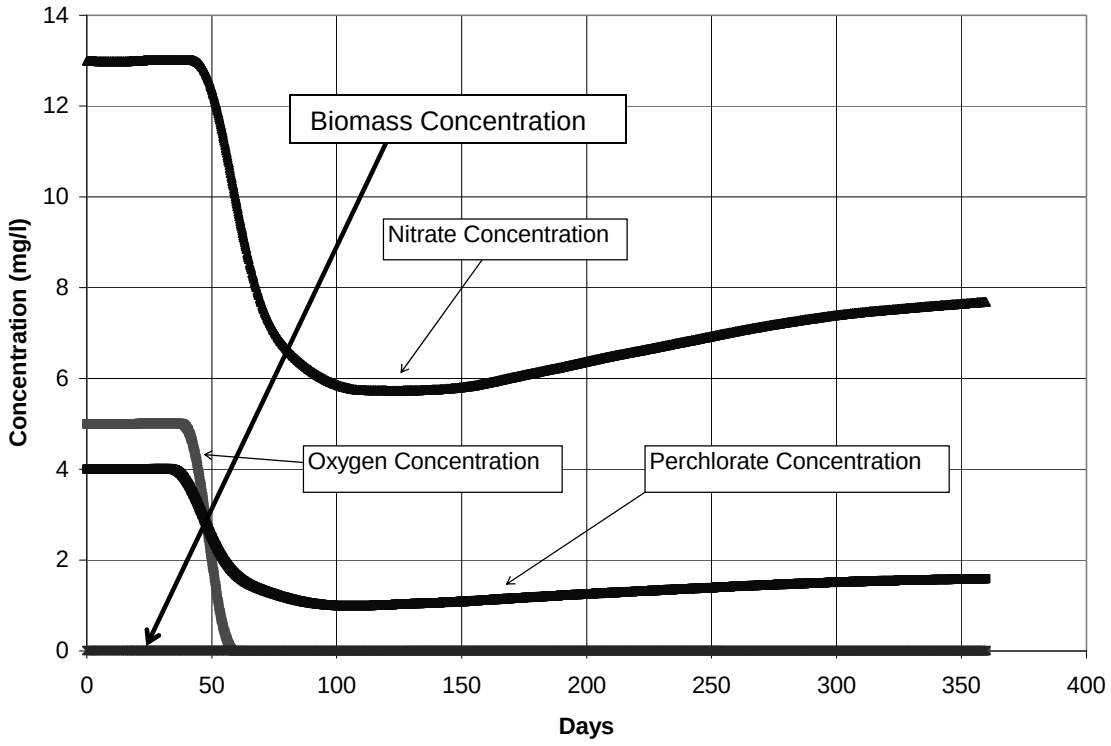

Figure 4.16 Electron acceptor concentration time series at observation well 3627 (baseline parameters)

The retarded transport of ethanol due to sorption can be seen in the model output shown in Figure 4.16. Ethanol was not observed at well 3627 until approximately day 75, yet the non-sorbing electron acceptor concentrations began to fall before day 50. This is observed because ethanol adsorbs to the porous matrix and therefore travels slower than oxygen, nitrate, and perchlorate through the aquifer. The treated groundwater which is devoid of oxygen and contains limited nitrate and perchlorate reaches well 3627 ahead of the ethanol plume

As expected, the oxygen and nitrate concentration within the aquifer was significantly reduced during the 360 day baseline simulation. Figure 4.17 represents the oxygen and

nitrate “holes” that appear in all layers of the model. Note that nitrate is not completely consumed, while the oxygen concentration is very close to zero within layer 1.

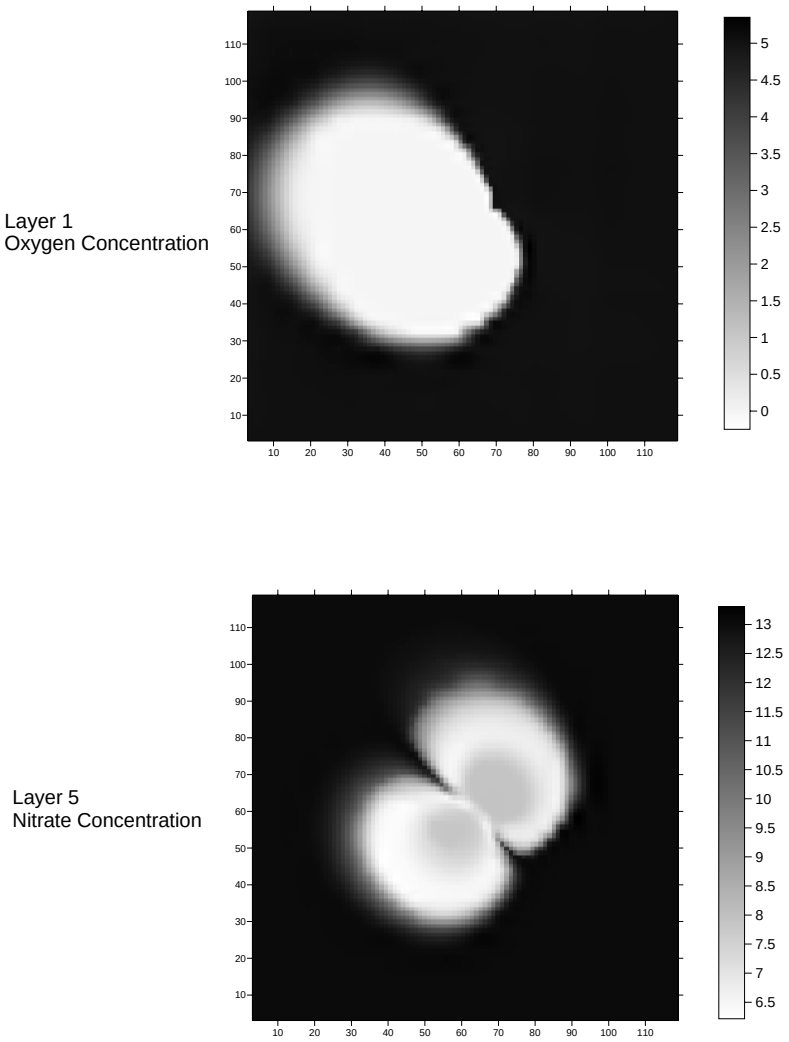

Figure 4.17 Oxygen concentration in layer 1 and nitrate concentration in layer 5 after 360 days (baseline parameters)

The amount of biomass that was present at the end of the 360 day baseline simulation was not significant throughout most of the aquifer. In fact, the amount of biomass was low enough at the end of 360 days that the porosity, and hence the hydraulic conductivity, did not change significantly as Figure 4.9 and Figure 4.10 indicate.

Nevertheless, some interesting observations regarding biomass accumulation can be made from the baseline simulation.

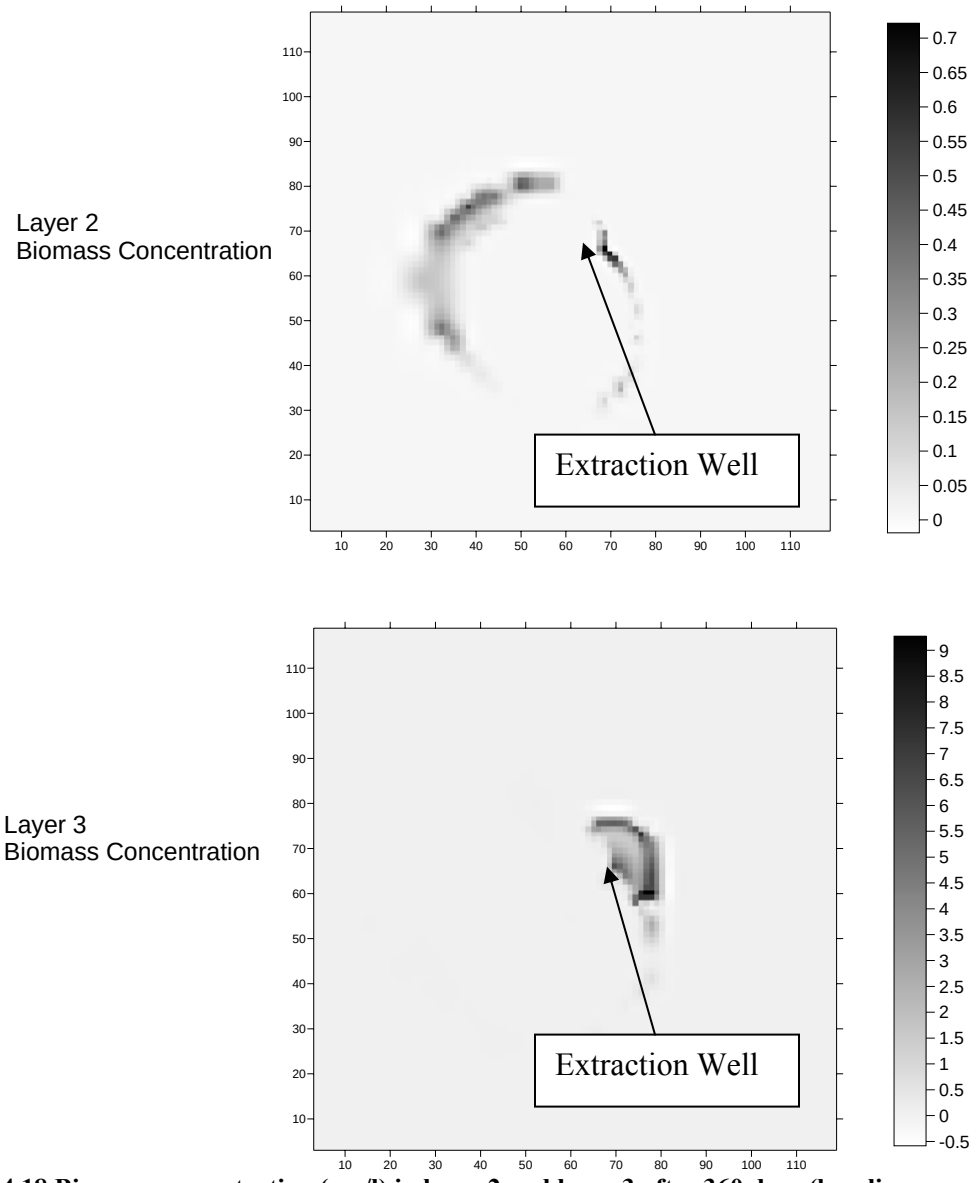

Figure 4.18 Biomass concentration (mg/l) in layer 2 and layer 3 after 360 days (baseline parameters)

In Figure 4.18, biomass grows the most near the extraction well. The same trend can be seen in the lower aquifer.

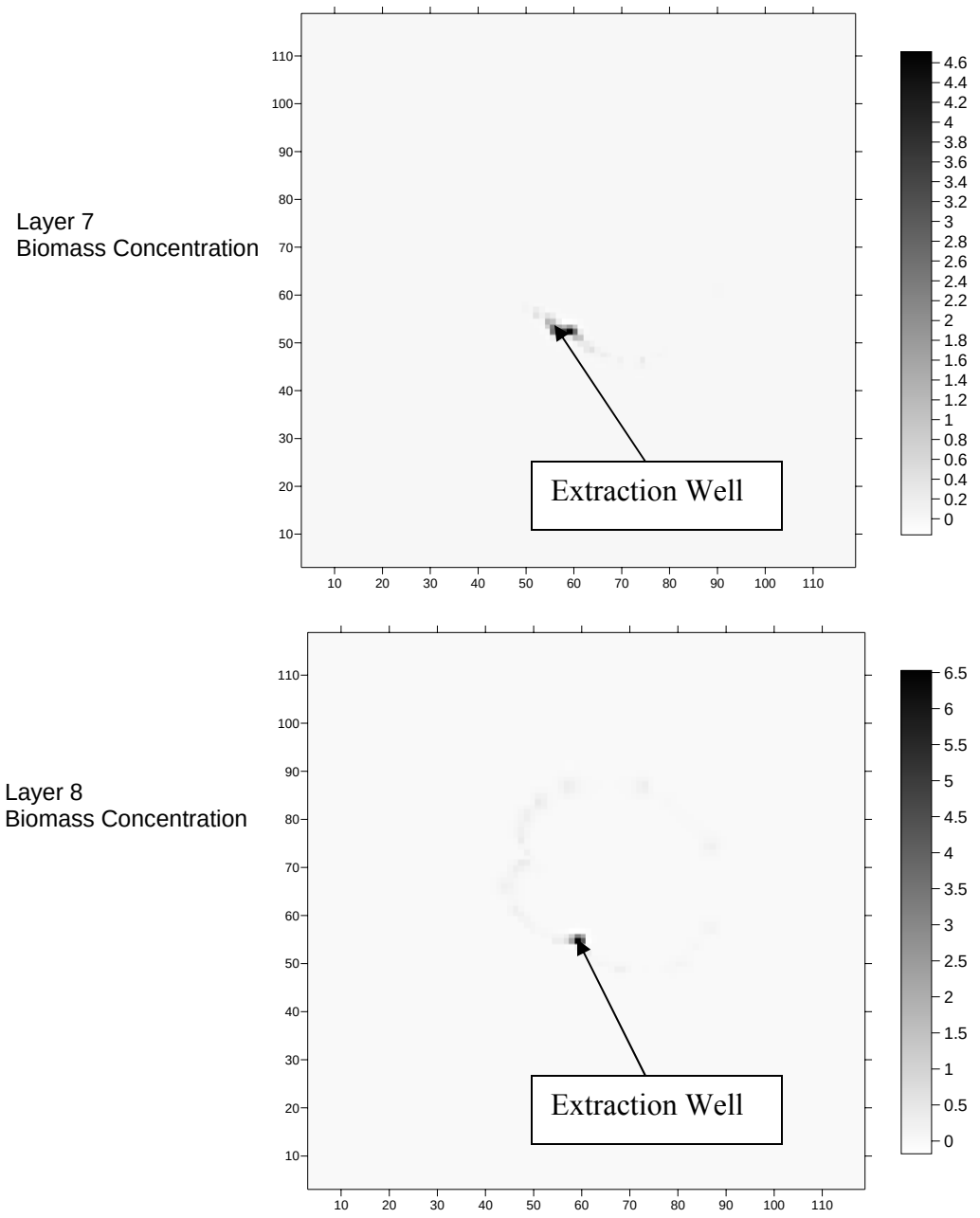

Figure 4.19 Biomass concentration (mg/l) in layer 7 and layer 8 after 360 days (baseline parameters)

Figure 4.19 shows the observed biomass growth concentrated around the extraction well in layer 7 and 8. As stated earlier, this phenomenon may occur because electron donor amended groundwater is continuously flowing towards the extraction well screens which facilitate greater accumulation of biomass.

The biomass concentration profiles in Figures 4.18 and 4.19 are "snapshots" taken at the end of the 360 day simulation. However, if biomass concentrations are changing over time, bioclogging may impact the HFTW performance earlier (or later) in the simulation. The following time series data taken from the extraction well screen located in layer 3 shows a significant spike in biomass concentration at day 50.

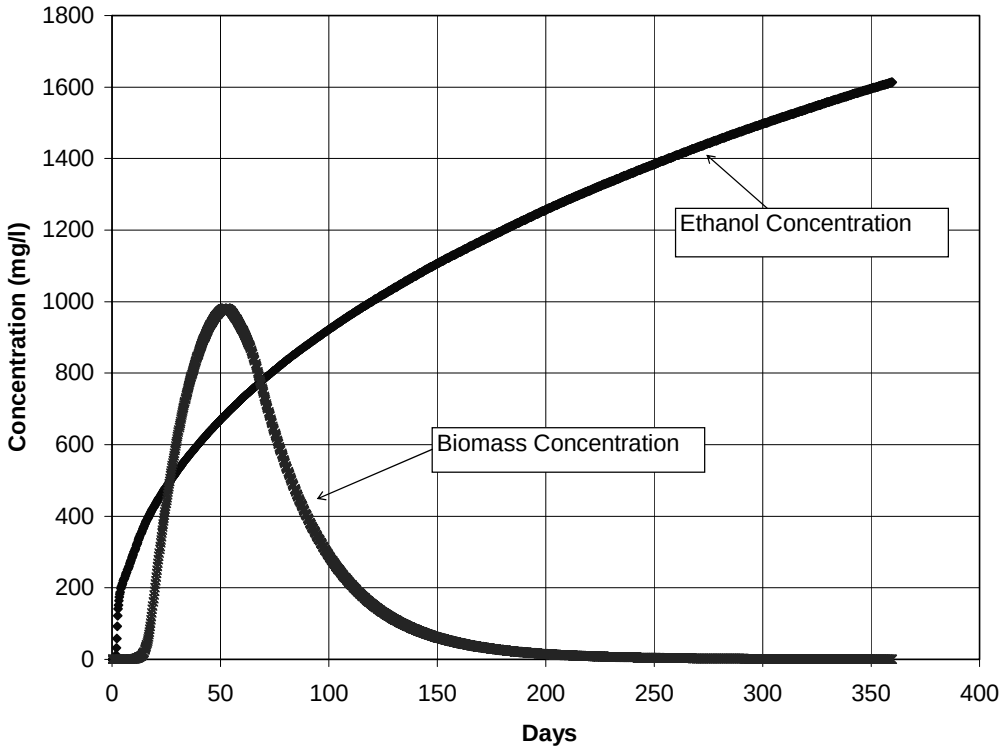

Figure 4.20 Concentration time series at layer 3 extraction well (baseline parameters)

In order to capture the impact on bioclogging that the biomass concentration spike at day 50 may have on HFTW performance, a 50 day simulation was conducted and the most significant porosity change (layer 3) within the aquifer is shown in Figure 4.21.

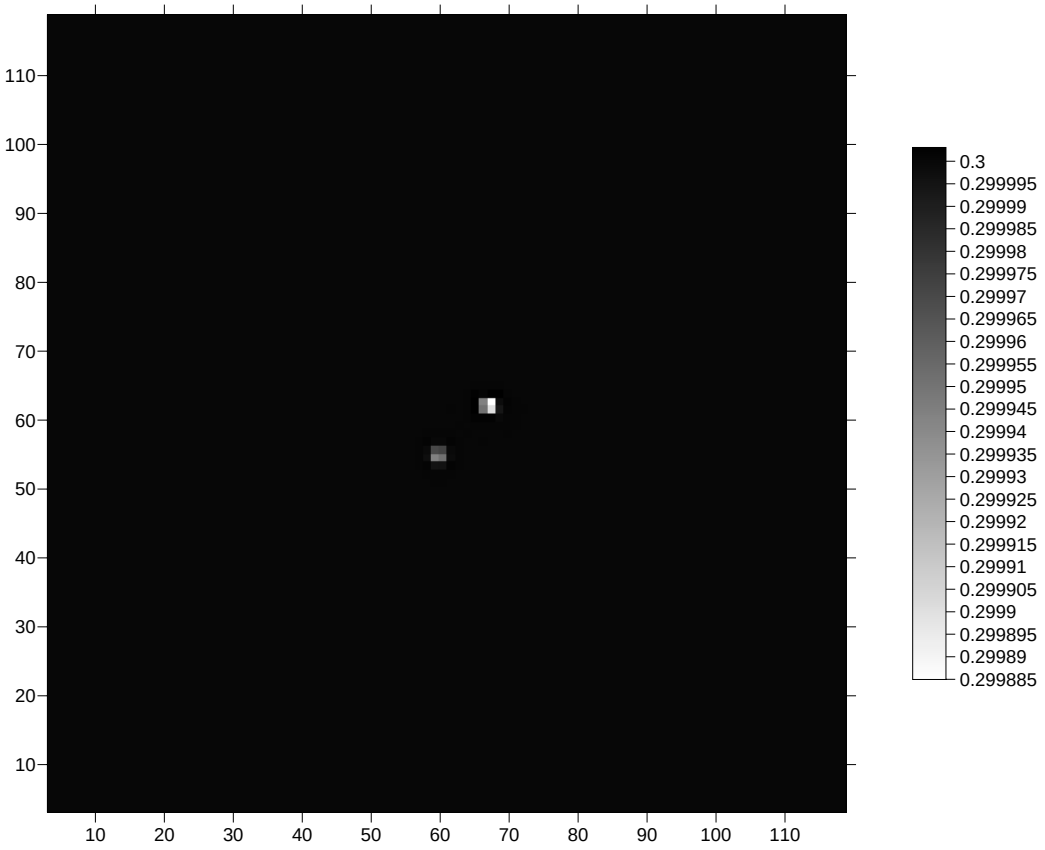

Figure 4.21 Porosity change in layer 3 (50 day baseline simulation)

Figure 4.21 clearly shows that little change in the aquifer porosity resulted from the highest biomass concentration realized during the 360 day baseline parameter simulation.

The next time series graph of the electron acceptor concentrations is also from the extraction well in layer 3. It is interesting to note that the decline in biomass concentration roughly coincides with the minimum aggregate electron acceptor concentration. This may indicate that the microbial utilization rate of nitrate and perchlorate as electron acceptors is not great enough at the concentrations encountered at the Aerojet site to overcome the rate of bacterial decay assumed in this study (0.0624 day^{-1}).

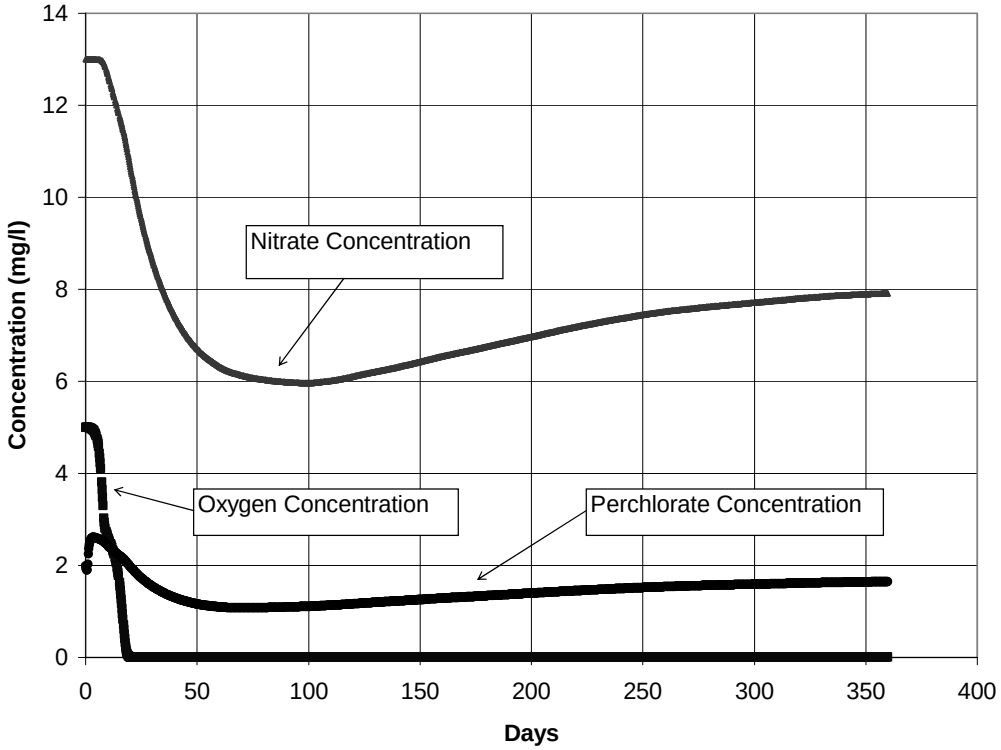

Figure 4.22 Electron acceptor concentration time series at layer 3 extraction well (baseline parameters)

Figure 4.22 also demonstrates that the nitrate and perchlorate concentrations rebound after the biomass concentration declines to its minimum level. On the other hand, the oxygen concentration barely rebounds during the 360 day simulation, indicating that the microbial population can more efficiently utilize oxygen as an electron acceptor than nitrate or perchlorate. It was also observed that the nitrate and perchlorate concentrations shown in Figure 4.22 are slightly higher than the concentrations observed at well 3627 (Figure 4.16), indicating that degradation continues to occur as the ethanol plume travels down gradient. However the amount of the perchlorate degradation that occurs as the plume moves down gradient is not extensive. The decrease in nitrate and perchlorate concentrations evident in Figure 4.16 represents a "pseudo degradation" effect at this well 3627. Most of the electron acceptor degradation occurs up-gradient of well 3627.

The fact that the microbial concentration at well 3627 does not rise above the survival concentration confirms this observation; too few electron acceptors, particularly oxygen, are delivered to the location of well 3627 to facilitate microbial growth. The next section investigates the effect of varying the time averaged electron donor concentration on HFTW performance.

4.3.2 EFFECTS OF TIME AVERAGED CONCENTRATION (TAC) ON HFTW TECHNOLOGY PERFORMANCE AT AEROJET SITE

In this section we investigate the effect of varying the time averaged concentration (TAC) of electron donor on the technology model simulation results. Table 4.2 shows the mass of perchlorate removed during 360 day model simulations using various TAC values.

Table 4.2 Perchlorate mass degraded at various TAC levels (pump rate = 100 m^3/d, continuous donor addition, 360 day simulation)

Time Averaged Concentration, TAC (mg/L)	Mass Perchlorate Degraded (kg)
200	20.5
400	22.7
600 (baseline)	23.9
800	25.0
1000	25.9
1200	26.7

From Table 4.2 we see that the mass of perchlorate degraded increases with increasing TAC. This increase may be caused by the microorganisms having more electron donor available for consumption.

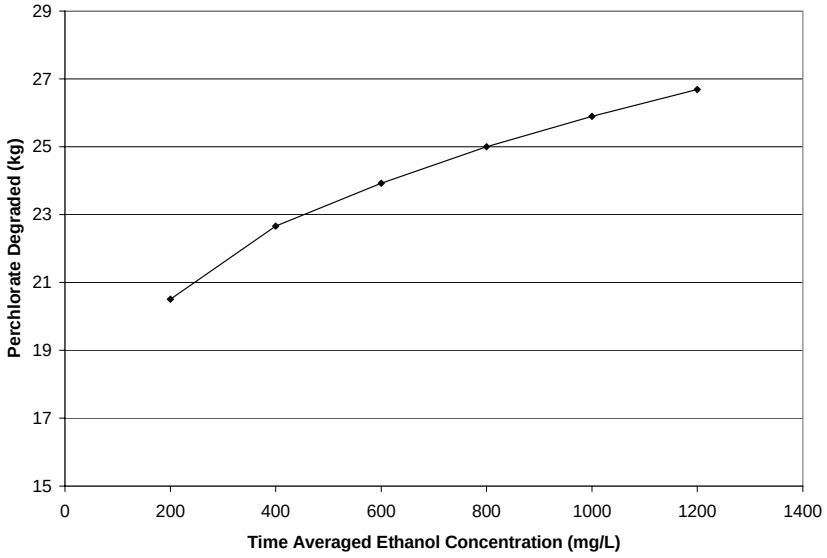

Figure 4.23 Mass of perchlorate degraded as a function of TAC level (pump rate = 100 m^3/d, continuous donor addition, 360 day simulation)

We see from Figure 4.23 that the relationship between the mass of perchlorate degraded and the time averaged concentration over a 360 day period is not linear. In fact, the mass of perchlorate degraded appears to be approaching some asymptotic value. Adding more electron donor may not guarantee an increase in perchlorate mass removed; a fact important to the cost effectiveness of the HFTW system.

Figure 4.24 displays the perchlorate concentration contours in layer seven under three time averaged concentration levels: 200 mg/L, 800 mg/L, and 1200 mg/L. Figure 4.24 shows the size of the perchlorate "hole" which results from the addition of ethanol to the aquifer via HFTWs. It is interesting to note that the size of the area in which perchlorate is degraded is about equal for different TAC levels; that is to say, the 3.8 mg/L concentration contour is nearly identical in all three scenarios. The difference in perchlorate concentrations occurs near the treatment wells. When TAC is equal to 1200

mg/L, the perchlorate concentration is reduced to nearly 1 mg/L. Conversely, when the TAC is set to 200 mg/L, the perchlorate concentration is only reduced to approximately 1.6 mg/L. This observation indicates that when the HFTW pumping rate and the donor addition schedule are held constant, the area of affected perchlorate reduction remains unchanged with increasing TAC levels while the extent of perchlorate degradation near the treatment wells increases.

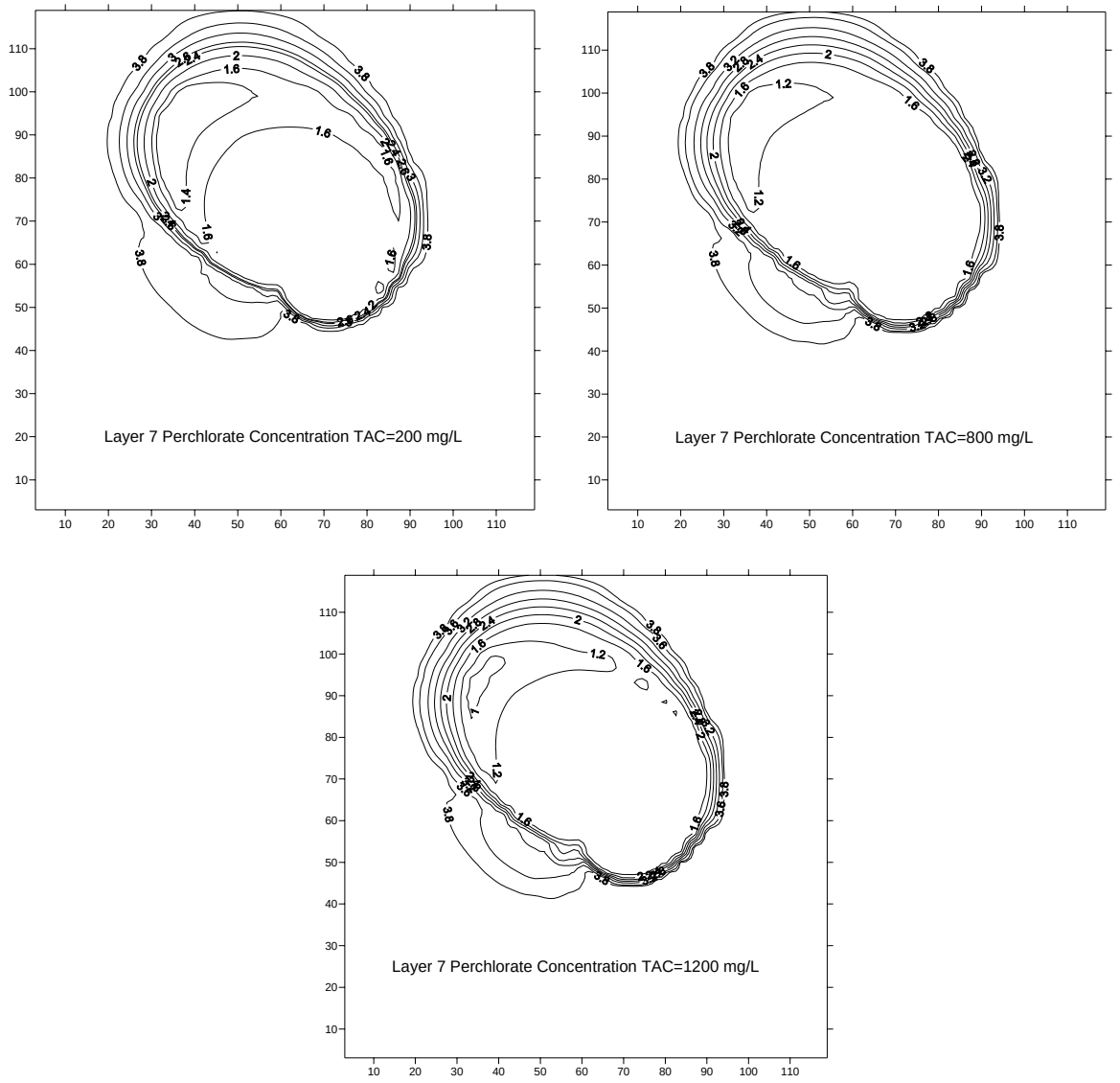

Figure 4.24 Perchlorate concentration contours in layer 7 at TAC=200 mg/L, TAC=800 mg/L, and TAC=1200 mg/L (pump rate = 100 m^3/d, continuous donor addition, 360 day simulation)

Recall from Figure 4.12 that the perchlorate concentration in layer 2 increases as a result of the operation of the HFTW system. The next set of image maps taken from layer 2 under the highest and lowest simulated TAC levels show the same trend.

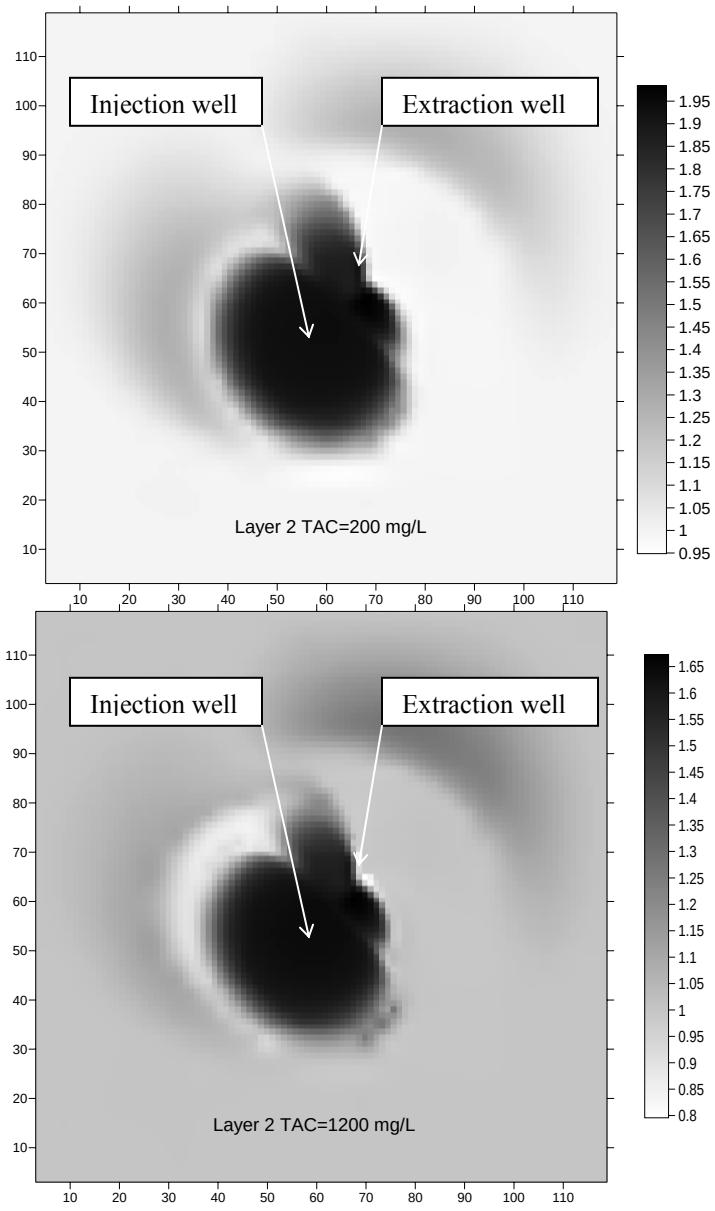

Figure 4.25 Perchlorate concentration in layer 2 at TAC=200 mg/L and TAC=1200 mg/L (pump rate = 100 m^3/d, continuous donor addition, 360 day simulation)

In Figure 4.25, the impacted area from both the highest and lowest under both TAC levels appears to be similar. However, as was previously discussed, the extent of

perchlorate degradation is greater under the TAC=1200 mg/L scenario which results in lower perchlorate concentrations in layer 2. This difference is realized by examining the concentration scales associated with each image map included in Figure 4.25.

The following time series data were obtained from well 3627 which is screened in layer 7. It also shows the increase in perchlorate removal as a result of increasing the TAC from 200 mg/L to 1200 mg/L.

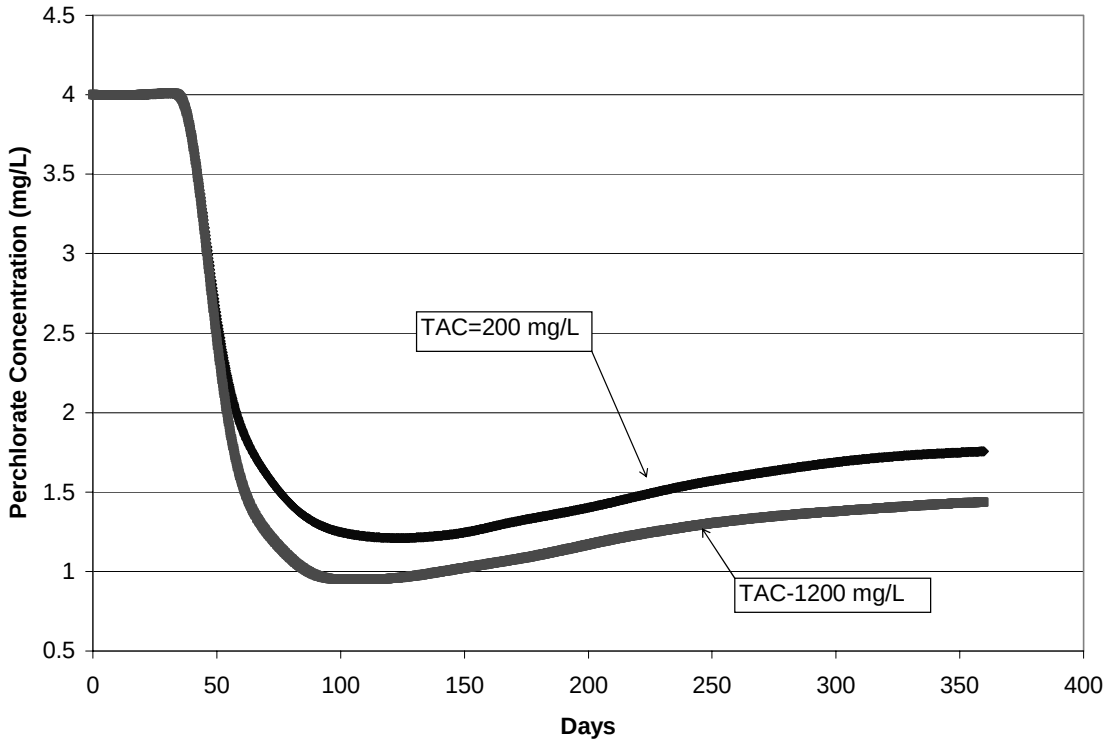

Figure 4.26 Perchlorate concentration at well 3627 at different TAC levels (pump rate = 100 m^3/d, continuous donor addition, 360 day simulation)

Figure 4.26 shows that even with a significant increase in TAC, only moderate decreases in down-gradient perchlorate concentrations are realized. However, we see from Figure 4.27 that the higher TAC levels do not correspond with higher biomass concentrations near the treatment wells.

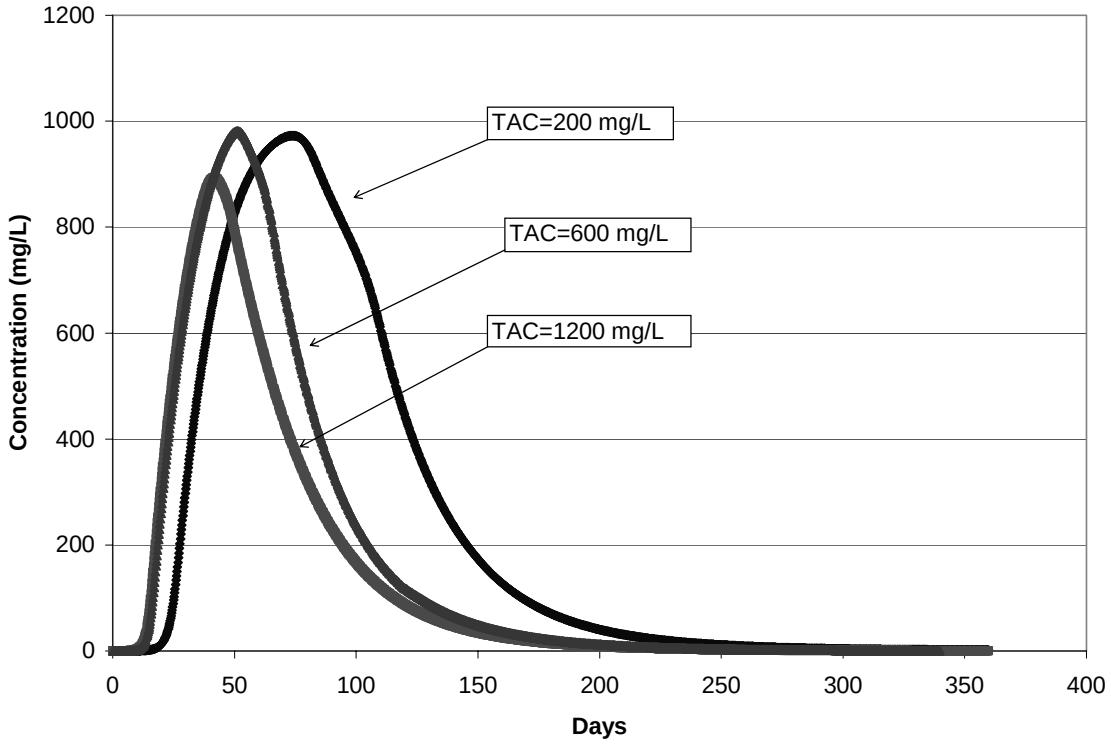

Figure 4.27 Biomass concentration time series at layer 3 extraction well as a function of ethanol TAC levels

The biomass accumulates much faster during the ethanol TAC=1200 mg/L simulation than at any other TAC level; a fact reflected in the lower down–gradient concentrations of perchlorate (see Figure 4.26). The rapid rate of biomass growth subsequently stimulates a rapid decline of electron acceptors. In contrast, when the electron donor TAC level is 200 mg/L, the biomass concentration does not increase as rapidly. As such, the electron acceptor concentration is not depleted as rapidly. The slower electron acceptor degradation rate that is due to the lower TAC, along with the electron acceptors continuously supplied from the boundaries of the model, allow for a longer period of sustained growth of biomass resulting in a larger peak concentration later in the simulation.

Finally, the porosity change at the time of the peak biomass concentration was not significant at the various TAC levels (data not shown). This was to be expected since the peak biomass concentrations at the various TAC levels are similar to the baseline peak biomass concentrations for which the porosity change is shown in Figure 4.21. The next section analyzes the effect of electron donor addition schedule on technology performance.

4.3.3 EFFECTS OF ELECTRON DONOR ADDITION SCHEDULE ON HFTW TECHNOLOGY PERFORMANCE AT AEROJET SITE

In this section we seek to identify the impacts of varying the ethanol dosing schedule on HFTW performance. Previous studies (McCarty *et al*., 1998) have demonstrated that varying the schedule which the electron donor is added to the aquifer may reduce the accumulation of biomass near the treatment wells; thereby reducing the amount of bioclogging near the wells as well as allowing the electron donor to travel further away from the treatment wells.

Table 4.3 indicates that the mass of perchlorate reduced decreases a very small amount as the pulse length of the electron donor dose is shortened. Parr *et al*., (2003) observed a similar trend and attributed the decreased treatment efficiency to the fact that the kinetic parameters used to describe the perchlorate respiring bacteria in their study, as well as this one, describe a lethargic microbial population which may be unable to effectively metabolize concentrated pulses of electron donor.

Table 4.3 Perchlorate mass degraded using various electron donor dosing schedules (pump rate = 100 m^3/d, TAC=600mg/l, 360 day simulation)

Electron Donor Dosing Schedule (hrs on/hrs off)	Mass of Perchlorate Degraded (kg)
8/0 (Baseline)	23.93
7/1	23.91
6/2	23.91
5/3	23.89
4/4	23.90
3/5	23.88
2/6	23.90

In each of the above simulations, the amount of electron donor added per day is the same to ensure that the time averaged concentration is constant (600 mg/L) during each simulation, i.e. a higher electron donor mass loading rate was used during the shorter pulse simulations to offset the time when no donor was added in order to maintain the baseline 600 mg/L TAC. Very little difference is observed in the amount of perchlorate degradation realized during the baseline simulation, i.e. continuous electron donor addition, and the various electron donor dosing schedules that were simulated. The biomass concentration time series at the layer 3 and layer 9 extraction wells are shown in Figure 4.28.

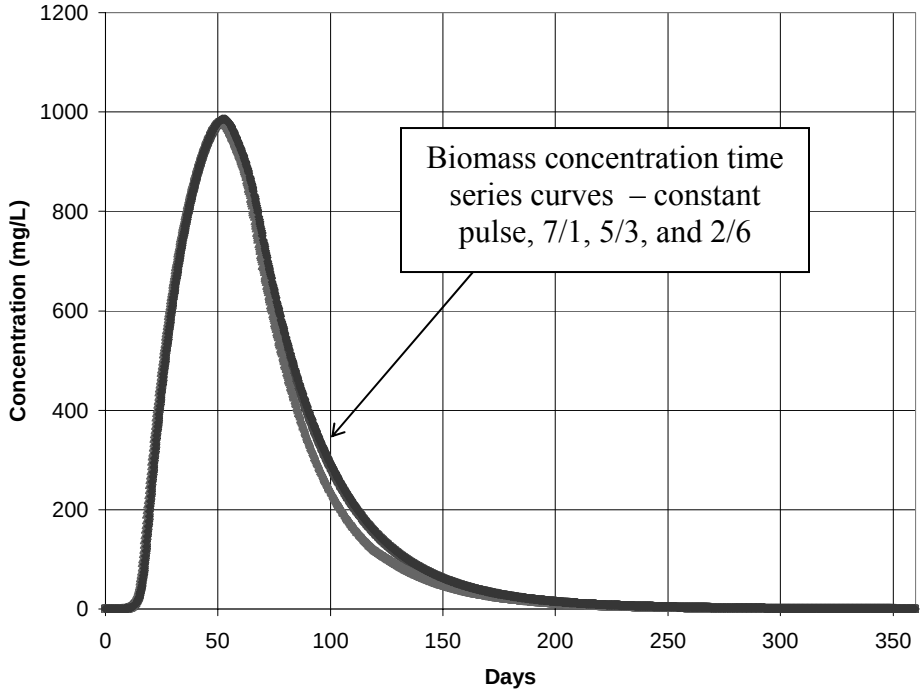

Figure 4.28 Biomass concentration time series for varying electron donor addition schedules at layer 3 extraction well (pump rate =100m^3/d, TAC=600 mg/L, 360 day simulation)

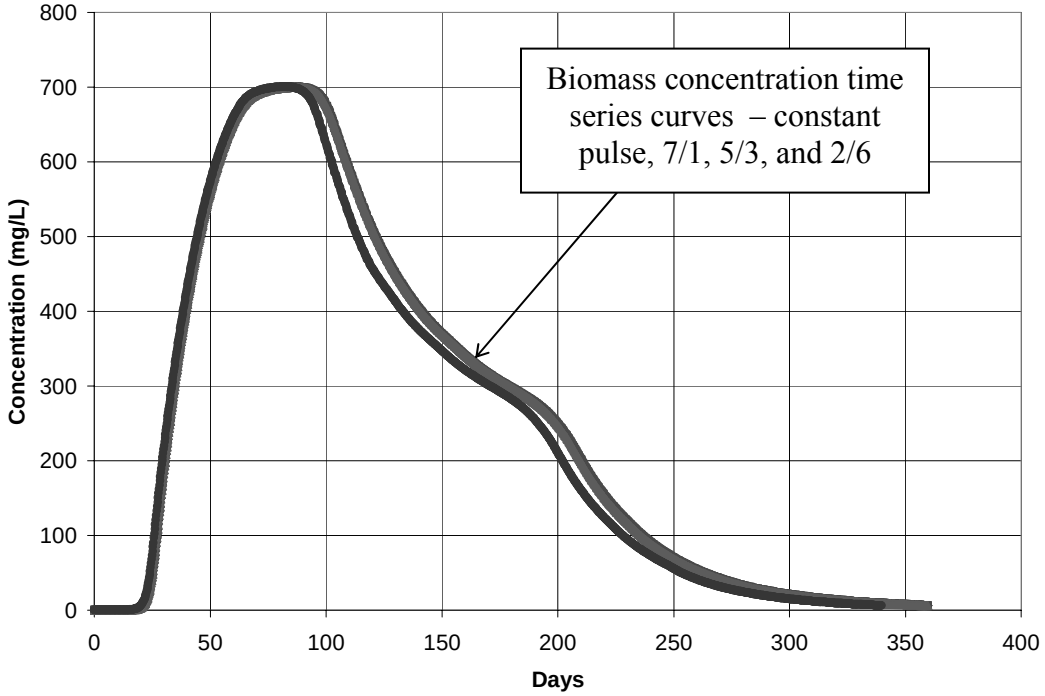

Figure 4.29 Biomass concentration time series for varying electron donor addition schedules at layer 9 extraction well (pump rate =100m^3/d, TAC=600 mg/L, 360 day simulation)

Figure 4.28 and Figure 4.29 show that the different electron donor pulsing schedules have a negligible effect on the biomass concentrations, and thus bioclogging, within the aquifer. Additionally, at the end of the 360 day simulation, very little difference in the distribution of the biomass within the aquifer was realized. Electron acceptor concentration time series data at various down-gradient monitoring wells from the various electron donor pulsing simulations was observed to be nearly identical to the baseline, continuous electron donor addition simulation (data not shown). There were also no marked differences between the electron acceptor concentration profiles from the different electron donor pulsing simulations and the electron acceptor concentration profiles obtained from the baseline simulation (data not shown).

The next section investigates the effect of different treatment well pumping rates on the performance of the HFTW system.

4.3.4 EFFECTS OF TREATMENT WELL PUMPING RATE ON HFTW TECHNOLOGY PERFORMANCE AT THE AEROJET SITE

In this section we vary a final engineered parameter, the HFTW pumping rate, in order to assess the effect of varying the HFTW pumping rate on *in situ* perchlorate biodegradation at the Aerojet site. Four pumping rates were investigated and compared to the baseline simulation (100 m^3/day); the four pumping rates simulated were: 75 m^3/day, 50 m^3/day, 25 m^3/day, and 10 m^3/day. All of the tested pumping rates are lower than the baseline pumping rate due to the inability of the actual wells at the Aerojet site to achieve a flow

rate greater than approximately 49 m^3/d (Goltz, 2004). The following table shows the mass of perchlorate degraded during 360 day simulations using different pumping rates.

Table 4.4 Perchlorate mass degraded using various HFTW pumping rates (TAC=600mg/l, 360 day simulation, continuous donor addition)

HFTW Pumping Rate (m^3/day)	Mass of Perchlorate Degraded (kg)
100	23.93
75	20.41
50	16.96
25	12.20
10	7.338

We see from Table 4.4 that, as expected, the mass of perchlorate degraded decreases as the treatment well pumping rates decrease. Figure 4.30 below shows the different sizes of the perchlorate "holes" that occur in layer 7 at various treatment well pumping rates.

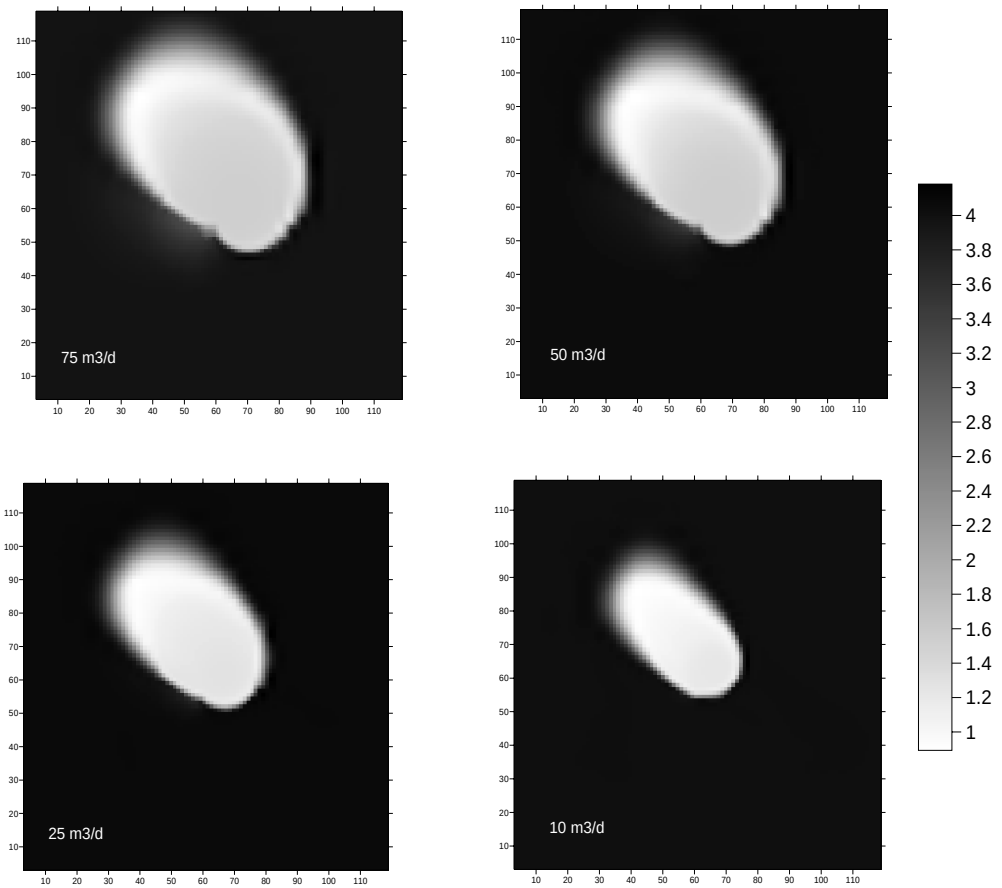

Figure 4.30 Perchlorate concentration profiles in layer 7 using various treatment well pumping rates (TAC=600 mg/l, continuous donor addition, 360 day simulation)

We see from Figure 4.30 that the area of affected perchlorate reduction is reduced as the treatment well pumping rate is reduced. The same trend was observed in other layers of the aquifer (data not shown). We also see from Figure 4.30 that the extent of perchlorate degradation near the treatment wells when the pump rate is 75 m^3/d and 50 m^3/d appears to be slightly less than when the pump rate is 10 m^3/d. The perchlorate concentration contours shown in Figures 4.31 and 4.32 confirm this.

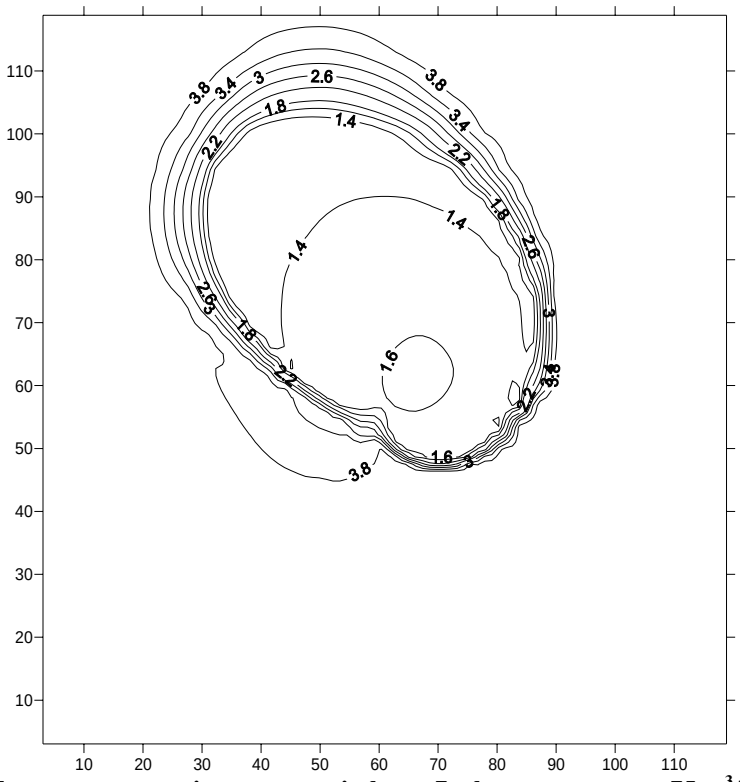

Figure 4.31 Perchlorate concentration contours in layer 7 when pump rate = 75 m^3/d (TAC=600 mg/l, continuous donor addition, 360 day simulation)

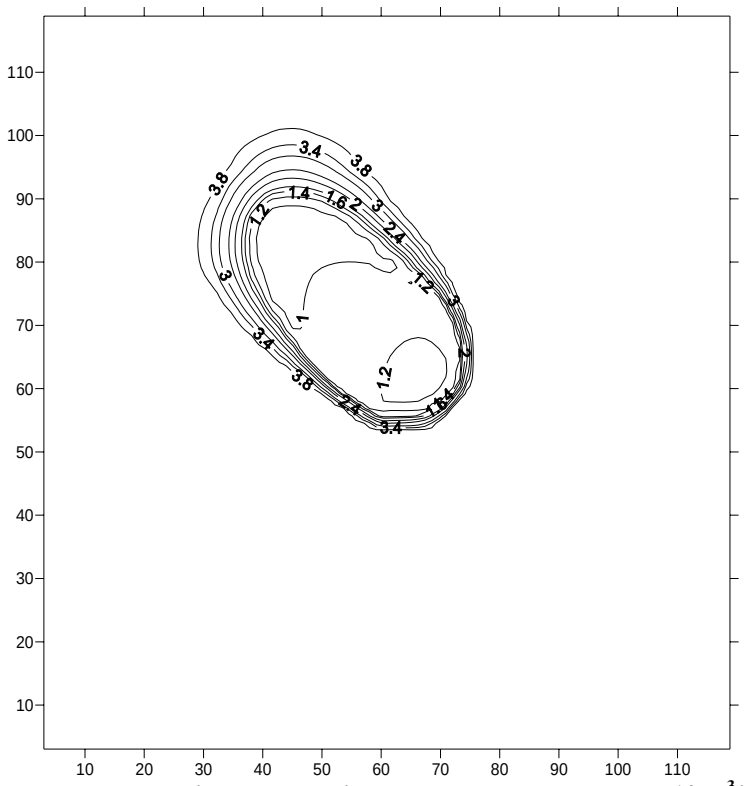

Figure 4.32 Perchlorate concentration contours in layer 7 when pump rate = 10 m^3/d (TAC=600 mg/l, continuous donor addition, 360 day simulation)

Comparing Figure 4.31 and Figure 4.32, we see that the extent of perchlorate degradation near the treatment wells is slightly higher when the pumping rate is 10 m^3/d. The lower perchlorate concentration contours near the treatment wells when the pumping rate is set to 10 m^3/d may be due to the fact that the groundwater is moving at a lower velocity and therefore spends more time in the bioactive zone. Figure 4.33 shows the perchlorate concentration time series at well 3627.

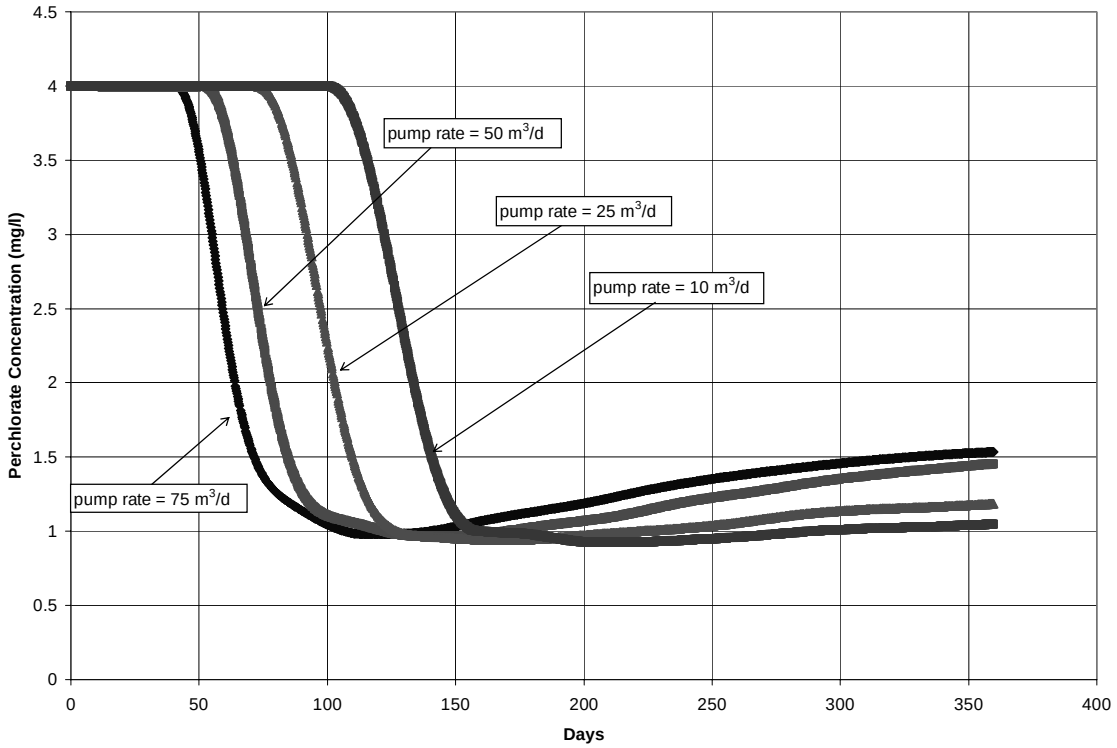

Figure 4.33 Perchlorate concentration time series at well 3627 under various pumping rates (TAC=600 mg/l, continuous donor addition, 360 day simulation)

The 10 m^3/d pump rate results in the lowest perchlorate concentration at well 3627 at the end of the 360 day simulation. The differences between the four curves shown in Figure 4.33 are 1) the time at which the perchlorate concentration begins to drop, *i.e.* the time when groundwater containing lower perchlorate concentrations arrives at well 3627 from up-gradient, and 2) the extent of the rebound in perchlorate concentration at the end of the simulation. The greater the pumping rate, the sooner the plume arrives at well 3627 and the greater the rebound in perchlorate concentration at the end of the simulation.

Slower groundwater velocities are induced by lower pumping rates. Consequently, the perchlorate "hole" arrives at well 3627 later for the low pump rate simulations. Furthermore, the reason the perchlorate concentration rebounds less during the simulations using lower pumping rates may be due to the lower electron donor mass

loading rate used in these simulations to maintain a constant TAC of 600 mg/l. The lower mass loading rates result in lower biomass growth (and decay) as shown in Figure 4.34.

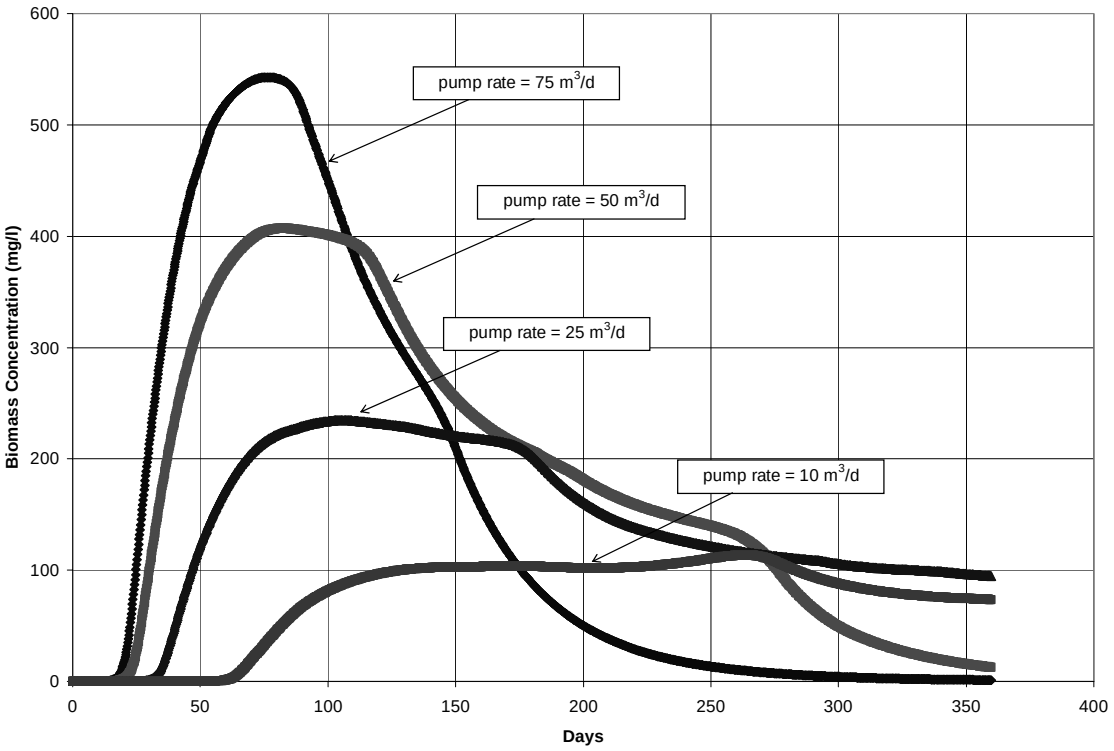

Figure 4.34 Biomass concentration time series at layer 7 extraction well under various pumping rates (TAC=600 mg/l, continuous donor addition, 360 day simulation)

Biomass does not accumulate as fast under the lower electron donor loading rate. Thus, as shown in Figure 4.34, there is less temporal variability of biomass at the lower electron donor loading rates. Since there is a significantly more biomass near the treatment wells at the end of the low pump rate/low electron donor loading rate simulations, the rebound in perchlorate concentration is not as pronounced as for the higher pump rate/electron donor loading rate simulations where the biomass concentrations near the wells drop rapidly over time.

Figure 4.35 compares the biomass concentration time series at the extraction screen in layer 3 at different pumping rates.

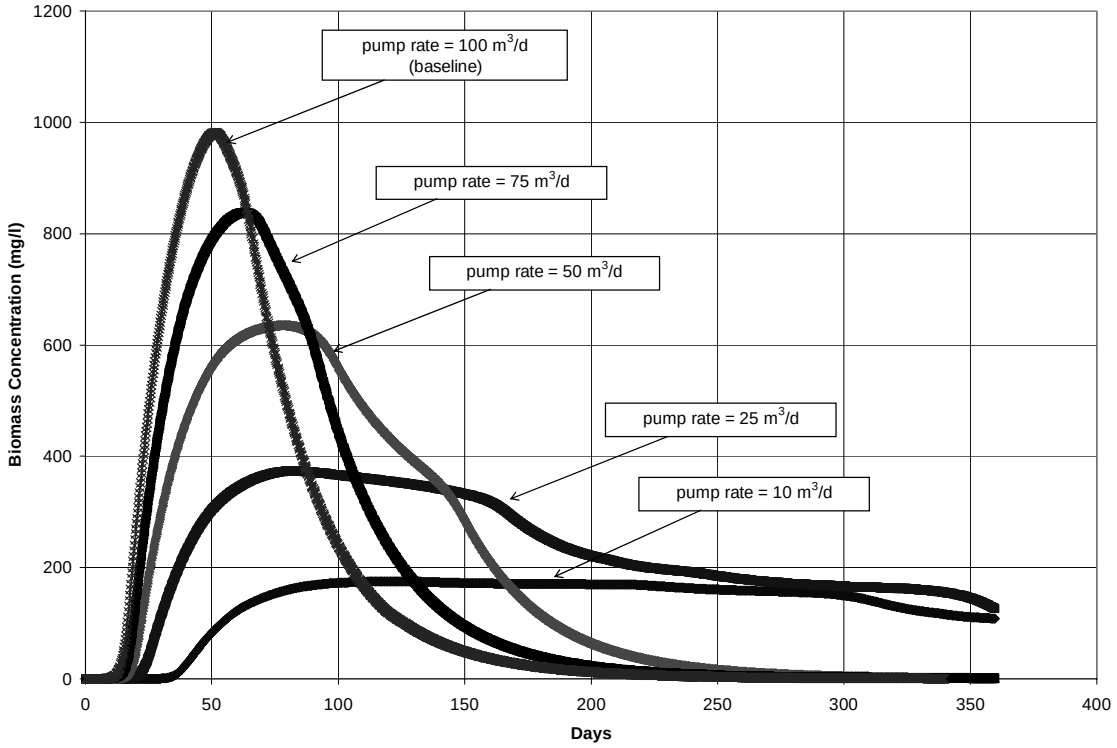

Figure 4.35 Biomass concentration time series at layer 3 extraction well under various pumping rates (TAC=600 mg/l, continuous donor addition, 360 day simulation)

We see from Figure 4.35 that the biomass reaches its highest concentration at the extraction well screen in layer 3 in the baseline simulation (pumping rate = 100 m^3 per d). It was shown earlier that this maximum observed biomass concentration has little effect on the porosity of the aquifer. Therefore, the bioclogging effects of the biomass for the lower pumping rates should be less than the bioclogging effects of the baseline simulation discussed previously.

Varying the pumping rate produces two different effects on the performance of the HFTW system. First, the lower pumping rate decreases circulation between the treatment wells and reduces the capture zone of the HFTW. Second, in order to maintain a constant TAC of 600 mg/l throughout each of the simulations, the electron donor mass loading rate must be reduced in each simulation. This also affects the performance of the technology by limiting the growth of biomass near the treatment wells.

The results of these competing effects can be seen in the seemingly contradictory results of the simulations presented in this section. Table 4.4 clearly shows that a lower pumping rate results in a lower amount of perchlorate degradation in terms of total mass of perchlorate destroyed. Yet the down-gradient perchlorate concentration time series data seem to indicate that the lower pumping rates are more effective in reducing perchlorate concentrations. These results illustrate the care that must be exercised when making decisions based upon modeling efforts. If the success of a remediation effort is measured solely on decreases in down-gradient concentration, low pumping rates may be preferable even though more perchlorate mass is removed from the aquifer using higher pumping rates.

The next section discusses a proposed set of engineering parameters to be used at the Aerojet site based on the analysis previously presented.

4.4 MODEL RESULTS USING PROPOSED ENGINEERED HFTW PARAMETERS

4.4.1 PROPOSED MODEL PARAMETERS

In this final section we propose a set of engineered HFTW parameters based on the analysis presented in the preceding sections. From the analysis conducted in section 4.3.2 it appears that a larger time averaged concentration provides the best results in terms of the total mass of perchlorate degraded and down-gradient concentration. The amount of biomass accumulation, and thus bioclogging, realized at higher TAC levels does not appear to have a detrimental effect on the performance of the HFTW system at the Aerojet site. Considering these observations, the proposed TAC to be used at the Aerojet site is 1200 mg/l. The simulations where the electron donor pulsing schedule was varied showed virtually no difference in model results. Therefore, a continuous electron donor pulse will be proposed because it facilitated the degradation of slightly more perchlorate mass.

The selection of the pumping rate to be employed at the Aerojet site seeks to simultaneously degrade the most perchlorate mass as well as minimize the down-gradient perchlorate concentration to the greatest extent possible. As such, a pumping rate that balances these two requirements, 25 m^3/d, is proposed for use at the Aerojet HFTW field demonstration site. This pumping rate was also chosen based on the maximum pumping rate that testing in the field has shown can be achieved and maintained at the Aerojet site.

4.4.2 MODEL RESULTS

The following table compares the amount of perchlorate mass degraded using a 25 m^3/d HFTW pumping rate and a TAC of 1200 mg/l with continuous electron donor addition with the simulation results obtained when the same HFTW pumping rate and electron donor addition schedule were used but the TAC was reduced to 600 mg/l.

Table 4.5 Mass of perchlorate degraded when TAC = 600 mg/l and TAC = 1200 mg/l. (pump rate = 25 m^3/d, continuous donor addition, 360 day simulation)

Time Averaged Ethanol Concentration (mg/l)	Mass of Perchlorate Degraded (kg)
600	12.20
1200	12.99

We see from Table 4.5, that the total mass of perchlorate degraded when the TAC is increased to the recommended level of 1200 mg/l, increases a little less than 1 kg. The cost of the increased ethanol required to realize this small increase in the mass of perchlorate degraded would have to be evaluated in order to determine if using a larger TAC is worthwhile.

Figure 4.36 below shows the perchlorate concentration time series results from well 3627 for the recommended HFTW engineered parameter set. The simulation results using the baseline TAC, 600 mg/l are also included in Figure 4.36.

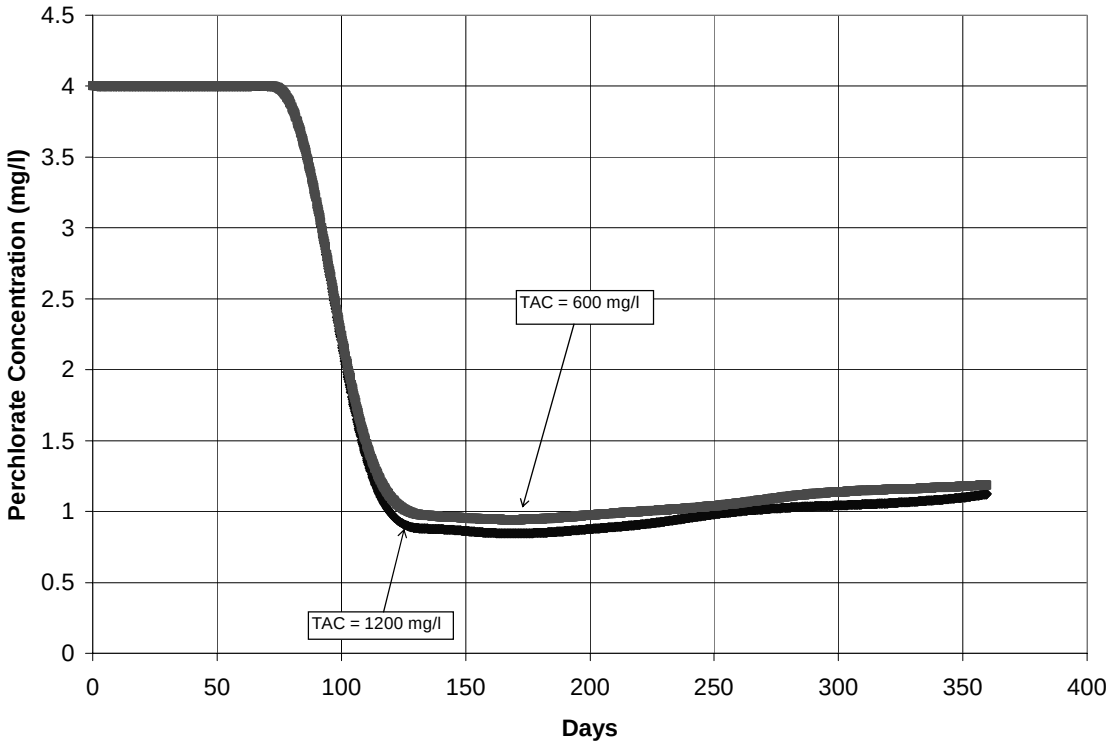

Figure 4.36 Perchlorate concentration time series at well 3627 comparing (a) ethanol TAC of 1200 mg/L and (b) ethanol baseline TAC (pump rate = 25 m^3/d, continuous electron donor addition, 360 day simulation)

Figure 4.36 shows us that only a slight decrease in perchlorate concentration is realized when the TAC is increased to 1200 mg/l. Figure 4.36 indicates that the recommended HFTW engineering parameter set is effective in decreasing the down-gradient perchlorate concentration observed at well 3627 from 4 mg/l to 1.12 mg/l, a decrease in perchlorate concentration of 72%. However, the baseline TAC, 600 mg/l, was able to effect a similar 70% decrease in the perchlorate concentration from 4 mg/l to 1.19 mg /l. The difference between the results of the two TAC levels may not be significant enough to warrant using an ethanol TAC level of 1200 mg/l.

Finally, Figure 4.37 shows the biomass concentration at the layer 3 extraction well screen, the location which previous simulations have shown is subject to the largest increase in biomass concentration.

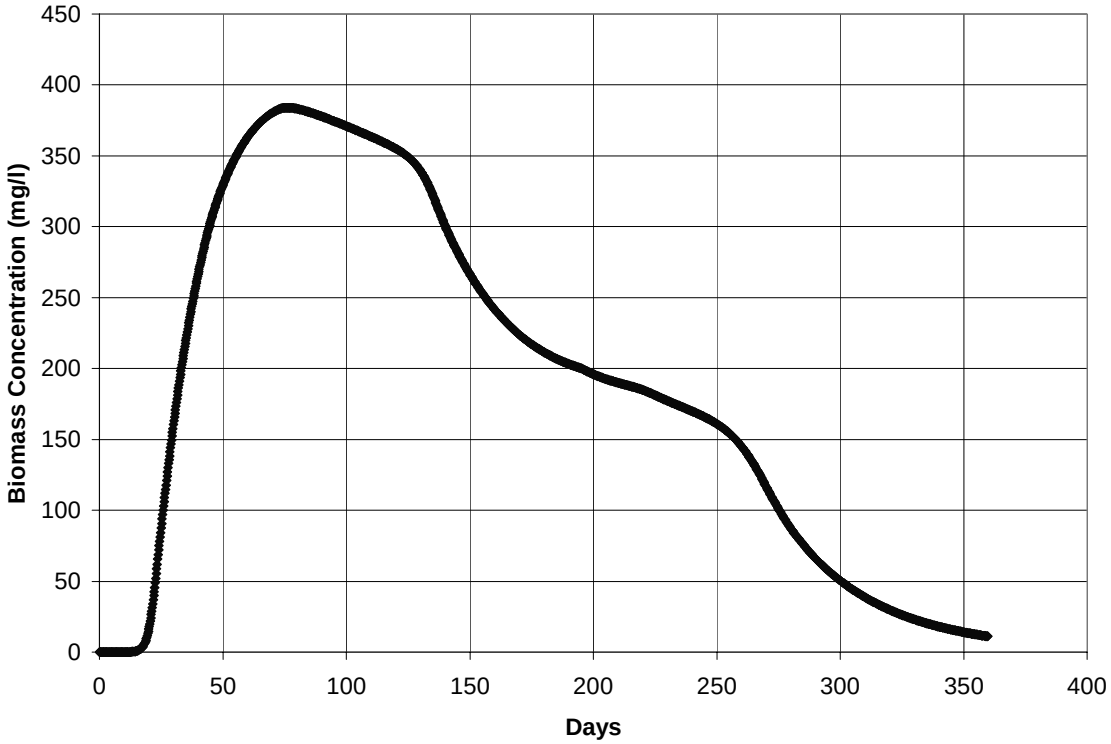

Figure 4.37 Biomass concentration time series at well 3627 for (a) ethanol TAC of 1200 mg/L and (b) ethanol baseline TAC (pump rate = 25 m^3/d, continuous donor addition, 360 day simulation)

Comparing Figure 4.37 biomass concentrations with earlier simulations shows that no reduction in conductivity due to bioclogging is anticipated. Porosity profiles of the various aquifer layers indicate little or no change (data not shown), confirming that bioclogging may not be an issue of concern when using the proposed HFTW engineered parameter set.

5.0 CONCLUSIONS

5.1 SUMMARY

In this thesis, the technology model developed by Parr *et al*. (2003) was modified to include a bioclogging submodel based on the relationship developed by Clement *et al*. (1996) which describes the change in hydraulic conductivity due to the accumulation of biomass within the porous medium. This combined technology model was then applied to simulate the *in situ* remediation of a perchlorate plume located at the Aerojet Superfund site in Sacramento, California.

Simulations based on the site characteristics of the Aerojet site and biological kinetic parameters developed by Envirogen (2002) predict that bioclogging will not have an adverse effect on *in situ* perchlorate biodegradation through the addition of an electron donor (ethanol).

5.2 CONCLUSIONS

- **Bioclogging does not occur solely due to the accumulation of biological mass.** The production of extra cellular polymers and gaseous byproducts also may present a significant source of hydraulic conductivity loss within a biologically active zone of an aquifer. Additionally, the biomass attached to the porous medium may increase the friction factor of the porous media and thereby reduce hydraulic conductivity.

- **Bioclogging appears to occur under a variety of subsurface conditions.** Both aerobic and anaerobic aquifer conditions can promote bioclogging. Evidence has also shown that bioclogging can occur under acidic aquifer conditions as well.

  The primary physical parameter that determines the extent of the impact bioclogging has on an aquifer is the grain size of the porous medium, with fine soil particles being most susceptible to bioclogging. First, coarse-grained soils have less specific surface area available for colonization by microorganisms. Therefore, there is less microbial growth and the bioclogging effect is less than in fine-grained soils with high specific surface area. Second, fine soil particles that may advect in the groundwater flow field are susceptible to being trapped by extra cellular polymers produced by subsurface microorganisms.

- **There are several methods available to mathematically model the processes involved in bioclogging.** Mathematically modeling bioclogging typically involves a fundamental assumption regarding how biomass accumulates within the subsurface. The most common type of model is based upon the assumption that the microorganisms within the subsurface grow in a uniform biofilm that coats the particles of the porous medium. Other mathematical models of bioclogging assume that the biomass accumulates as aggregates or plugs within the pore throats of the porous medium. Still other models of bioclogging assume that biomass accumulates in an incomplete biofilm or "microcolony".

A final class of bioclogging models makes no assumptions regarding the way biological mass accumulates within the subsurface. It was determined that this class of bioclogging models was more appropriate for use in this work than those models that make unverifiable assumptions regarding how biomass accumulates.

- **Bioclogging does not appear to adversely impact the HFTW system being used to effect *in situ* perchlorate biodegradation at the Aerojet site.** Simulations using the combined technology model were conducted using a variety of engineered parameters (time averaged electron donor concentration, electron donor addition schedule, and HFTW pumping rates). The results of the various simulations do not indicate that bioclogging has a detrimental effect on *in situ* perchlorate biodegradation achieved through electron donor addition via an HFTW system.

5.3 RECOMMENDATIONS

- **Validate the combined technology model.** The next step in refining our model of HFTW effected *in situ* perchlorate biodegradation is to compare the results obtained in this study with actual field data obtained from the Aerojet field demonstration site.

- **Develop an alternative model describing bioclogging that is more sensitive to low levels of microbial growth.** The version of the Clement *et al*. (1996) equation used in this study relates the hydraulic conductivity ratio to the change in

the biomass concentration. The reader is referred to the Appendix for a detailed discussion regarding this issue. The resultant maximum concentration of biomass within the aquifer, X_{as}, used in this study was equal to 1.1×10^6 mg/l. This large value makes the bioclogging submodel insensitive to the relatively low level biomass concentrations encountered in the simulations conducted as part of this study. The impact of relatively low levels of biological growth on hydraulic conductivity, particularly near the treatment wells, may be better described by a bioclogging model that makes fundamental assumptions regarding how biomass grows within the porous matrix.

- **Obtain kinetic parameters for microbial consumption of oxygen, nitrate, and perchlorate using ethanol as an electron donor.** The present study used kinetic parameters obtained from experiments which used acetate as the electron donor for oxygen, nitrate, and perchlorate reduction (Envirogen, 2002). The Aerojet field demonstration used ethanol as the electron donor. More accurate model predictions may result if the kinetic parameters associated with biological growth using ethanol as the electron donor were available for use in the multi-electron acceptor dual-Monod biological submodel.

A.0 APPENDIX: TECHNOLOGY MODEL EQUATIONS AND PARAMETERS

A.1 INTRODUCTION

The purpose of this appendix is to expand upon Section 3.3 and provide the reader with more detail regarding the technology model for *in situ* perchlorate bioremediation using HFTWs. First, the model equations used in each of the elements in Figure 3.8 are presented. The next section of this appendix will describe the three dimensional model space used in this study. In the final section, the parameter values used in this study are presented.

A.2 MODEL EQUATIONS

In order to calculate groundwater velocities for use in the transport equation, MODFLOW must first solve equation A.1, Laplace's equation, for user-specified boundary conditions and source/sinks.

$$\nabla^2 h = 0 \qquad \text{(A.1)}$$

where

h = *hydraulic head (L)*

The solution to equation A.1 is the three-dimensional hydraulic head field. Then, using the hydraulic conductivities that were either input initially, or calculated by the bioclogging model, Darcy's law, Equation A.2, is used by MODFLOW to calculate the three-dimensional velocity field (v).

$$v = -\frac{K}{n}\nabla h \quad \text{(A.2)}$$

where

K = hydraulic conductivity tensor (L/T)

n = measured porosity of porous media

The velocity field is then used in Equations A.3 through A.6 the chemical advective/dispersive transport equations. These equations are developed from conservation of mass principles, and describe the transport and fate of dissolved ethanol, oxygen, nitrate, and perchlorate in terms of the temporal and spatial changes in their respective concentrations C^{don}, C^{oxy}, C^{nit}, and C^{per}.

$$\frac{\partial C^{don}}{\partial t}(1+\frac{k_d \rho_{bulk}}{n}) = D\cdot\nabla^2 C^{don} - v\cdot\nabla C^{don} + r_{donor} \quad \text{(A.3)}$$

$$\frac{\partial C^{oxy}}{\partial t}(1+\frac{k_d \rho_{bulk}}{n}) = D\cdot\nabla^2 C^{oxy} - v\cdot\nabla C^{oxy} + r_{oxy} \quad \text{(A.4)}$$

$$\frac{\partial C^{nit}}{\partial t}(1+\frac{k_d \rho_{bulk}}{n}) = D\cdot\nabla^2 C^{nit} - v\cdot\nabla C^{nitn} + r_{nit} \quad \text{(A.5)}$$

$$\frac{\partial C^{per}}{\partial t}(1+\frac{k_d \rho_{bulk}}{n}) = D\cdot\nabla^2 C^{per} - v\cdot\nabla C^{per} + r_{per} \quad \text{(A.6)}$$

The quantity in the parenthesis on the left hand side of Equation A.3 through Equation A.6 is known as the retardation coefficient. The bulk density of the porous medium, ρ_{bulk}, and the porosity, n, has been defined previously. k_d is known as the soil-water partitioning coefficient which is defined as the ratio of the concentration of a compound adsorbed to the solid phase of a porous media (mass of compound per mass of soil) to the concentration of the compound in solution (mass of compound per volume of water). For

the electron donor, in this case, ethanol, k_d was set equal to 0.2 L/kg. For oxygen, nitrate, and perchlorate, the partitioning coefficient was set equal to zero.

The first terms on the right hand side of the transport equations (A.3-A.6) represent dispersive transport. Dispersion is not explicitly modeled in the present study. Rather, numerical dispersion, resulting from the truncation errors associated with numerically solving Equations A.3 through A.6 by finite differences, is used to model dispersive phenomenon in a porous medium (Parr, 2002). No parameter representing the dispersion coefficient, *D*, is input into the technology model, but according to Charbeneau (2000) and reported by Parr (2002), the dispersion can be estimated using the following relationship.

$$D_{x,y,z} = \frac{v_{x,y,z}\Delta(d_{x,y,z})}{2} + \frac{(v_{x,y,z})^2 \Delta t}{2} \qquad \text{(A.7)}$$

where

$v_{x,y,z}$ = *groundwater velocity in the x, y, and z directions*

$\Delta d_{x,y,z}$ = *cell size in the x, y, and z directions*

Δt = *time step*

The last terms on the right hand side of Equations A.3 through A.6 represent the biodegradation sink terms defined in the following equations.

$$r_{donor} = \frac{dC^{don}}{dt} = -X \cdot (r_{don,oxy} + r_{don,nit} + r_{don,per}) \qquad \text{(A.8)}$$

$$r_{oxy} = \frac{dC^{oxy}}{dt} = -X \cdot (F_{oxy} \cdot r_{don,oxy}) \qquad \text{(A.9)}$$

$$r_{nit} = \frac{dC^{nit}}{dt} = -X \cdot (F_{nit} \cdot r_{don,nit}) \qquad \text{(A.10)}$$

$$r_{per} = \frac{dC^{per}}{dt} = -X \cdot (F_{per} \cdot r_{don,per}) \qquad \text{(A.11)}$$

where

r_{donor} = *rate of electron donor consumption (mg donor/L/day)*

r_{oxy}= *rate of oxygen consumption (mg oxygen/L/day)*

r_{nit}= *rate of nitrate consumption (mg nitrate/L/day)*

r_{per}= *rate of perchlorate consumption (mg perchlorate/L/day)*

$r_{don,oxy}$ = *specific rate of electron donor consumption using oxygen as an electron acceptor (mg donor/mg biomass/day)*

$r_{don,nit}$ = *specific rate of electron donor consumption using nitrate as an electron acceptor (mg donor/mg biomass/day)*

$r_{don,per}$ = *specific rate of electron donor consumption using perchlorate as an electron acceptor (mg donor/mg biomass/day)*

X = *concentration of active biomass (mg/L)*

F_{oxy} = *0.83 (mg oxygen/mg donor)*

F_{nit} = *1.3 (mg nitrate/mg donor)*

F_{per}= *1.45 (mg perchlorate/mg donor)*

The reader is referred to Parr (2002) and Parr *et al.* (2003) for the stoichiometric equations used to determine the values of *F*, the ratios of electron acceptor reduced per electron donor oxidized. The dual-Monod expressions for the specific rates of donor consumption used in Equations A.8 through A.11 are (Parr, 2002; Parr *et al.,* 2003):

$$r_{don,oxy} = k_{\max}^{don/oxy}\left[\frac{C^{don}}{K_S^{don/oxy} + C^{don}}\right]\cdot\left[\frac{C^{oxy}}{K_S^{oxy} + C^{oxy}}\right] \quad \text{(A.12)}$$

$$r_{don,nit} = k_{\max}^{don/nit}\left[\frac{C^{don}}{K_S^{don/nit} + C^{don}}\right]\cdot\left[\frac{C^{nit}}{K_S^{nit} + C^{nit}}\right]\cdot\left[\frac{K_i^{oxy}}{K_i^{oxy} + C^{oxy}}\right] \quad \text{(A.13)}$$

$$r_{don,per} = k_{\max}^{don/per}\left[\frac{C^{don}}{K_S^{don/per} + C^{don}}\right]\cdot\left[\frac{C^{per}}{K_S^{per} + C^{per}}\right]\cdot\left[\frac{K_i^{oxy}}{K_i^{oxy} + C^{oxy}}\right]\cdot\left[\frac{K_i^{nit}}{K_i^{nit} + C^{nit}}\right] \quad \text{(A.14)}$$

where

$k_{max}^{don/oxy}$ = *maximum specific rate of substrate utilization in the presence of oxygen when donor concentration is varied and limiting (mg donor/mg biomass/day)*

$k_{max}^{don/nit}$ = *maximum specific rate of substrate utilization in the presence of nitrate when donor concentration is varied and limiting (mg donor/mg biomass/day)*

$k_{max}^{don/per}$ = *maximum specific rate of substrate utilization in the presence of perchlorate when donor concentration is varied and limiting (mg donor/mg biomass/day)*

$K_S^{don/oxy}$ = *half saturation concentration of the electron donor in the presence of oxygen when donor (ethanol) concentration is varied and limiting (mg donor/L)*

$K_S^{don/nit}$ = *half saturation concentration of the electron donor in the presence of nitrate when donor (ethanol) concentration is varied and limiting (mg donor/L)*

$K_S^{don/per}$ = *half saturation concentration of the electron donor in the presence of perchlorate when donor (ethanol) concentration is varied and limiting (mg donor/L)*

K_S^{oxy} = *half saturation concentration when oxygen (an electron acceptor) concentration is varied and limiting (mg/L)*

K_S^{nit} = *half saturation concentration when nitrate (an electron acceptor) concentration is varied and limiting (mg/L)*

K_S^{per} = *half saturation concentration when perchlorate (an electron acceptor) concentration is varied and limiting (mg/L)*

K_i^{oxy} = *oxygen inhibition coefficient (mg/L)*

K_i^{nit} = *nitrate inhibition coefficient (mg/L)*

Equations A.12, A.13, and A.14 are used in Equations A.8 through A.11 in order to calculate the consumption rates of the various chemical species of interest. Note that the first two Monod terms in Equations A.12 through A.14 indicate that the rate of electron donor consumption is dependent upon the concentration of the electron donor as well as the electron acceptor. Recall from the discussion in Chapter 2 that oxygen is the preferred electron acceptor utilized by perchlorate respiring bacteria. The reduction in donor consumption using nitrate as an acceptor, due to the presence of oxygen, is captured in Equation A.13 by the inhibition term, the third term on the right hand side of the equation. Similarly, the reduction in donor consumption using perchlorate as an acceptor, due to the presence of oxygen and nitrate, is captured in Equation A.14 by inhibition terms, the third and fourth terms on the right hand side of the equation.

The biomass growth/decay equation is shown below.

$$\frac{dX}{dt} = X \cdot \left[Y_{biomass} \cdot (r_{don,oxy} + r_{don,nit} + r_{don,per}) - b \right]; \quad X > X_{\min} \tag{A.15a}$$

$$\frac{dX}{dt} = 0; X \le X_{\min} \tag{A.15b}$$

where

$Y_{biomass}$ = *the biomass yield per mass of donor consumed (mg biomass/mg electron donor)*

b = *biomass decay rate (1/day)*

X_{min} = *minimum survival concentration of biomass (mg/l)*

Equation A.15b ensures that the microbial population never is totally depleted anywhere in space. Parr (2002) presents a body of literature indicating that even in the absence of electron donor or acceptor, a small population of microorganisms (X_{min}) will survive.

The final element of the technology model is the relationship that describes bioclogging. Recall from Chapter 3, that the Clement *et al.* (1996) bioclogging equation was selected for integration into the Parr (2002) numerical model of *in situ* biodegradation of perchlorate. The Clement *et al.* (1996) bioclogging relationship is shown here:

$$\frac{K_s}{K_{so}} = (1 - \frac{n_b}{n})^{19/6} \qquad \text{(A.16)}$$

where

K_s = *clogged hydraulic conductivity (Lt/T)*

K_{so} = *hydraulic conductivity under sterile conditions (L/T)*

n = *initial porosity* (L^3/L^3)

n_b = *fraction of total volume occupied by biomass* (L^3/L^3)

The version of Equation A.16 that is integrated into the technology model is:

$$\frac{K_s}{K_{so}} = (1 - \frac{X}{X_{as}})^{19/6} \qquad \text{(A.17)}$$

where

X = *active biomass concentration* (M/L^3)

X_{as} = *maximum biomass concentration* (M/L^3)

Equation A.17 is used in the technology model code so that *X*, the active biomass concentration that is calculated from equation A.15, can be used directly to determine hydraulic conductivity reduction rather than having to convert active biomass concentration to n_b in order to apply equation A.16.

If we define biomass density, ρ_b, as $mass_{bio}$/ $volume_{bio,}$ we see:

$$X = \frac{n_b}{n} * \rho_b \quad \text{(A.18)}$$

When biomass has accumulated to the point where all of the pore space is completely occupied by biomass ($n_b/n = 1$), we find:

$$X_{as} = \rho_b \quad \text{(A.19)}$$

Assuming that bacterial biomass has a specific gravity of 1.1 as suggested in Maier *et al.* (2000), Equation A.18 would result in $X_{as} = 1.1x10^6$ mg/L. Finally, it should be noted that K_{so} can never be reached because there is always the survival population of microorganisms present, X_{min}, and according to Equation A.17, K_s and K_{so} are only equal when X = 0.

The next section describes the model space used to simulate the Aerojet HFTW demonstration site.

A.3 SITE MODEL

The site model is a finite difference grid created using MODFLOW. Figure A.1 is a plan view of a portion of the site model, showing the locations of the HFTWs and monitoring wells at the Aerojet Site, in relation to the groundwater flow direction.

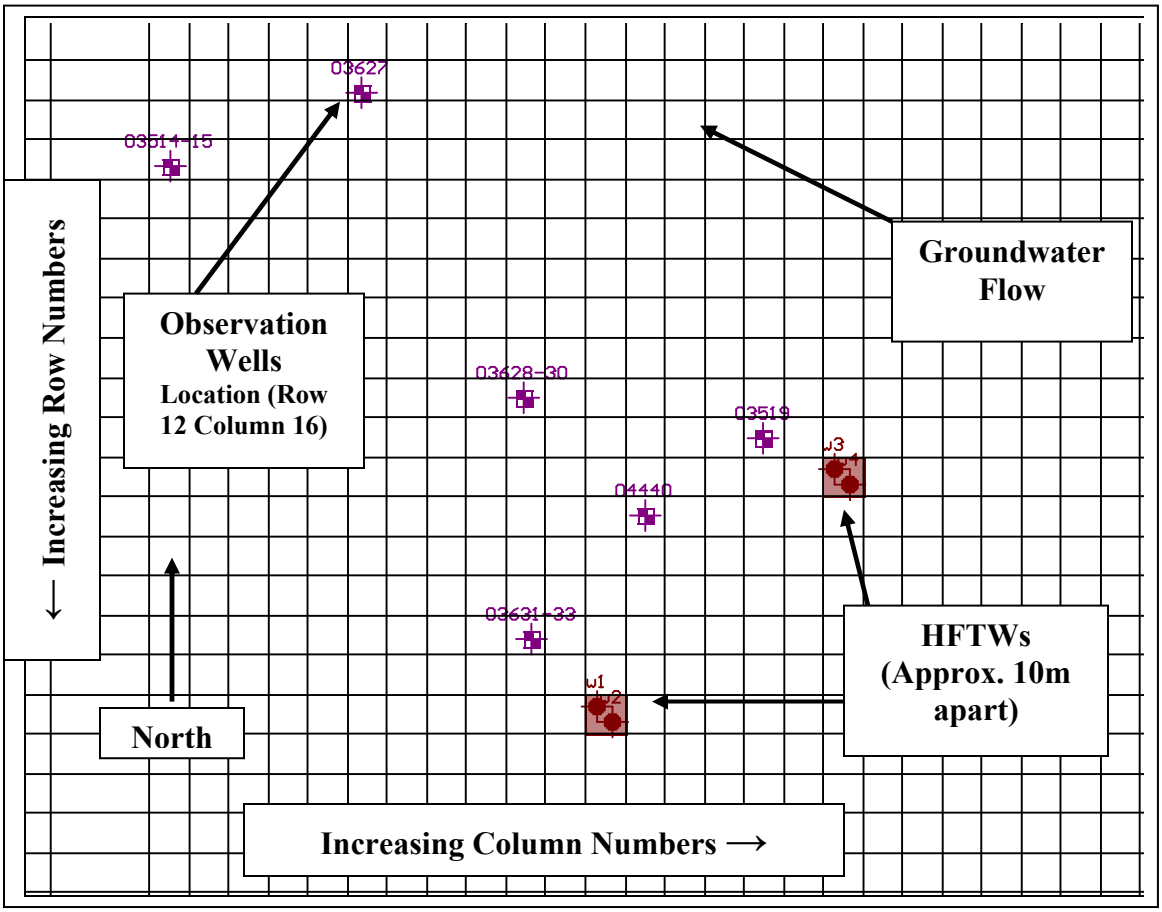

Figure A.1 Plan view of site model

The grid shown in Figure A.1 is only a portion of the total site model. The full site model consists of a 45 unit long x 45 unit wide x 12 layer deep grid representing a 121.92m x 121.92m x 40.843m rectangular solid. Not all of the cells of the grid are the same size. Cells close to the HFTWs are smaller to better capture hydrologic, chemical, and biological activity that occurs close to the treatment wells. It is also worth noting that several of the observation wells consist of multiple wells screened at different depths below ground surface (bgs). Nearly all of the observation wells are screened at 30.48 meters bgs or less.

Figure A.2 illustrates the 12 vertical layers used in the site model. The hatched areas represent the layers that are spanned by the upper and lower well screens of the HFTWs. Each layer is assigned a single hydraulic conductivity. Hydraulic conductivity homogeneity and isotropy within each layer is assumed.

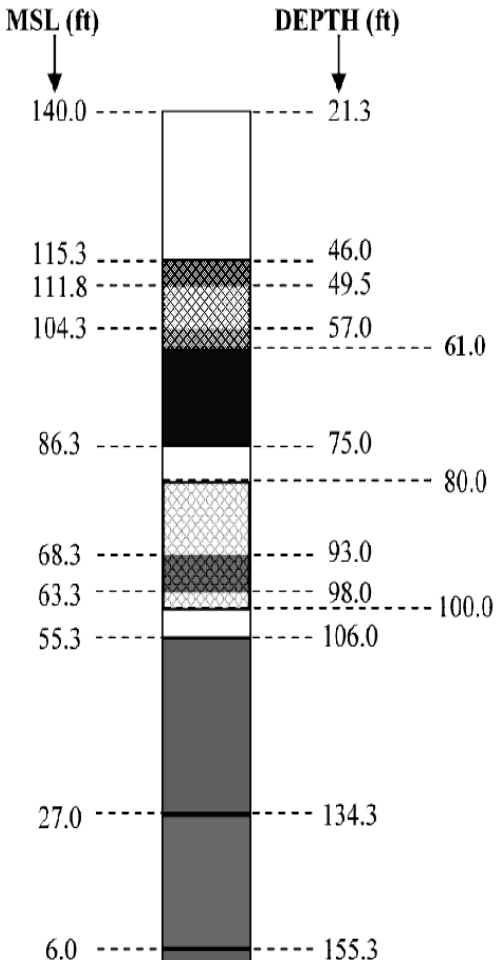

Figure A.2 Layers in site model (depths in feet below ground surface)

A.4 PARAMETER VALUES

There are a number of parameters that must be input into the technology model. This section breaks these parameters down into three sections: geologic/hydrogeologic parameters, biological/chemical parameters, and boundary conditions.

Table A.1 Geologic/hydrogeologic parameters

Layer	Thickness (m)	Transmissivity (m^2/day)	Hydraulic conductivity (m/day)	Effective Porosity
1	7.529	Unconfined Layer	2.286	0.3
2	1.067	0.076	0.071	0.3
3	2.286	5.226	2.286	0.3
4	1.219	0.087	0.071	0.3
5	4.267	0.303	0.071	0.3
6	1.524	3.484	2.286	0.3
7	3.962	9.057	2.286	0.3
8	1.524	0.108	0.071	0.3
9	0.61	1.394	2.286	0.3
10	1.829	4.181	2.286	0.3
11	8.626	4.925	0.571	0.3
12	6.401	0.173	0.027	0.3

The data in Table A.1 were obtained from optimization calculations based on pump tests conducted at the HFTW demonstration site (Shaw Environmental and Infrastructure, 2003). All dimensions have been converted to metric to facilitate operation of the technology model.

Table A.2 presents the chemical and biological parameters used in this study. The source of the parameter values is indicated in the table, with most of the parameters obtained from the final report for SERDP project CU-1136 (Envirogen, 2002). The kinetic parameters shown in Table A.2 were determined using acetate as the electron donor. The field study at the Aerojet site will use ethanol as the electron donor. The corresponding set of biological kinetic parameters describing the growth of microorganisms metabolizing oxygen, nitrate, and perchlorate through the oxidation of ethanol were not available. Therefore, for the purposes of the present study, it is assumed that the

parameters shown below accurately reflect the kinetic behavior of subsurface microorganisms metabolizing ethanol.

Table A.2 Biological/chemical parameters

Parameter	Value	Description	Reference
$k_{max}^{don/oxy}$	5.04	maximum specific rate of ethanol utilization in the presence of oxygen when the ethanol concentration is varied and limiting (mg ethanol/mg biomass/day)	Envirogen, 2002
$k_{max}^{don/nit}$	3.48	maximum specific rate of ethanol utilization in the presence of nitrate when the ethanol concentration is varied and limiting (mg ethanol/mg biomass/day)	Envirogen, 2002
$k_{max}^{don/per}$	3.36	maximum specific rate of ethanol utilization in the presence of perchlorate when the ethanol concentration is varied and limiting (mg ethanol/mg biomass/day)	Envirogen, 2002
$K_S^{don/oxy}$	90.0	half saturation concentration of ethanol in the presence of oxygen when the ethanol concentration is varied and limiting (mg ethanol/L)	Envirogen, 2002
$K_S^{don/nit}$	70.0	half saturation concentration of ethanol in the presence of nitrate when the ethanol concentration is varied and limiting (mg ethanol/L)	Envirogen, 2002
$K_S^{don/per}$	120.0	half saturation concentration of ethanol in the presence of perchlorate when the ethanol concentration is varied and limiting (mg ethanol/L)	Envirogen, 2002
K_S^{oxy}	1.0	half saturation concentration of oxygen when oxygen concentration is varied and limiting (mg oxygen/L)	Envirogen, 2002
K_S^{nit}	180.0	half saturation concentration of nitrate when nitrate concentration is varied and limiting (mg nitrate/L)	Envirogen, 2002
K_S^{per}	150.0	half saturation concentration of perchlorate when perchlorate concentration is varied and limiting (mg perchlorate/L)	Envirogen, 2002
K_i^{oxy}	1.0	inhibition coefficient of oxygen (mg oxygen/L)	Envirogen, 2002
K_i^{nit}	180	inhibition coefficient of nitrate (mg nitrate/L)	Envirogen, 2002
Y	0.236	biomass yield coefficient (mg biomass/ mg ethanol)	Envirogen, 2002

b	0.0624	Biomass decay rate (1/day)	Envirogen, 2002
Foxy	0.83	stiochiometric ratio of oxygen to ethanol utilization for biomass growth	Envirogen, 2002
Fnit	1.30	stiochiometric ratio of nitrate to ethanol utilization for biomass growth	Envirogen, 2002
Fper	1.45	stiochiometric ratio of perchlorate to ethanol utilization for biomass growth	Envirogen, 2002
bimn	0.01	minimum biomass concentration (mg biomass/L)	Envirogen, 2002
Xas	1.1×10^6	saturated biomass concentration (mg biomass/L)	See text (Section A.2)
kd	0.2	ethanol distribution coefficient (L/kg)	Arbitrary

To complete the site model, boundary conditions must be defined. Figure A.3 is a plan view of the entire site model, showing the constant head boundary conditions. Groundwater flow is from the bottom right corner of the figure to the top left corner of the figure.

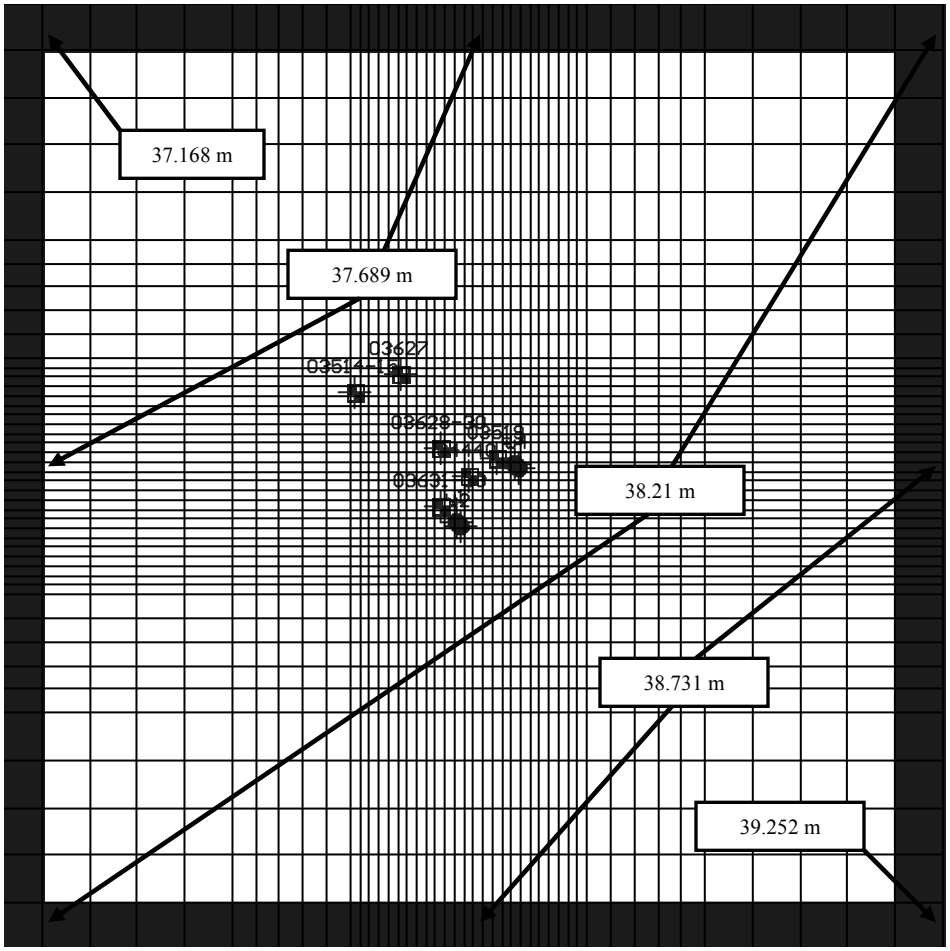

Figure A.3 Constant head boundary conditions

Selected values of the constant head boundary are displayed to give the reader a sense of the direction of decreasing head and consequently groundwater flow at the site. Hydraulic head values are input for the corner cells and MODFLOW linearly interpolates between them to determine the hydraulic head value of each boundary cell. Each of the twelve layers of the model has hydraulic head boundary conditions identical to those shown in Figure A.3, so that there is no vertical flow due to the natural hydraulic gradient. The cluster of dots in the middle of Figure A.3 represents the HFTWs and the downstream observation wells.

The boundary conditions for the electron acceptors (oxygen, nitrate, and perchlorate) are held constant for two of the four boundaries of the site model as shown in Figure A.4.

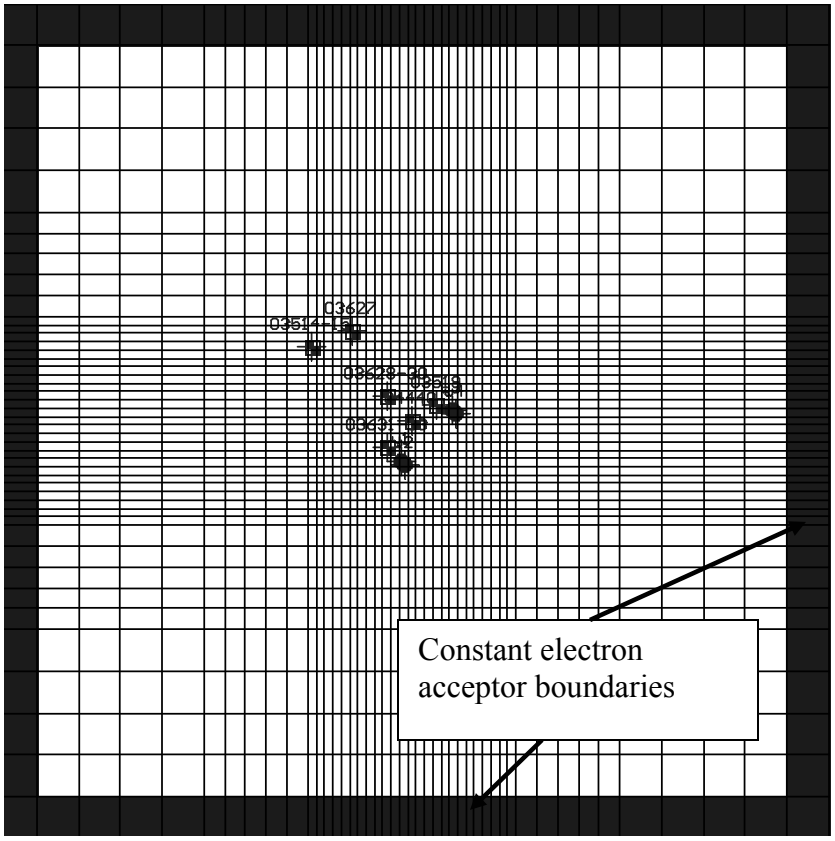

Figure A.4 Constant electron acceptor boundaries

As stated earlier, groundwater flow is from the lower right corner to the upper left corner of the site model. The oxygen and nitrate concentration within the indicated boundary cells is held constant; oxygen and nitrate concentrations within the rest of the site model change with time and space. Thus, the right and lower boundaries represent a constant source of oxygen and nitrogen for the site model. The initial and boundary oxygen and nitrate concentrations of all twelve layers of the site model are assumed to be homogeneous and equal to the on site concentrations reported in Table 3.1.

The lower and right hand boundaries also serve as a constant source of perchlorate. Unlike the other electron acceptors, however, Table 3.2 clearly shows that perchlorate concentrations increase with depth below ground surface. To capture this trend, it is assumed that the initial and boundary conditions for perchlorate concentration vary from layer to layer as shown in Table A.3.

Table A.3 Initial and boundary concentrations of model constituents

Constituent	Concentration (mg/L)
Ethanol	0
Oxygen	5.0
Nitrate	13.0
Microorganisms	0.01
Perchlorate – Layer 1	1.0
Perchlorate – Layer 2	1.0
Perchlorate – Layer 3	2.0
Perchlorate – Layer 4	2.0
Perchlorate – Layer 5	3.0
Perchlorate – Layer 6	4.0
Perchlorate – Layer 7	4.0
Perchlorate – Layer 8	4.0
Perchlorate – Layer 9	4.0
Perchlorate – Layer 10	4.0
Perchlorate – Layer 11	4.0
Perchlorate – Layer 12	4.0

Furthermore, in the absence of any measurement of indigenous perchlorate respiring microorganisms, it is assumed that the microorganisms are initially distributed uniformly at their minimum survival concentration (X_{min}).

BIBLIOGRAPHY

Air Force Center for Environmental Excellence (AFCEE). Bioreactors. Perchlorate Treatment Technology Fact Sheet, AFCEE/ERT, August 2002a. http://www.afcee.brooks.af.mil/ER/ert/perchloratetreatment/bioreactors.pdf

Air Force Center for Environmental Excellence (AFCEE). Permeable Reactive Barriers. Perchlorate Treatment Technology Fact Sheet, AFCEE/ERT, August 2002b. http://www.afcee.brooks.af.mil/ER/ert/perchloratetreatment/permeablereactivebarriers.pdf

Aerojet General Corporation, Personal Communication, Scott Neville, Aerojet Aquifer Depths. 2004.

Baveye, P., Vandervivere P., Hoyle, B.L., DeLeo, P.C., and De Lozada, D.S. Environmental Impact and Mechanisms of the Biological Clogging of Saturated Soils and Aquifer Materials. *Critical Reviews in Environmental Science and Technology*, 28(2): 123-191, 1998.

Baveye, P., Vandervivere, P., and De Lozada, D. Comment of Biofilm Growth and the Related Changes in the Physical Properties of a Porous Medium: 1. Experimental Investigations. *Water Resources Research*, 28: 543-550, 1989.

Bear, J. Dynamics of Fluids in Porous Media. New York, USA: Elsiver Publishing Company, 1972.

Bear, J., and Verruijt, A. Modeling Groundwater Flow and Pollution. Dordrecht, Holland: D. Reidel Publishing Company, 1987.

Bender, K.S., O'Connor, S.M., Chakraborty, R., Coates, J.D., and Achenbach, L.A. Sequencing and Transcriptional Analysis of the Chlorite Dismutase Gene of *Dechloromonas agitate* and Its Use as a Metabolic Probe. *Applied and Environmental Microbiology*, 68(10): 4820-4826, October, 2002.

Bohlke, J.K., Ericksen, G.E., Revesz, K. Stable Isotope Evidence for an Atmospheric Origin of Desert Nitrate Deposits in Northern Chile and Southern California, USA. *Chemical Geology*, 136: 135-152, 1997.

Brechner, R.J., Parkhurst, G.D., Humble, W.O., Brown, M.B., and Herman, W.H. Ammonium Perchlorate Contamination of Colorado River Drinking Water is Associated with Abnormal Thyroid Function in Newborns in Arizona. *Journal of Occupational and Environmental Medicine*, 42: 777-782, 2000.

California Department of Health Services (CDHS). Biological Treatment to Remove Perchlorate Given Conditional California DHS Approval. Department of Health Services, Sacramento, California. 2002 www.safe.drinkingwater.com/archive/sdwn051502.htm

California Department of Health Services (CDHS). Perchlorate in California Drinking Water: Status of Regulations and Monitoring Results. Department of Health Services, Sacramento, California. Updated August 6, 2003. www.dhs.cawnet.gov/ps/ddwem/chemicals/perchl/perchlindex.htm

Cao, J., Elliot, D., and Zhang, W. Nanoscale Iron Particles for Perchlorate Reduction. *Division of Industrial and Engineering Chemistry, the 225th ACS National Meeting*. New Orleans, LA, March 23-27, 2003.

Chang, A. C., Olmstead, W. R., Johansen, J. B., Yamashita, G. The Sealing Mechanism of Wastewater Ponds. *Journal of the Water Pollution Control Federation*, 46: 1715-1721, 1974.

Charbeneau, R.J. *Groundwater Hydraulics and Pollutant Transport.* Prentice-Hall Inc., pp. 428-435, 2000.

Chaudhuri, S.K., O'Connor, S.M., Gustavson, R.L., Achenbach, L.A., and Coates, J.D. Environmental Factors that Control Microbial Perchlorate Reduction. *Applied and Environmental Microbiology*, 68(9): 4425-4430, 2002.

Chu, M., Kitanidis, P.K., and McCarty, P.L. Effects of Biomass Accumulation on Microbially Enhanced Dissolution of a PCE Pool: A Numerical Simulation. *Journal of Contaminant Hydrology*, 65: 79-100, 2003.

Clark, J.J. Toxicology of Perchlorate. In *Perchlorate in the Environment* Ed. Urbansky, E. T.; Kluwer Academic/Plenum Publishers, New York, 2000.

Clement, T.P., Hooker, B.S., and Skeen, R.S. Macroscopic Models for Predicting Changes in Saturated Porous Media Properties Caused by Microbial Growth. *Groundwater*, 34(5): 934-942, 1996.

Coates, J. D., Michaelidou, U., Bruce, R. A., O'Connor, S. M., Crespi, J. N., and Achenbach, L. A. Ubiquity and and Diversity of Dissimilatory (Per)chlorate-Reducing Bacteria, *Applied and Environmental Microbiology*, *65*(12): 5234-5241, 1999.

Coates, J.D., Michaelidou, U., O'Connor, S.M., Bruce, R.A., and Achenbach, L.A. The Diverse Microbiology of (Per)Chlorate Reduction. In *Perchlorate in the Environment* Ed. Urbansky, E. T.; Kluwer Academic/Plenum Publishers, New York, 2000.

Coleman, M.L., Ader, M., Chaudhuri, S., Coates, J.D. Microbial Isotopic Fractionation of Perchlorate Chlorine. *Applied and Environmental Microbiology*, 69(8): 4997-5000, 2003.

Cox, E.E., Edwards, E., and Neville, S. In Situ Bioremediation of Perchlorate in Groundwater, *Perchlorate in the Environment*. Ed. Urbansky, E. T.; Kluwer Academic/Plenum Publishers, New York, 2000.

CRC. *CRC Handbook of Chemistry and Physics*. 84th Edition. Ed. Lide, D.R. CRC Press, Boca Raton, Florida, 2003.

Crump, C., Michaud, P., Tellez, R., Reyes, C., Gonzalez, G., Montgomory, E.L., Crump, K.S., Lobo, G, Becerra, C., and Gibbs, J.P. Does Perchlorate in Drinking Water Affect Thyroid Function in Newborns or School-Aged Children. *Journal of Occupational and Environmental Medicine*, 42(6): 603-612, 2000.

Cunningham, A. B., Charackilis, W. G., and Abedeen, F., and Crawford, D. Influence of Biofilm Accumulation on Porous Media Hydrodynamics. *Environmental Science and Technology*, 25(7): 1305-1311, 1991.

Cunningham, A.B., and Wanner, O. Modeling Biofilm Accumulation and Mass Transport in a Porous Medium Under High Substrate Loading. *Biotechnology and Bioengineering*, 47: 703-712, 1995.

Damien, P., and Pontius, F.W. From Rockets to Remediation: The Perchlorate Problem. *Environmental Protection*, 10(6): 24-31, June 1999.

Davis, S., Fairbank, W., and Weisheit, H. Dairy Waste Ponds Effectively Self-Sealing. *Trans. ASAE*, 16: 69-71, 1973.

Dupin, H.J., and McCarty, P.L. Mesoscale and Microscale Observations of Biological Growth in a Silicon Pore Imaging Element. *Environmental Science and Technology*, 33:1230-1236, 1999

Dupin, H. J., McCarty, P. L. Impact of Colony Morphologies and Disinfection on Biological Clogging in Porous Media. *Environmental Science and Technology*, 34: 1513-1520, 2000.

Dupin, H. J., Kitanidis, P. K., McCarty, P. L. Pore-Scale Modeling of Biological Clogging Due to Aggregate Expansion: A Material Mechanics Approach. *Water Resources Research*, 37(12): 2965-2979, 2001a.

Dupin, H. J., Kitanidis, P. K., McCarty, P. L. Simulations of Two Dimensional Modeling of Biomass Aggregate Growth in Network Models. *Water Resources Research*, 37(12): 2981-2994, 2001b.

Ellis, D.E., Lutz, J.E., Odom, J.M., Buchanen Jr., R.J., Bartlett, C.L., Lee, M.D. Harkness, M.R., and Deweerd, K.A. Bioaugmentation for Accelerated In Siu Anaerobic Bioremediation. *Environmental Science and Technology*, 34(11): 2254-2260, 2000.

Emsley, J. The Elements. Clarendon England: Oxford University Press, 1989.

Envirogen. *In Situ* Bioremediation of Perchlorate. SERDP project CY-1136 Final Report. 21 May, 2002.

Environmental Security Technology Certification Program (ESTCP). Ammonium Perchlorate Biodegredation for Industrial Wastewater Treatment. United States Department of Defense. June 2000.

Evans, P., Chu, A., Liao, S., Price, S., Moody, M., Headrick, D., Min, B., and Logan B.E. Pilot Testing of a Bioreactor for Perchlorate Contaminated Groundwater Treatment. In *Remediation of Chlorinated and Recalcitrant Compounds* Ed. Gavaskar, A.R., and Chen, A.S.C.; Battelle Press, Columbus, Ohio, 2002.

Flowers, T.C., and J.R. Hunt. Long-Term Release of Perchlorate as a Potential Source Of Groundwater Contamination. *Perchlorate in the Environment*. Ed. Urbansky, E. T.; Kluwer Academic/Plenum Publishers, New York, 2000.

Gandhi, R.K., Hopkins, G.D., Goltz, M.N., Gorelick, S.M., McCarty, P.M. Full-Scale Demonstration of In Situ Biodegradation of Trichloroethylene in Groundwater 1. Dynamics of a Recirculating Well System. *Water Resources Research*, 38(4): 10-1 – 10-16, 2002a.

Gandhi, R.K., Hopkins, G.D., Goltz, M.N., Gorelick, S.M., McCarty, P.M. Full-Scale Demonstration of In Situ Biodegradation of Trichloroethylene in Groundwater 2. Comprehensive Analysis of Field Data Using Reactive Transport Modeling. *Water Resources Research*, 38(4): 11-1 – 11-19, 2002b.

Geosyntec Consultants, Pilot Test of *In Situ* Bioremediation to Treat Perchlorate in GET D Recharge Water, Final Report. Prepared for Aerojet, Rancho Cordova, California. GeoSyntec project Number TR0018.15., January, 2002a.

Geosyntec Consultants, Pilot Test For In Situ Bioremediation of Perchlorate and Trichloroethene in Groundwater Using an Active Biobarrier, Final Report. Prepared for Aerojet, Rancho Cordova, California. GeoSyntec project Number TR0018.11., June, 2002b.

Goleman, W.L., Carr, J.A., and Anderson, T.A. Environmentally Relevent Concentrations of Ammonium Perchlorate Inhibit Thyroid Function and Alter Sex Ratios in Developing *Xenopus laevis*. *Environmental Toxicology and Chemistry*, 21(3): 590-597, 2002.

Giblin, T.L., Herman, D.C., and Frankenberger Jr., W.T. An Autotrophic System for the Bioremediation of Perchlorate From Groundwater. In *Perchlorate in the Environment* Ed. Urbansky, E. T.; Kluwer Academic/Plenum Publishers, New York, 2000.

Giblin, T, Losi, M.E., Hosangadi, V., and Frankenberger Jr., W.T. Bacterial Perchlorate Reduction in Simulated Reverse Osmosis Rejectate. *Bioremediation Journal*, 6(2); 105-111, 2002.

Goltz, M.N., Bouwer, E.J., Huang, J. Transport Issues and Bioremediation Modeling for the *In Situ* Aerobic Co-Metabolism of Chlorinated Solvents. *Biodegradation*, 12: 127-140, 2001.

Goltz, M.N. Personal conversation, Maximum flow rate of HFTWs at the Aerojet site. 2004.

Greene, M.R., and Pitre, M.P. Treatment of Groundwater Containing Perchlorate Using Biological Fluidized Bed Reactors With GAC or Sand Media. In *Perchlorate in the Environment* Ed. Urbansky, E. T.; Kluwer Academic/Plenum Publishers, New York, 2000.

Gurol, M. D., Kim, K. Investigation of Perchlorate Removal in Drinking Water Sources by Chemical Methods. In *Perchlorate in the Environment* Ed. Urbansky, E. T.; Kluwer Academic/Plenum Publishers, New York, 2000.

Hatzinger, P.B., Whittier, M.C., Arkins, M.D., Bryan, C.W., and Guarini, W.J. *In Situ* and *Ex Situ* Biormediation Options for Treating Perchlorate in Groundwater. Remediation: *The Journal of Environmental Cleanup Costs, Technologies, and Techniques*, 12(2): 69-86, Spring 2002.

Hatzinger P. B., In Situ Bioremediation of Perchlorate in Groundwater, ESTCP Project Proposal. 2001.

Hines, M.E., von Hippel, F., Kennish, J., Mach, M., and Pilson, D. Biological Effects of Inadvertent Perchlorate Releases During Launch Operations. Technical Report Prepared for U.S. Air Force Space and Missile Systems Center Environmental Management Branch, Contract No. F04701-00-D-0203, 30 September, 2002.

Hogue, C., Of Lettuce and Rocket Fuel. *Chemical and Engineering News*, 81(18): 11, May 5, 2003.

Ives, K.J., and Pienvichitr, V. Kinetics of the Filtration of Dilute Suspensions. *Chemical Engineering Science*, 20: 965-973, 1965.

Jackson, P.E., and Chassaniol, K. Advances in the Determination of Inorganic Ions in Potable Waters by Ion Chromatography, *Journal of Environmental Monitoring*, 4(1): 10-15, 2002

Jackson, P.E., Gokhale, S., and Rohrer, J.S. Recent Developments in the Analysis of Perchlorate Using Ion Chromatography. In *Perchlorate in the Environment* Ed. Urbansky, E. T.; Kluwer Academic/Plenum Publishers, New York, 2000.

Kengen, S. M., Rikken, G. B., Hage, W. R., Van Ginkel, C. G., Stams, A. M. Purification and Characterization of (Per)Chlorate Reductase From the Chlorate-Respiring Strain GR-1. *Journal of Bacteriology*, 181(21): 6706-6711, 1999.

Kildsgaard, J., and Engesgaard, P. Numerical Analysis of Biological Clogging in Two-Dimensional Sand Box Experiments. *Journal of Contaminant Hydrology*, 50: 261-285, 2001.

Kim, K., and Logan, B.E. Fixed-Bed Bioreactor Treating Perchlorate-Contaminated Waters. *Environmental Engineering and Science*, 17(5): 257-265, 2000.

Kirk, A.B., Smith, E.E., Tian, K., Anderson, T.A., and Dasgupta, P.K. Perchlorate in Milk. *Environmental Science and Technology*, 37(21): 4979-4981, 2003.

Lamm, S.H., and Doemland, M. Has Perchlorate in Drinking water Increased the Rate of Congenital Hypothyroidism? *Journal of Occupational and Environmental Medicine*, 41: 409-411, 1999.

Li, Z., Li, F.X., Byrd, D., Deyhle, G.M., Sesser, D.E., Skeels, M.R., and Lamm, S.H. Neonatal Thyroxine Level and Perchlorate in Drinking Water. *Journal of Occupational and Environmental Medicine*, 42(2): 200-205, 2000.

Linke, W.F. Solubilities: Inorganic and Metal Organic Compounds, Volume 1. American Chemical Society, Washington D.C. 1958.

Linke, W.F. Solubilities: Inorganic and Metal Organic Compounds, Volume 2. American Chemical Society, Washington D.C. 1965.

Logan, B.E. Evaluation of Biological Reactors to Degrade Perchlorate to Levels Suitable for Drinking Water. In *Perchlorate in the Environment* Ed. Urbansky, E. T.; Kluwer Academic/Plenum Publishers, New York, 2000.

Logan, B.E. Assessing the Outlook for Perchlorate Remediation. *Environmental Science and Technology*, 35(23): 482A-487A, 2001a.

Logan, B.E. Analysis of Overall Perchlorate Removal Rates in Packed-Bed Bioreactors. *Journal of Environmental Engineering*, 127(5): 469-471, 2001b.

Logan, B.E., Kim, K., and Price, S. Perchlorate Degradation in Bench and Pilot Scale Ex Situ Bioreactors. In *Bioremediation of Inorganic Compounds* Ed. Leeson A., Peyton, B.M., Means, J.L., and Mager, V.S.; Battelle Press, Columbus Ohio, 2001.

Logan, B.E., and LaPoint, D. Treatment of Perchlorate and Nitrate Contaminated Groundwater in an Autotrophic, Gas Phase, Packed Bed, Bioreactor. *Water Research*, 36: 3647-3653, 2002.

Losi, M. E., Giblin, T., Hosangadi, V., Frankenberger Jr, W. T. Bioremediation of Perchlorate-Contaminated Groundwater Using a Packed Bed Biological Reactor. *Bioremediation Journal,* 6(2): 97-103, 2002.

Maier, R.M., Pepper, I.L., and Gerba, C.P., *Environmental Microbiology*. San Diego: Academic Press, 2000.

Magnuson, M.L., Urbansky, E.T., and Kelty, C.A. Determination of Perchlorate at Trace Levels in Drinking Water by Ion-Pair Extraction with Electrospray Ionization Mass Spectrometry. *Analytical Chemistry*, 72(1): 25-29, 2000.

Mattison, R.G., Taki, H., and Harayama, S. The Bacterivorous Soil *Flagellate Heromita globosa* Reduces Bacterial Clogging under Denitrifying Conditions in Sand-Filled Aquifer Columns. *Appled and Environmental Microbiology*, (68)9: 4539-4545, 2002.

McCarty, P. L., Goltz, M. N., Hopkins, G. D., Dolan, M. E., Allan, J. P., Kawakami, B. and T., Carrothers, T. J. Full Scale Evaluation of In Situ Cometabolic Degradation of Trichloroethylene in Groundwater Through Toluene Injection. *Environmental Science and Technology*, 32: 88-100, 1998.

McMaster, M.L. Cox, E.E., Neville, S.L, and Bonsack, L.T. Successful field Demonstration of In Situ Bioremediation of Perchlorate in Groundwater. In *Bioremediation of Inorganic Compounds* Ed. Leeson A., Peyton, B.M., Means, J.L., and Mager, V.S.; Battelle Press, Columbus Ohio, 2001

Michaelidou, U. Achenbach, L.A., and Coates, J.D. Isolation and Characterization of Two Novel (Per)Chlorate-Reducing Bacteria From Swine Waste Lagoons. In *Perchlorate in the Environment* Ed. Urbansky, E. T.; Kluwer Academic/Plenum Publishers, New York, 2000.

Miller, J.P., and Logan, B.E. Sustained Perchlorate Degradation in an Autotrophic, Gas-Phase, Packed-Bed Bioreactor. *Environmental Science and Technology*, 34(14): 3018-3022, 2000.

Miyazaki, T. Bulk Density Dependence of Air Entry Suctions and Saturated Hydraulic Conductivities of Soils. *Soil Science*, 161: 484-490, 1996.

Molz, F.J., Widdowson, M.A., and Benefield, L.D. Simulations of Microbial Growth Dynamics Coupled to Nutrient and Oxygen Transport in Porous Media. *Water Resources Research*, 22, 1207-1216, 1986.

Moore, A.M, De Leon, C.H., and Young, T.M. Rate and Extent of Aqueous Perchlorate Removal by Iron Surfaces. *Environmental Science and Technology*, 37(14): 3189-3198, 2003.

Munakata, N., Cunningham, J.A., Reinhard, M., Ruiz, R., Lebron, C. Palladium Catalysis in Horizontal Flow Treatment Wells: Field Scale Design and Laboratory Study. In *Remediation of Chlorinated and Recalcitrant Compounds* Ed. Gavaskar, A.R., and Chen, A.S.C.; Battelle Press, Columbus, Ohio, 2002.

Murray, A.B. Seeking Explanation Affects Numerical Modeling Strategies. *Eos,* 83(38): 418-419, 2002.

Nambi, I.M., Werth, C.J., Sanford, R.A., and Valocchi, A.J. Pore-Scale Anaerobic Halorespiring Bacterial Growth Along the Transverse Mixing Zone of an Etched Silicon Pore Network. *Environmental Science and Technology*, 37(24): 5617-5624, 2003.

Nuttel, E.J, Investigations of Biofilms in Sand Column Experiments. Unpublished data. Received October 2003.

O'Connor, S.M., and Coates, J.D. Universal Immunoprobe for (Per)Chlorate-Reducing Bacteria. *Applied and Environmental Microbiology*, 68(6): 3108-3113, June 2002.

Oya, S., and Valocchi, A. J. Transport and Biodegradation of Solutes in Stratified Aquifers Under Enhanced *In Situ* Bioremediation Conditions. *Water Resources Research*, 34: 3323-3334, 1998.

Parr, J.C. Application of Horizontal Flow Treatment Wells for In Situ Treatment of Perchlorate Contaminated Groundwater. MS Thesis, AFIT/GEE/ENV/02M-08, 2002. School of Engineering and Management, Air Force Institute of Technology, (AU), Wright-Patterson AFB OH, March 2002.

Parr, J.C., Goltz M.N., Huang J., Hatzinger P.B., and Farhan, Y.H. Modeling *In Situ* Bioremediation of Perchlorate-contaminated Groundwater. *Seventh International In Situ and On-site Bioremediation Symposium*, Orlando, FL, 2-5 June 2003.

Paulsen, J.E., Oppen, E., and Bakke, R. Biofilm Morphology in Porous Media, A Study With Microscopic and Image Techniques. *Water Science Technology*, 36(1): 1-9, 1997.

Perlmutter, M.W., Britto, R., Cowan, J.D., Patel, M., Jacobs, A., logan, B., and Craig, M. Bioremediation of Perchlorate Contaminated Groundwater at Naval Weapons Reserve Plant McGregor, Texas. *National Defense Industrial Association Proceedings, 26th Environmental Symposium and Exhibition*, Long Beach, CA: 27-30 March, 2000.

Pontius, F.W., Damian P., and Eaton, A.D. Regulating Perchlorate in Drinking Water. *Perchlorate in the Environment.* Ed. Urbansky, E. T.; Kluwer Academic/Plenum Publishers, New York, 2000.

Polk, J., Onewokae, C., Guarini, W.J., Murray, C., Tolbert, D.E., and Togna, A.P. Army Success Story: *Ex Situ* Biological Treatment of Perchlorate-Contaminated Groundwater. *Federal Facilities Environmental Journal*, 13(2): 85-94, Summer 2002.

Ragusa, S., R., de Zoysa, D. S., and Rengasamy, P. The Effect of Microorganisms, Salinity, and Turbidity on Hydraulic Conductivity of Irrigation Channel Soil. *Irrigation Science*, 15: 159-166, 1994.

Rittmann, B.E. The Significance of Biofilms in Porous Media. *Water Resources Research*, 29(7): 2195-2202, 1993.

Rice, R., C. Soil Clogging During Infiltration of Secondary Effluent. *Journal of the Water Pollution Control Federation*, 46: 708-716, 1974.

Rikken, G.B., Kroon, A.G.M, and van Ginkel, C.G. Transformation of (per)chlorate into Chloride by a Newly Isolated Bacterium: Reduction and Dismutation. *Applied Microbiology and Biotechnology*, 45: 420-426, 1996.

Seki, K., and Miyazaki, T. A Mathematical Model for Biological Clogging of Uniform Porous Media. *Water Resources Research*, 37(12): 2995-2999, 2001.

Seki, K., Suko, T., and Miyazaki, T. Bioclogging of Glass Beads by Bacteria and Fungi. *Transactions of the World Congress of Soil Science*, Symposium no. 51, Paper no. 1244: 1244-1 – 144-8, 2002.

Shaw Environmental and Infrastructure. *In Situ Bioremediation of Perchlorate Using Horizontal Flow Treatment Wells*. ESTCP Technology Demonstration Plan, Project CU-0224 Final. 2003.

Stoppel, C. M., and Goltz, M. N. Modeling Pd-Catalyzed Destruction of Chlorinated Ethenes in Groundwater. *Journal of Environmental Engineering*, 129(2): 147-154, February 2003.

Strategic Environmental Research and Development Program (SERDP), *Annual Report to Congress – Fiscal Year 2002*. Washington D.C., March 2003.

Sturchio, N.C., Hatzinger, P.B., Arkins, M.D., Suh, C., Heraty, L.J. Chlorine Isotope Fractionation During Microbial Reduction of Perchlorate. *Environmental Science and Technology*, 37(17): 3859-3863, 2003.

Suchomel, B.J., Chen, B.M., and Allen III, M.B. Network Model of Flow, Transport and Biofilm effects in Porous media. *Transportation in Porous Media*, 30(1), 1-23, 1998.

Taylor, S.W., and Jaffe, P.R. Biofilm Growth and related Changes in the Physical Properties of a Porous Medium: 1. Experimental Investigation. *Water Resources Research*, 26(9), 2153-2159, 1990a.

Taylor, S.W., and Jaffe, P.R. Biofilm Growth and related Changes in the Physical Properties of a Porous Medium: 3. Dispersivity and Model Verification. *Water Resources Research*, 26(9), 2171-2180, 1990b.

Taylor, S.W., and Jaffe, P.R. Substrate and Biomass Transport in a Porous Medium. *Water Resources Research*, 26(9), 2181-2194, 1990c.

Taylor, S.W., Milly, C.D., Jaffe, P.R. Biofilm Growth and related Changes in the Physical Properties of a Porous Medium: 2. Permeability. *Water Resources Research*, 26(9), 2161-2169, 1990.

Taylor, T.P., Longmire, P., Counce, D.A., Chipera, S.J., Kaszuba, J.P., and Conca, J.L. Permeable Reactive Barrier Treatment Technology for Remediation of Inorganic Contaminated Groundwater. In *Remediation of Chlorinated and Recalcitrant Compounds* Ed. Gavaskar, A.R., and Chen, A.S.C.; Battelle Press, Columbus, Ohio, 2002.

Texas Department of Health, Public Health Service, Health Assessment and Toxicology Program, Environmental Epidemiology and Toxicology Division. Physician Fact Sheet: Perchlorate. Electronic Publication No. E09-11579, October 2002. www.tdh.state.tx.us/epitox/physpch.pdf.

Thuett, K.A., Roots, E.H., Mitchell, L.P., Gentles, B.A., Anderson, T., Kendall, R.J., Smith, E.E. Effects of In Utero and Lactational Ammonium Perchlorate Exposure on Thyroid Gland Histology and Thyroid and Sex Hormones in Developing Deer Mice (*Peromyscus maniculatus*) Through Postnatal Day 21. *Journal of Toxicology and Environmental Health, Part A*, 65: 2119-2130, 2002.

Thullner, M., Mauclaire, L., Schroth, M. H., Kinzelbach, W., Zeyer, J. Interaction Between Water Flow and Spatial Distribution of Microbial Growth in a Two-Dimensional Flow Field in Saturated Porous Media. *Journal of Contaminant Hydrology*, 58: 169-189, 2002.

Tipton, D.K., Rolston, D.E., and Scow, K.M. Transport and Biodegradation of Perchlorate in Soils. *Journal of Environmental Quality*, 32: 40-46, 2003.

Togna, A.P., Guarini, W.J., Frisch, S., Del Vecchio, M., Polk, J., Murray, C., and Tolbert, D.E. Case Study of Ex Situ Biological Treatment of Perchlorate-Contaminated Groundwater. . In *Bioremediation of Inorganic Compounds* Ed. Leeson A., Peyton, B.M., Means, J.L., and Mager, V.S.; Battelle Press, Columbus Ohio, 2001.

United States Army Center for Health Promotion and Preventive Medicine. Perchlorate in Drinking Water. May 2002. http://chppm-www.apgea.army.mil/documents/FACT/31-003-0507.pdf

United States Environmental Protection Agency (USEPA). Region 9 Perchlorate Update. Washington D.C., June 1999a.

United States Environmental Protection Agency (USEPA). Interim Assessment Guidance for Perchlorate. Washington D.C , June 18, 1999b.

United States Environmental Protection Agency (USEPA). Survey of Fertlizers and Related Materials for Perchlorate (ClO_4^-) (EPA/600/R-01/049). Office of Research and Development, Cincinnati, OH, 2001.

United States Environmental Protection Agency (USEPA). Status of EPA's Interim Assessment Guidance for Perchlorate. Washington D.C. January 22, 2003a.

United States Environmental Protection Agency (USEPA). Perchlorate Releases as of April, 2003. 22 August 2003b. http://www.clu-in.org/download/contaminantfocus/perchlorate/usrel_titleless.pdf

United States House of Representatives, H.R. 2123, *Preventing Perchlorate Pollution Act of 2003*, Washington D.C. May 15, 2003.

United States Senate, S.820, *Perchlorate Community Right-to-Know Act of 2003*, Washington D.C. April 8, 2003.

Urbansky, E. T., Perchlorate Chemistry: Implications for Analysis and Remediation. *Bioremediation Journal*, *2*: 81-95, 1998.

Urbansky, E.T., Schock, M.R. Issues in Manageing the Risks Associated With Perchlorate in Drinking Water. *Journal of Environmental Management*, 56: 79-95, 1999.

Urbansky, E.T., Magnuson, M.L., Kelty, C.A., Brown, S.K. Perchlorate Uptake by Salt Cedar (*Tamarix ramosissima*) in the Las Vegas Wash Riparian Ecosystem. *The Science of the Total Environment,* 256: 227-232, 2000.

Urbansky, E. T., Perchlorate as an Environmental Contaminant. *Environmental Science and Pollution Research*, 9(3): 187-192, 2002.

Vandevivere, P., and Baveye P. Effect of Bacterial Extracellular Polymers on the Saturated Hydraulic Conductivity of Sand Columns. *Applied Environmental Microbiology*, 58: 1690-1698, 1992a.

Vandevivere, P., and Baveye P. Relationship Between Transport of Bacteria and Their Clogging Efficiency in Sand Columns. *Applied Environmental Microbiology*, 58: 2523-2530, 1992b.

Vandevivere, P., and Baveye P. Saturated Hydraulic Conductivity Reduction Caused by Aerobic Bacteria in Sand Columns. *Soil Science Societyof America Journal*, 56: 1-13, 1992c.

Vandevivere, P., Baveye, P., de Lozada, Diego, and Sanchez, DeLeo, P. Microbial Clogging of Saturated Soils and Aquifer Materials: Evaluation of Mathematical Models. *Water Resources Research*, 31(9): 2173-2180, 1995.

Waterloo Hydrogeologic Inc. *Users Manual for Visual MODFLOW*. Waterloo, Ontario: Waterloo Hydrogeologic Incorporated, 1999.

Weise, E., Studies Find Disturbing Amounts of Chemical Contamination in Lettuce. *USA Today*, pg 4D, April 29, 2003.

Widdowson, M.A. Comment on An Evaluation of Mathematical Models of the Transport of Biologically Reacting Solutes in Saturated Soils and Aquifers. *Water Resources Research*, 27: 1378-1378, 1991.

Wolff, J. Perchlorate and the Thyroid Gland. *Pharmacological. Rev., 50*: 89-95, 1998.

Wu, J., Unz, R.F., Zhang, H., and Logan, B.E. Persistence of Perchlorate and Chlorate Respiring Microorganisms in Natural Waters, Soils, and Wastewater. *Bioremediation Journal*, 5(2): 119-130, 2001.

Xu, J., Song, Yanguang, Min, Booki, Steinberg, L., and Logan, B.E. Microbial Degradation of Perchlorate: Principles and Applications. *Environmental Engineering Science*, 20(5): 405-422, 2003.

Xu, J., and Logan, B.E. Measurement of Chlorite Dismutase Activities in Perchlorate Respiring Bacteria. *Journal of Microbiological Methods*, 54: 239-247, 2003.

Vita

Captain Peter G. Chosa graduated from Baraga High School located in Baraga Michigan in 1993. He entered undergraduate studies at Michigan Technological University in Houghton Michigan where he graduated Magna Cum Laude with a Bachelor of Science degree in Civil Engineering in 1999. He was commissioned through Detachment 400 AFROTC at Michigan Technological University.

His first assignment was to Eielson AFB, Alaska where he served as a project manager and project programmer in the 354th Civil Engineering Squadron. In September 2000 he deployed to Kuwait in support of Operation Southern Watch. While in Kuwait, Captain Chosa worked as the environmental flight commander in the 332nd Expeditionary Civil Engineering Squadron. In September of 2002, he entered the Graduate School of Engineering and Management, Air Force Institute of Technology. Upon graduation, he will be assigned to Osan AB, Republic of Korea.

REPORT DOCUMENTATION PAGE

Form Approved
OMB No. 074-0188

The public reporting burden for this collection of information is estimated to average 1 hour per response, including the time for reviewing instructions, searching existing data sources, gathering and maintaining the data needed, and completing and reviewing the collection of information. Send comments regarding this burden estimate or any other aspect of the collection of information, including suggestions for reducing this burden to Department of Defense, Washington Headquarters Services, Directorate for Information Operations and Reports (0704-0188), 1215 Jefferson Davis Highway, Suite 1204, Arlington, VA 22202-4302. Respondents should be aware that notwithstanding any other provision of law, no person shall be subject to an penalty for failing to comply with a collection of information if it does not display a currently valid OMB control number.

PLEASE DO NOT RETURN YOUR FORM TO THE ABOVE ADDRESS.

1. REPORT DATE *(DD-MM-YYYY)*	**2. REPORT TYPE**	**3. DATES COVERED** *(From – To)*
23-03-2004	Master's Thesis	Sep 2002 – Mar 2004

4. TITLE AND SUBTITLE

MODELING A FIELD APPLICATION OF *IN SITU* BIOREMEDIATION OF PERCHLORATE-CONTAMINATED GROUNDWATER USING HORIZONTAL FLOW TREATMENT WELLS (HFTWs)

5a. CONTRACT NUMBER

5b. GRANT NUMBER

5c. PROGRAM ELEMENT NUMBER

6. AUTHOR(S)

Pete G. Chosa, Capt, USAF

5d. PROJECT NUMBER
NA

5e. TASK NUMBER

5f. WORK UNIT NUMBER

7. PERFORMING ORGANIZATION NAMES(S) AND ADDRESS(S)

Air Force Institute of Technology
Graduate School of Engineering and Management (AFIT/EN)
2950 Hobson Way, Building 641
WPAFB OH 45433-7765

8. PERFORMING ORGANIZATION REPORT NUMBER

AFIT/GEM/ENV/04M-05

9. SPONSORING/MONITORING AGENCY NAME(S) AND ADDRESS(ES)

Air Force Center for Environmental Excellence
Attn: Ms. Erica Becvar
3300 Sydney Brooks
Brooks AFB, TX 78235-5112
(210) 536-4330

Environmental Security Technology Certification Program
Attn: Dr. Andrea Leeson
901 N Stuart St., Ste 303
Arlington, VA 22203
(703) 696-2118

10. SPONSOR/MONITOR'S ACRONYM(S)
AFCEE/ERS
ESTCP

11. SPONSOR/MONITOR'S REPORT NUMBER(S) – Mark Goltz, (937)255-3636 x4638, mark.golz@afit.edu

12. DISTRIBUTION/AVAILABILITY STATEMENT

APPROVED FOR PUBLIC RELEASE; DISTRIBUTION UNLIMITED.

13. SUPPLEMENTARY NOTES

14. ABSTRACT

Perchlorate contaminated groundwater is rapidly becoming a significant environmental remediation issue for the Department of Defense. In this study, an existing numerical model that simulates the operation of a Horizontal Flow Treatment Well (HFTW) system to effect the *in situ* biodegradation of perchlorate through the addition of an electron donor is modified to include a submodel that describes bioclogging. Bioclogging restricts flow out of the HFTW due to the accumulation of biomass directly adjacent to the well. The modified model is then applied to an existing perchlorate contaminated site that will be used for an evaluation of the HFTW technology. Simulations were conducted to determine the impact of altering various engineered parameters on HFTW performance. Simulation results indicate that higher time averaged electron donor concentrations and HFTW pumping rates lead to more perchlorate degradation in terms of total mass of perchlorate removed. Simulation results also indicate that varying the electron donor addition schedule has little impact on HFTW performance. The simulations conducted in this study show that, regardless of the engineered parameter values, bioclogging does not impact the ability of the HFTW technology to effect *in situ* biodegradation of perchlorate at the evaluation site.

15. SUBJECT TERMS

Groundwater contamination, perchlorate, bioremediation, modeling, bioclogging, biofouling

16. SECURITY CLASSIFICATION OF:			**17. LIMITATION OF ABSTRACT**	**18. NUMBER OF PAGES**	**19a. NAME OF RESPONSIBLE PERSON**
a. REPORT	**b. ABSTRACT**	**c. THIS PAGE**			Professor Mark N. Goltz, ENV
U	**U**	**U**	**UU**	193	**19b. TELEPHONE NUMBER** *(Include area code)* (937) 255-3636, ext 4638 mark.goltz@afit.edu

Standard Form 298 (Rev. 8-98)
Prescribed by ANSI Std. Z39-18

Form Approved
OMB No. 074-0188